A PALAEOMAGNETIC STUDY OF UPPER PALAEOZOIC TO LOWER MESOZOIC
SEDIMENTS OF THE GONDWANA SYSTEM FROM COALFIELDS OF
THE KOEL-DAMODAR VALLEY AND THE SON VALLEY, N.E. INDIA
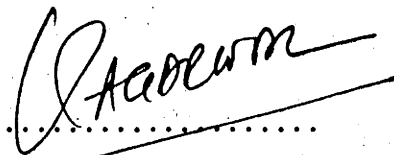
by

VINOD KUMAR AGARWAL

A Thesis Submitted for the Degree of
Master of Science
at the
Australian National University

Research School of Earth Sciences
Australian National University
Canberra

November, 1980

STATEMENT

Results and interpretations presented in this thesis
are the original work of the author, unless otherwise
acknowledged in the text.   No part of this study has
been previously submitted to any other university or
institution.   The study described herein was conducted
during my tenure of an Australian National University
Scholarship from February, 1977 to March, 1979 and
afterwards at my own expense.

VINOD KUMAR AGARWAL

Canberra, November 1980

ACKNOWLEDGEMENTS

TABLE OF CONTENTS

(iii) The Permo-Triassic Panchet Formation D = 115.3°;
       I = +55.6°.

(iv) The Middle-Late Triassic Tiki Formation and the
      Parsora Formation D = 300.2°; I = -28.2° and
      D = 317.2°, I = -42.9° respectively.

(c) A secondary early Tertiary component related to the Deccan Traps
     magmatic activity, which is broken down gradually between
     temperatures 300°C - 675°C. This component has been observed in
     the late Early Triassic-Early Jurassic Mahadeva Formation and
     in the Carnian-early Norian Tiki Formation. The mean magnetization
     direction is D = 337.0°, I = -43.0°.

The palaeomagnetic results from Permo-Carboniferous to late-Early
Permian rocks are open to two interpretations - Primary or Secondary of
Triassic-Jurassic age. For primary interpretation the results are seemingly
in disagreement with some earlier established results and invoke an
appreciable polar wandering during Permian time. An alternative explanation
in terms of a Triassic-Jurassic remagnetization may be invoked because of
their similarity with the Triassic-Jurassic trajectory in the Indo-Pakistan
APWP as proposed before. This interpretation however, seems less likely
because of the predominantly reversed polarities of the results obtained,
compared with the world-wide normal polarity bias which has been established
for the Triassic-Jurassic.

The Permo-Triassic and middle to Late Triassic results are in
gross agreement with established results of the Indo-Pakistan and add
further support for the existence of a Triassic-Jurassic loop in the APWP.

Palaeomagnetic directions obtained from both the thermal and the
chemical demagnetization techniques have shown good agreement in the
characteristic directions obtained. Chemical demagnetization was more
effective in separating the primary component from a chemical magnetization
component related to the early Tertiary Deccan Trap magmatic activity. Such
Deccan Trap remagnetization was observed in the present study in coalfields
located both far from and near to the present exposures of Deccan Traps.
It is argued that since this remagnetization seems to be a locally prevalent
effect which has not been observed on a regional scale, that hydrothermal
fluids associated with the Deccan Trap magmatic activity must be seen as a
major cause for remagnetization of these rocks in addition to regional heating.

A comparison of the Indo-Pakistan APWP as updated on the basis of
the here obtained results, with APWP trajectories for the other Gondwanaland

continents, such as Australia, South America, "Stable" Africa and NW
Africa, shows that the Permian loop interpreted in the Indo-Pakistan
APWP (in case of primary magnetization) can be recognized in data from
"Stable" Africa but is not evidently present in data from the other
continents. This discrepancy awaits further study. The Triassic-Jurassic
loop, however, exists also in the Australian APWP and may be interpreted,
though tentatively as yet, in the data from "Stable" Africa, N.W. Africa,
Morocco and South America.

This common Triassic-Jurassic loop may be interpreted as reflecting
an initial rifting stage of Gondwanaland's northern rim, associated with
the formation of the NeoTethys during late Palaeozoic and early Mesozoic
times.

CHAPTER 1

A REVIEW OF INDIAN PALAEOMAGNETIC DATA AND THEIR INTERPRETATION

1.1   Introduction

Palaeomagnetic studies during the fifties revived interest in the continental drift theory as advocated earlier this century by workers such as Alfred Wegener (1924) and Alex du Toit (1937). Du Toit, in particular pointed to the existence of a supercontinent called Gondwanaland, which contained all the southern hemisphere continents and India. The Gondwanaland concept was initially based on the widespread occurrences of traces of a late Palaeozoic glaciation . The glacial evidence suggested that Gondwanaland passed the (south) polar region during the late Palaeozoic. Indo-Pakistan is the most obvious Gondwanaland fragment which is now situated in the northern hemisphere. It must have drifted at a much higher latitudinal speed than other Gondwanaland continents. For this reason, a palaeomagnetic study of Indo-Pakistan's drift is particularly interesting because latitudinal as well as rotational movements can be traced by palaeomagnetic methods.

In a wider perspective, the former unity of Indo-Pakistan within Gondwanaland and the subsequent breakup of this supercontinent can be studied by comparing the Apparent Polar Wander Paths (APWP's) from the various Gondwana continents. This is most appropriately acheived with the continents reconstructed in one of the proposed pre-drift configurations. The configuration generally used is the Gondwana reconstruction of Smith and Hallam (1970), modified for the Australia-Antarctica fit according to Griffiths (1974). This type of comparison depends heavily on the reliability of existing APWP's for the various continents. The Indo-Pakistan APWP as known heretofore is ambiguous in various respect as will be summarised below:

1.   Interpretation of Precambrian palaeomagnetic data in terms of an APWP is not possible because of poor constraints on the radiometrical or chronostratigraphic age of the rocks studied. For most of the results, only uncertain relative ages are available, based mainly on superposition criteria and lithologic correlation (see review by Klootwijk, 1979a).

2.   A remagnetization of strata on the Indian shield during Deccan Trap time (60-65 My., Wellman and McElhinny 1970, Kaneoka and Haramura 1973, Wensink et al., 1977) observed in widely separated areas of peninsular Indo-Pakistan.

3.   Rocks of Palaeozoic and Tertiary ages are not widely represented in peninsular Indo-Pakistan, which make the determination of these parts of the Indo-Pakistan APWP diffcult. Tertiary pole positions however, have been simulated from DSDP core data from the Ninety East Ridge and from the Arabian Sea.

4.   Palaeozoic and Tertiary rocks are better developed in extrapeninsular Indo-Pakistan but interpretation of palaeomagnetic results is more difficult here, because of the allochthonous nature of parts of the studied structural units.

Klootwijk and Binhgam (1980) have derived a tentative Indo-Pakistan APWP based on palaeomagnetic results from both peninsular and extrapeninsular Indo-Pakistan (Fig. 1.2, Table 1.1) This will be reviewed as an introduction to the interpretation and discussion of the new results from the more basal part of the Gondwana System (Permo-Carboniferous to Upper Triasic) of the Koel-Damodar Valley and Son Valley (Fig. 1.1).

Though the current study deals with Permo-Carboniferous to Upper Triasic rocks, a discussion of the whole of the late Palaeozoic to Tertiary trajectory of the Indo-Pakistan APWP is necessary for a better

understanding of the various secondary magnetic components observed in rocks from both the peninsular and the extrapeninsular regions. The main observations that can be drawn from the Klootwijk and Bingham (1980) APWP for Indo-Pakistan (Fig. 1.2) are:

1. A considerable scatter in Permo-Carboniferous poles.

2. A reasonably good agreement in the Permo-Triassic poles.

3. Existence of a Triassic-Jurassic loop in the APWP.

4. A fairly well defined Early Cretaceous and Tertiary trajectory.

These points will be discussed in detail with respect to data from peninsular and extrapeninsular Indo-Pakistan. An overview of previously studied localities from these regions is given in Figs. 1.1 and 1.4a, and results obtained are summarised in Table 1.1.

1.2   Palaeomagnetic data from Peninsular Indo-Pakistan

Figure 1.1 gives a generalised geology of peninsular Indo-Pakistan and is discussed in greater detail in Chapter 2. Precambrian metamorphic rocks form the foundation of the Craton which in some regions is covered with unaltered Precambrian sediments. The late Precambrian-early Palaeozoic to Permo-Carboniferous timespan was a period of regressive conditions on the Craton and only a scanty sedimentation record is available. From the Permo-Carboniferous untill the Early Cretaceous, predominantly continental type sediments were deposited. These are grouped into the Gondwana System, and are now exposed along three main river valleys in central and eastern India, i.e. the Koel-Damodar Valley, the Son-Mahanadi Valley, the Wardha-Pranhita Godavari Valley and the Satpura basin (Fig. 1.1). The peninsular depositional history was interrupted twice by major volcanic activity, Early Cretaceous extrusion of the Rajmahal Traps (100-105 My., McDougall and McElhinny, 1970) in NE India, and the Palaeocene or

Figure 1.1   Simplified geological map of Indian Shield.   Solid circles showing the palaeomagnetic sampled localities of rocks of mainly Gondwana age (latest Carboniferous to Early Cretaceous).   The numbers correspond with results in Table 1.1 and Figure 1.2a.

Legend:
- Indogangetic alluvium L. Cretaceous & Cenozoic
- Rajmahal Traps, Gondwana & marginal marine equivalents
- Deccan Traps
- Precambrian of Peninsula

RAJMAHAL TRAPS

KOEL – DAMODAR BASINS

SON–MAHANADI BASINS

SATPURA BASIN

WARDHA–GODAVARI BASINS

Calcutta

Rajahmundry

Madras

Bombay

Badhura

Jaisalmer

Bhuj
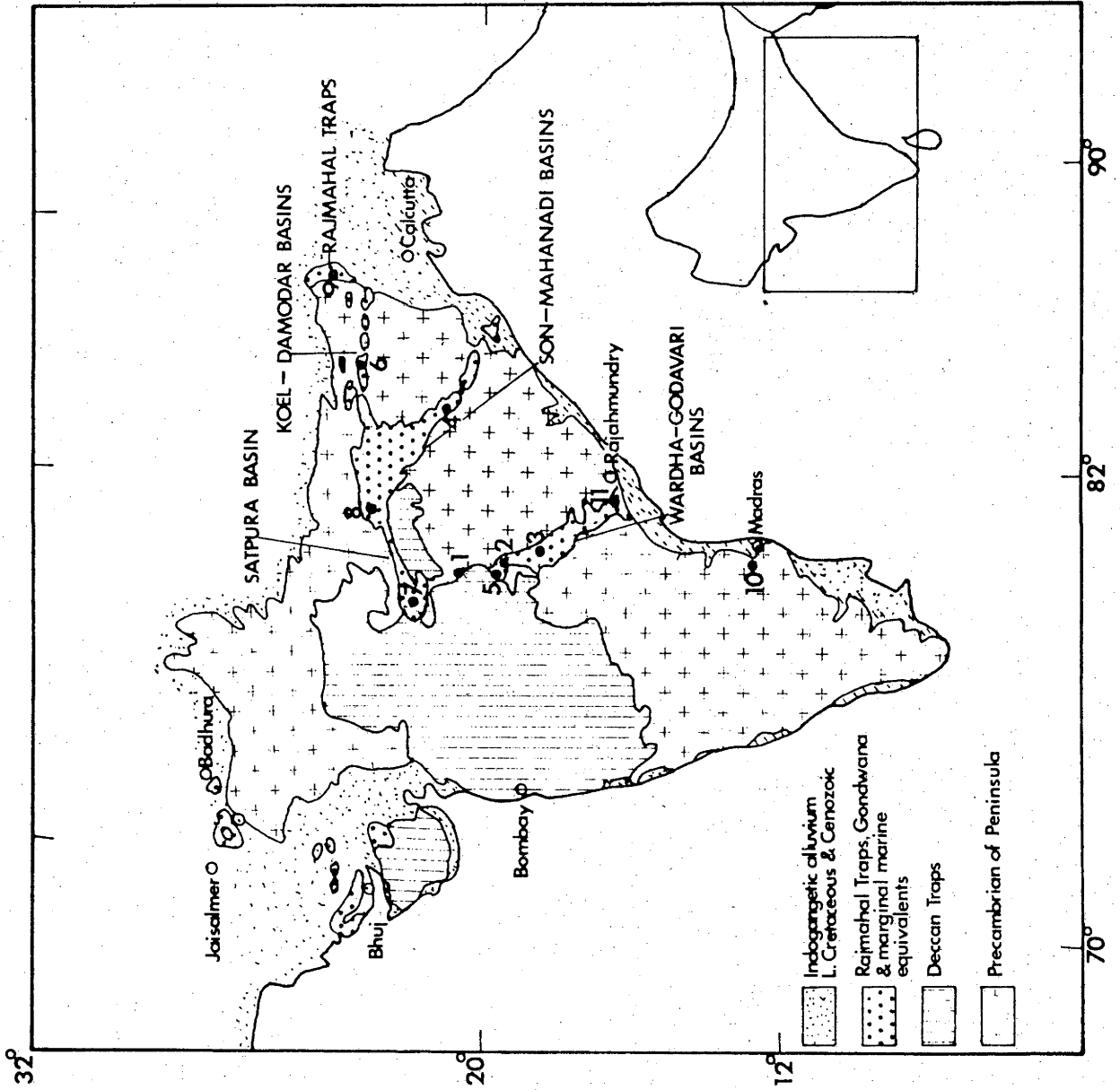
older Deccan Traps (60-65 My., Wellman and McElhinny, 1970., Kaneoka and Haramura,1973 .,Wensink et al., 1977) in western India. It is suspected that the Deccan Traps once covered an even larger area than their present 500.000 square kilometer outcrop. They were in part eroded during the Tertiary and the Quaternary as indicated by outliers which occur as far as the east coast near Rajahmundry (Fig. 1.1). Tertiary rocks are not very well developed on the peninsular region except for a few minor outcrops along the eastern and western coasts of India.

For many years, palaeomagnetic studies of rocks from peninsular India have concentrated on those formations whose magnetic content could be analysed with relatively simple and unsophisticated equipment such as the Astatic Magnetometer. Considerable emphasis was therefore placed on the study of igneous rocks and in particular on the early Tertiary Deccan Traps and the Early Cretaceous Rajmahal Traps (see review of Klootwijk, 1979a). These early palaeomagnetic studies were then extended to sedimentary successions, mainly red beds intercalated in the more basal part of the Gondwana System. Red beds were preferred because of their high intensity of Natural Remanent Magnetization (NRM) and their stable magnetic characteristics. Palaeomagnetic results were obtained during the sixties by Indian workers from red bed successions, of the Kamthi Formation, the Himgir beds, the Tirupati and Satyavedu beds (Table 1.1, Figs. 1.1,1.2, Localities 3,4,11,10, Poles 5,6,13 and 12). These results were not supported by later studies on Gondwana red beds, carried out by the palaeomagnetic group from Utrecht University (the Netherlands). Results obtained by the Dutch workers for the Kamthi Formation , the Mangli Formation and for the Panchet Formations showed the necessity of detailed thermal demagnetization (up to 675 degrees centigrade) in order to remove hard secondary magnetic components of early Tertiary age (Table1.1, Figs.1.1,1.2, Localities
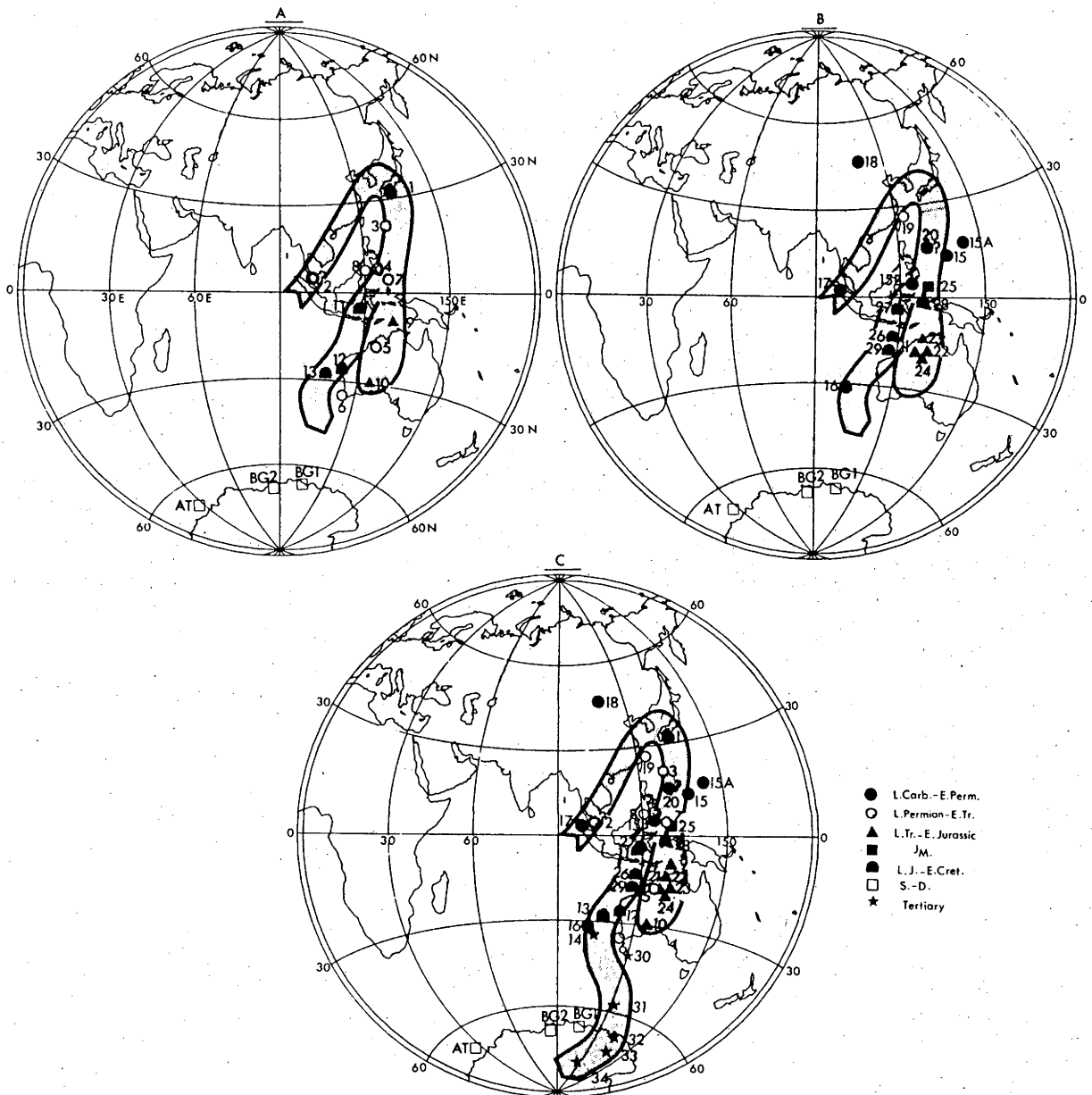
Figure 1.2   Trajectories of the Indo-Pakistan APWP according to the pole
positions listed under Table 1.1.   Swath width = 10°.

(A)   Corresponds to pole positions from peninsular Indo-Pakistan.
(B)   Corresponds to pole positions from extrapeninsular Indo-Pakistan.
(C)   Combined A and B plus mean pole positions from DSDP cores and
        Silurian-Devonian pole positions.

Legend: Solid Circles   = L.Carboniferous-E.Permian
            Open Circles   = L.Permian-E.Triassic
            Solid Triangles = L.Triassic-E.Jurassic
            Solid Squares   = M.Jurassic
            Solid D   = L.Jurassic-E.Cretaceous
            Open Squares   = Silurian-Devonian
            Stars   = Tertiary   Linear polar projection.
Details of Figure 1.2 A,B,C are given on the following pages.

Figure 1.2a

Figure 1.2b

C

60 60

30 30

●18

11

19 3

●15A

20 15

17 2 13 25

0 0
30 60 150

24

13 12
16
14 10

6
★30

31

BG2 BG1
32
AT 33

34
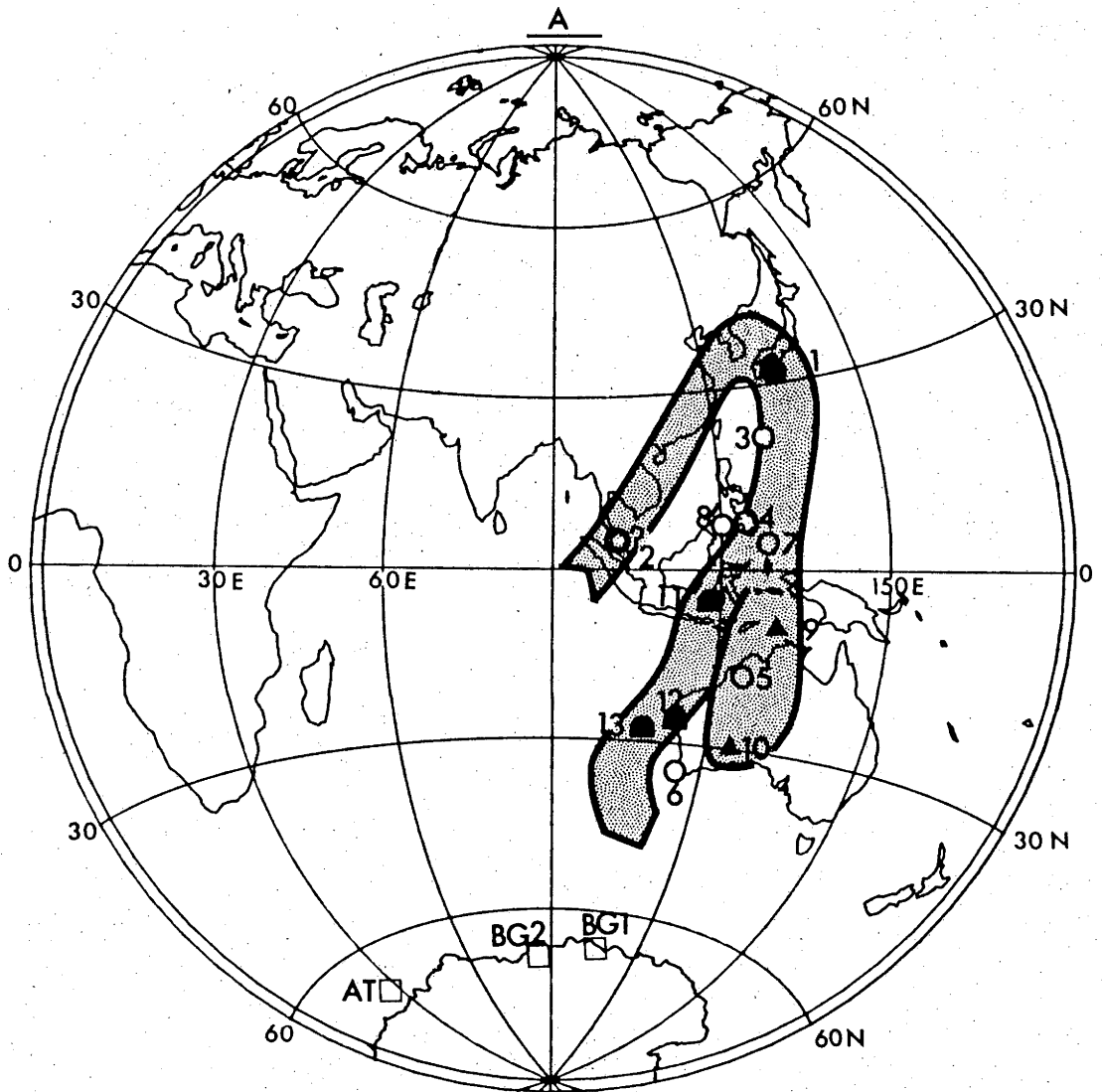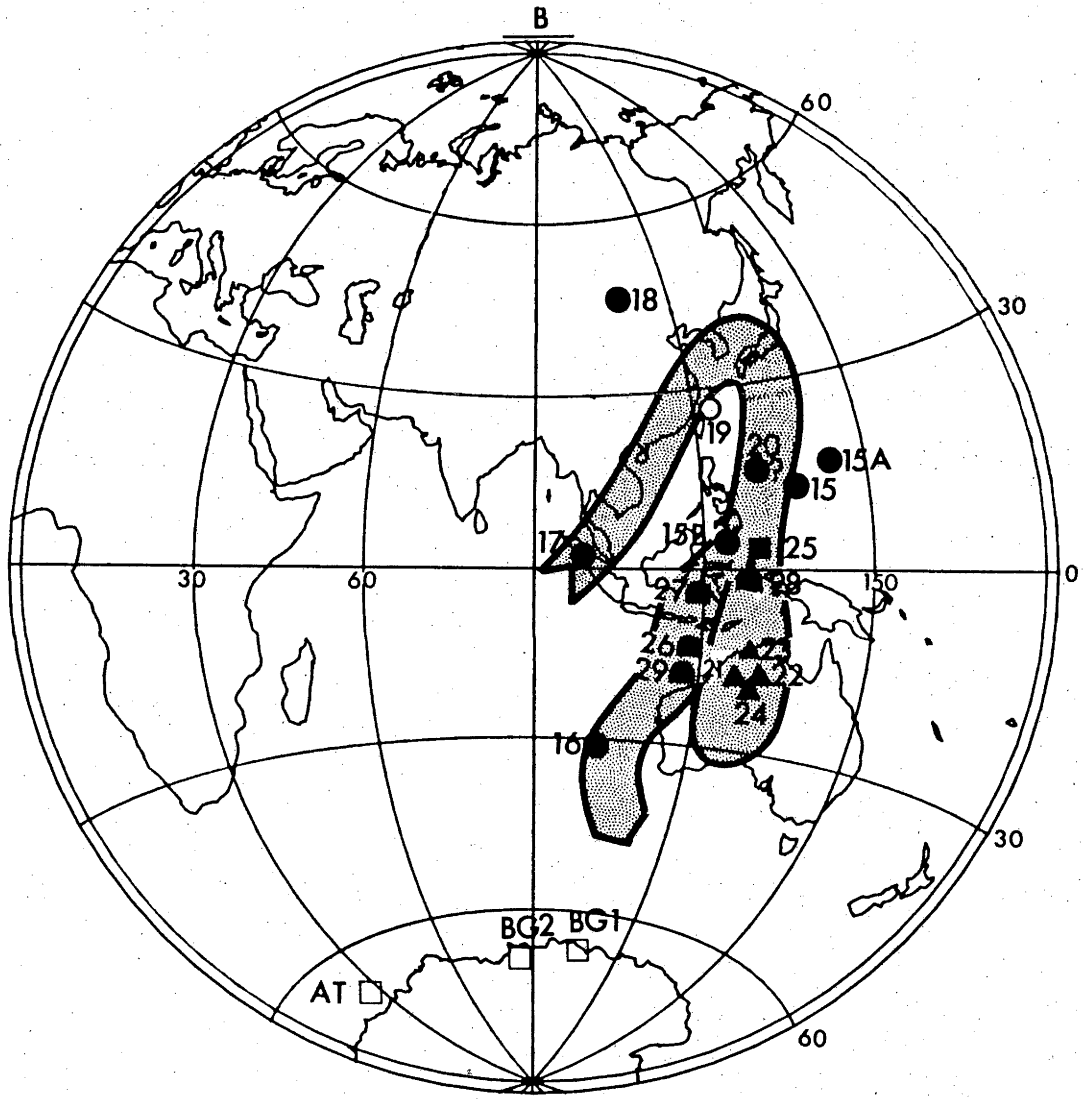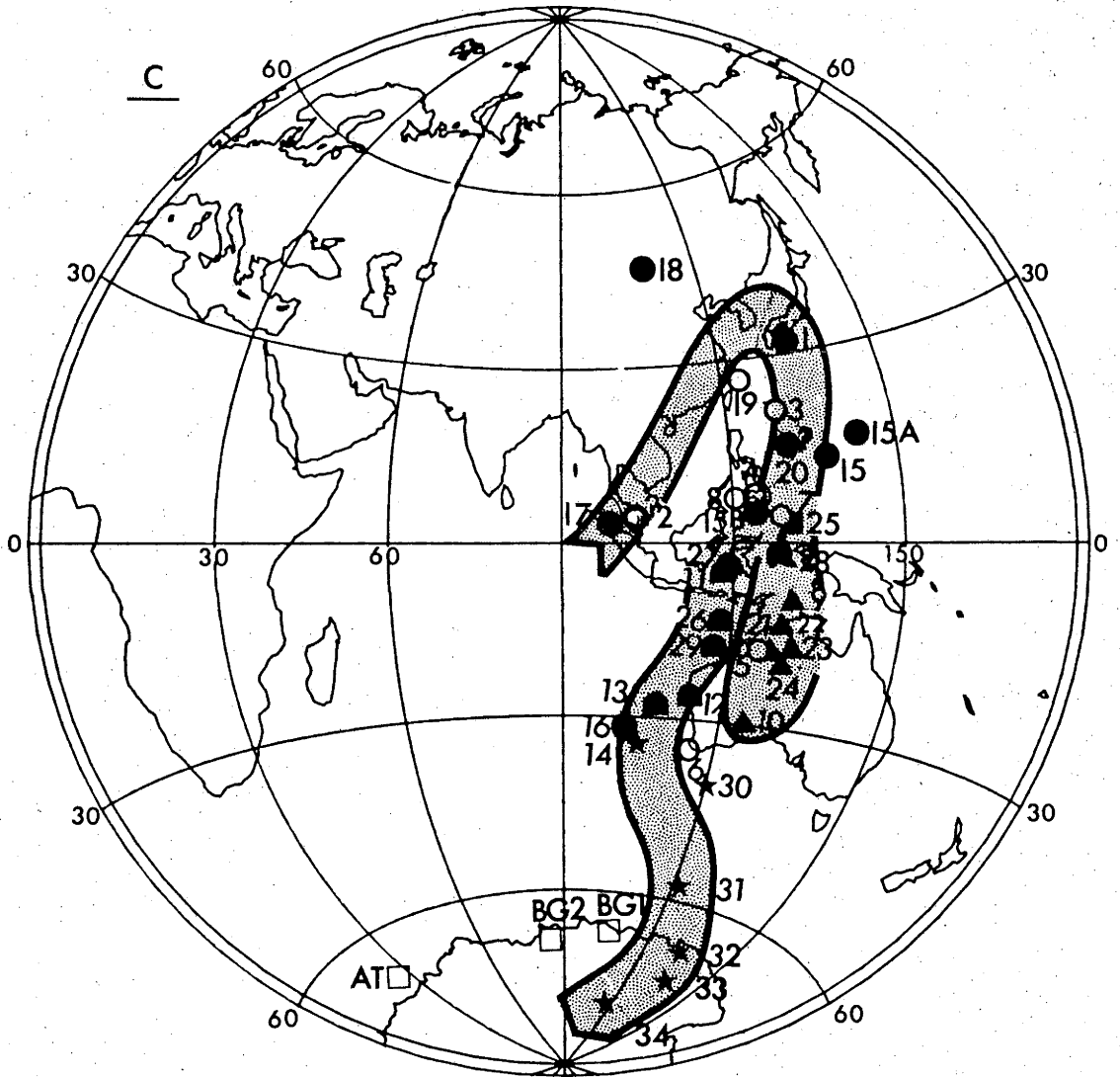
Figure 1.2c

2,5,6, Poles 3,4,7,8). This hard secondary overprint was related to the Deccan Trap magmatism (Klootwijk, 1974, 1975). An example of this predominant Deccan Trap overprinting is shown in Fig. 1.3. The Permo-Triassic red beds from the Wardha Valley (Klootwijk, 1975) clearly show partial and sometimes complete remagnetization during Deccan Trap time.

Secondary components due to this remagnetization were observed not only in Gondwana red beds but also in other red beds at distances up to several hundred kilometers away from the present outcrop of the Deccan Traps, e.g. in late Proterozoic-early Palaeozoic red beds of the Upper Vindhyan System (Klootwijk, 1973: McElhinny et al., 1978).

Several tentative explanations for the acquisition of this remagnetization in Deccan Trap times have been given.

1. Regional heating associated with the Deccan Trap magmatism at low to moderate temperatures and over a prolonged period, may have induced a Viscous Partial Thermoremanence, VPTRM (Chamalaun, 1964: Irving and Opdyke, 1965: Briden, 1965: Pullaiah et al., 1975). In addition to this phenomenon, Klootwijk (1975, 1976) suggested a possible thermo-chemical remagnetization, resulting from circulating hydrothermal fluids associated with the Deccan Traps magmatism.

2. Acquisition of a secondary Thermal Remanent Magnetization (TRM) due to direct heating under influence of the Deccan Trap flood basalts. The model studies of Jaeger (1957,1959) on the temperature distribution near to a cooling intrusive sheet show that remagnetization by direct heating must have been of very limited areal extent.

The Dutch group have generally observed in the red beds studied that separation of the hard secondary magnetic overprint from the primary magnetic component (if any) was possible only through elaborate thermal cleaning. Alternating field demagnetization generally proved to
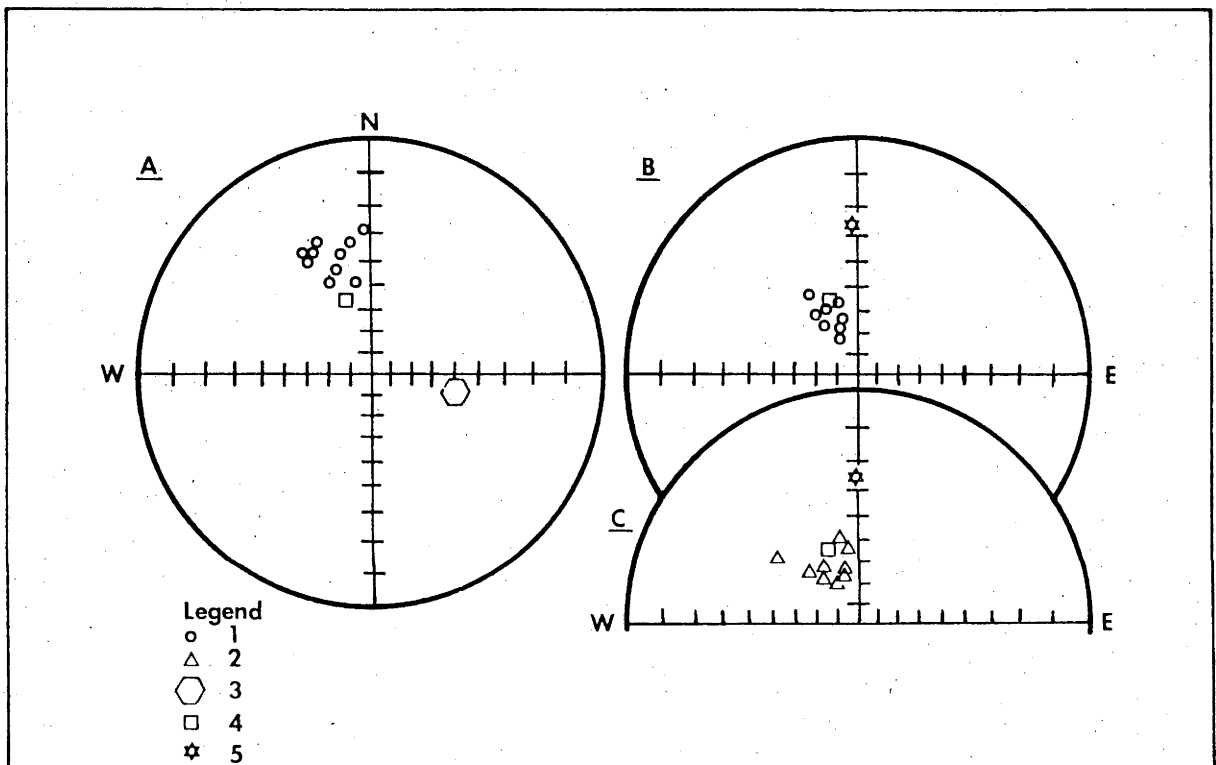
Figure 1.3 Stereographic projection showing directions of eliminated secondary magnetization component associated with Deccan Trap magmatism, from Klootwijk (1979a).

A) Permo-Triassic Kamthi Formation from the Wardha Valley (Klootwijk, 1975) where the rocks were partially remagnetized by the Deccan Traps.
B),C) Permo-Triassic results from the Wardha Valley where the rocks were fully remagnetized by the Deccan Traps.

Legend:
1. Secondary component eliminated by thermal demagnetization.
2. Secondary component eliminated by alternating field demagnetization.
3. Mean direction of primary magnetization component.
4. Upper Deccan Trap direction at the sampling locality extrapolated according to the axial dipole field formulae.
5. Present field direction at the sampling area.

be inadequate to separate individual components of a multicomponent magnetization system. No chemical demagnetization studies have yet been made on these red beds. The method could prove potentially more useful. It is for these reasons that interpretation of earlier obtained results from peninsular Indo-Pakistan seem ambiguous on occasion and it is suspected that secondary Deccan Trap remagnetization components have not been completely eliminated in some of the studies.

1.3 Palaeomagnetic results from DSDP cores

Apart from the Deccan Traps no Tertiary palaeomagnetic data are available from Indo-Pakistan because Tertiary rocks are not very well developed in the peninsular region . The Tertiary is better developed in extrapeninsular Indo-Pakistan but tectonic complications creates diffculties with the interpretation of the results obtained. Attempts have been made to obtain palaeomagnetic results from DSDP cores from the Ninety East Ridge and from the Arabian Sea (Peirce 1976,1978, Klootwijk 1979a). The palaeomagnetic data unfortunately suffer from the absence of declination control. As a result the arithmetic mean of individual inclination values underestimates the true palaeoinclination. Peirce (1976) following Cox (unpublished manuscript) describes an algorithm to correct for this effect and published a list of corrected palaeolatitude determinations. Since the comparison of results is best carried out through the use of pole positions there is a clear need for declnation control. Klootwijk (1979a) simulated declinations for various time intervals at various sites using the relative motion data for the Indian Ocean derived by Powell et al (1978). From these simulated declinations and corrected inclinations for various sites on the Ninety East Ridge and the Arabian Sea, Klootwijk (1979a) calculated

mean pole positions at 10 My. intervals for the Tertiary period (Table 1.1, Fig 1.2). The Tertiary APWP so deduced for Indo-Pakistan appears to be in good agreement with the Australian Tertiary APWP, when transferred to the Australian plate (Klootwijk and Peirce, 1979). Further confirmation of this Tertiary APWP by direct palaeomagnetic observations from peninsular Indo-Pakistan is very desirable, particulary since this APWP is used as a frame of reference for determining rotational movements of allochthonous structural units from extrapeninsular Indo-Pakistan with respect to the Indian Shield.

1.4. Palaeomagnetic results from Extra-peninsular Indo-Pakistan

The Phanerozoic System is not very well developed in peninsular Indo-Pakistan, Palaeozoic and Tertiary rocks being particularly poorly preserved in surface outcrop. To obtain a better palaeomagnetic coverage of the Phanerozoic, palaeomagnetic studies were started in the extrapeninsular region of Indo-Pakistan (Klootwijk, 1979b, in P.S. Saklani). Marine sedimentary successions in this region cover the Phanerozoic more completely and it can be expected that any effect of Deccan Trap remagnetization would be significantly reduced. On the other hand the Alpine-Himalayan belt was highly tectonized during and after the the early Tertiary collision between Indo-Pakistan and the Eurasian plate. Consequently, the magnetization of the rocks has proved to be generally complex. Palaeomagnetic studies carried out in the northern mountain belts of Indo-Pakistan (Fig.1.4a, Table 1.1) showed the consistent presence of an early Tertiary or younger magnetic overprint. Primary magnetic components could be determined only from part of the formations studied. A further complication is that both the secondary and primary directions may have to be corrected for local

Table 1.1 Summary of late Palaeozoic–early Tertiary Palaeomagnetic Results from Peninsular and Extra-Peninsular Indo-Pakistan

Locality No. (Fig.1.1)	Rock Unit	Age	Cleaning Technique	S.Pole Lat.(°)	Long.(°)	d_m[*1] (°)	d_p[*1] (°)	E_{95}[*2] (°)	Pole Position (Fig.1.2)	Reference
1	Talchir Beds	Permo-Carboniferous	300 mT	31.6N	134.3E	4.5	3.4	-	1	Wensink & Klootwyk (1968)
2	Taroba Beds	L.Permian-E.Triassic	280 mT 700°C	4.1N	102.8E	3.3	3.0	-	2	Wensink (1968)
2	Kamthi Wardha Valley	L.Permian-E.Triassic	280 mT 700°C	21.0N	129.7E	3.7	2.9	-	3	Wensink (1968.)
2	Mangli Beds	L.Permian-E.Triassic	280 mT 700°C	7.2N	124.3E	7.2	5.7	-	4	Wensink (1968)
3	Kamthi Godavari Valley	L.Permian-E.Triassic	60 mT	18.1S	126.6E	2.7	1.8	-	5	Verma & Bhalla (1968)
4	Himgir Beds	L.Permian-E.Triassic	80 mT	35.1S	115.1E	7.5	4.7	-	6	Athvale et al. (1970)
5	Kamthi Wardha Valley	L.Permian-E.Triassic	300 mT 700°C	4.1N	128.6E	9.6	7.2	-	7	Klootwyk (1975)
6	Panchet Clays	L.Permian-E.Triassic	300 mT 700°C	7.2N	120.3E	10.2	8.7	-	8	Klootwyk (1974)
7	Pachmarhi Beds	L.Triassic	280 mT 700°C	10.0S	130.3E	6.1	4.6	-	9	Wensink (1968)
8	Parsora Beds	L.Triassic	60 mT 550°C	30.1S	125.0E	6.8	4.1	-	10	Bhalla and Verma (1969)
9	Rajmahal Traps (Mean)	100-105 m.y.	100 mT 580°C 200 mT 600°C	6.1S	117.4E	6.0	5.0	-	11	McDougall & McElhinny (1970) Klootwyk (1971)
10	Satyavedu Beds	E.Cretaceous	40 mT 660°C	26.4S	113.2E	5.9	4.3	-	12	Mital et al. (1970)
11	Tirupati Beds	E.Cretaceous	40 mT 650°C	33.4S	109.3E	15.0	10.3	-	13	Pullaiha and Verma (1970)
12	Deccan Traps (Mean)	60-65 m.y.	150 mT 600°C**3	33.0S	101.0E	4.0	2.0	-	14	Klootwyk (1974) and many others

Table 1.1 (continued)

Locality No. (Fig.1.4a)	Rock Unit	Age	Cleaning Technique	S.Pole Lat. (°)	S.Pole Long. (°)	d_m[*1] (°)	d_p[*1] (°)	E_{95}[*2] (°)	Pole Position (Fig.1.2b)	Reference
	Warchha Sandstone (Formerly speckled sandstone)									
13	a) Milawan & Sardhi Gorge	E.Permian	680°C	16.4N	143.4E	7.8	4.8	--	15A	Wensink (1975)
13	b) Nurpur-Kushab Road	E.Permian	680°C	4.6N	124.4E	10.8	7.2	-	15B	Wensink (1975)
	c) a & b combined	E.Permian	680°C	13.0N	137.5E	9.4	6.1	-	15	Wensink (1975)
14	Panjal Traps	Permo-Carboniferous may be up to L.Triassic	30 mT 580°C	32.0S	102.0E	11.2	6.3	-	16	McElhinny et al. (1978)
15	Lower Blaini Diamictite	Permo-Carboniferous	675°C	3.0N	98.5E	-	-	12.0	17	Jain et al (1979]
15	Blaini Limestone	Permo-Carboniferous	675°C	46.5N	109.0E	-	-	7.5	18	Jain et al (1979)1979)
15	Krol A Limestone	Permo-Triassic	675°C	26.5N	123.5E	-	-	15.0	19	Jain et al (1979)1979)
16	Thini Chu Formation	Middle?Permian	675°C	15.6N	130.4E	-	-	7.5	20	Klootwyk & Bingham (1980)
16	Thinigaon Limestone	Carnian	675°C	18.0S	125.5E	-	-	5.5	21	Klootwyk & Bingham (1980)
16	Thinigaon Limestone	Norian	675°C	17.6S	130.9E	-	-	10.0	22	Klootwyk & Bingham (1980)
16	Jomosom Quartzite	Rhaetic	675°C	13.8S	128.8E	-	-	8.0	23	Klootwyk & Bingham (1980)
16	Jomosom Limestone	Lias	675°C	20.7S	128.7E	-	-	6.0	24	Klootwyk & Bingham (1980)
16	Lumachelle Formation	Dogger	675°C	3.8N	126.9E	-	-	8.5	25	Klootwyk & Bingham (1980)
16	Kagbeni Sandstone	Wealden	675°C	13.5S	116.6E	-	-	6.5	26	Klootwyk & Bingham (1980)
16	Dzong Sandstone	L.Aptian	675°C	5.6S	117.6E	-	-	5.0	27	Klootwyk & Bingham (1980)
17	Loralai Limestone E.Baluchistan, Pakistan	M-L Jurassic	210 mT 675°C	1.9S	128.1E	-	-	8.0	28	Klootwyk (1979b)
17	Goru Formation - Parm Limestone E.Baluchistan, Pakistan	Aptian/Albian to Santonian/Coniacian	210 mT 675°C	17.7S	116.8E	-	-	3.0	29	Klootwyk (1979b)

Table 1.1 (continued)

Locality No. (Fig.1.4a)	Rock Unit	Age	S.Pole Lat.(°)	Long.(°)	d_m [*1] (°)	d_p [*1] (°)	E_{95} [*2] (°)	Pole Position (Fig.1.2b)	Reference
Mean pole positions from DSDP cores from Indian Ocean and Arabian Sea									
		65-55 m.y.	40.7S	119.9E	-	-	10.7	30	Klootwyk (1979a)
		45-55 m.y.	57.7S	121.3E	-	-	9.1	31	Klootwyk (1979a)
		35-45 m.y.	67.5S	132.2E	-	-	12.0	32	Klootwyk (1979a)
		25-35 m.y.	72.5S	135.8E	-	-	3.5	33	Klootwyk (1979a)
		5-22.5 m.y.	78.7S	114.7E	-	-	-	34	Klootwyk (1979a)

[*1] d_m, d_p Semi major and semi minor axes of the polar error ellipse: the ellipse describes a region surrounding an estimated palaeomagnetic pole position within which the true pole lies at the 95% probability level.

[*2] E_{95} Semi angle of the cone whose apex lies at the region and whose axis coincides with the estimated mean pole calculated from a population of poles and within which the true mean pole lies within the 95% probability level.

[*3]   Cleaning technique refers to Klootwyk (1974).
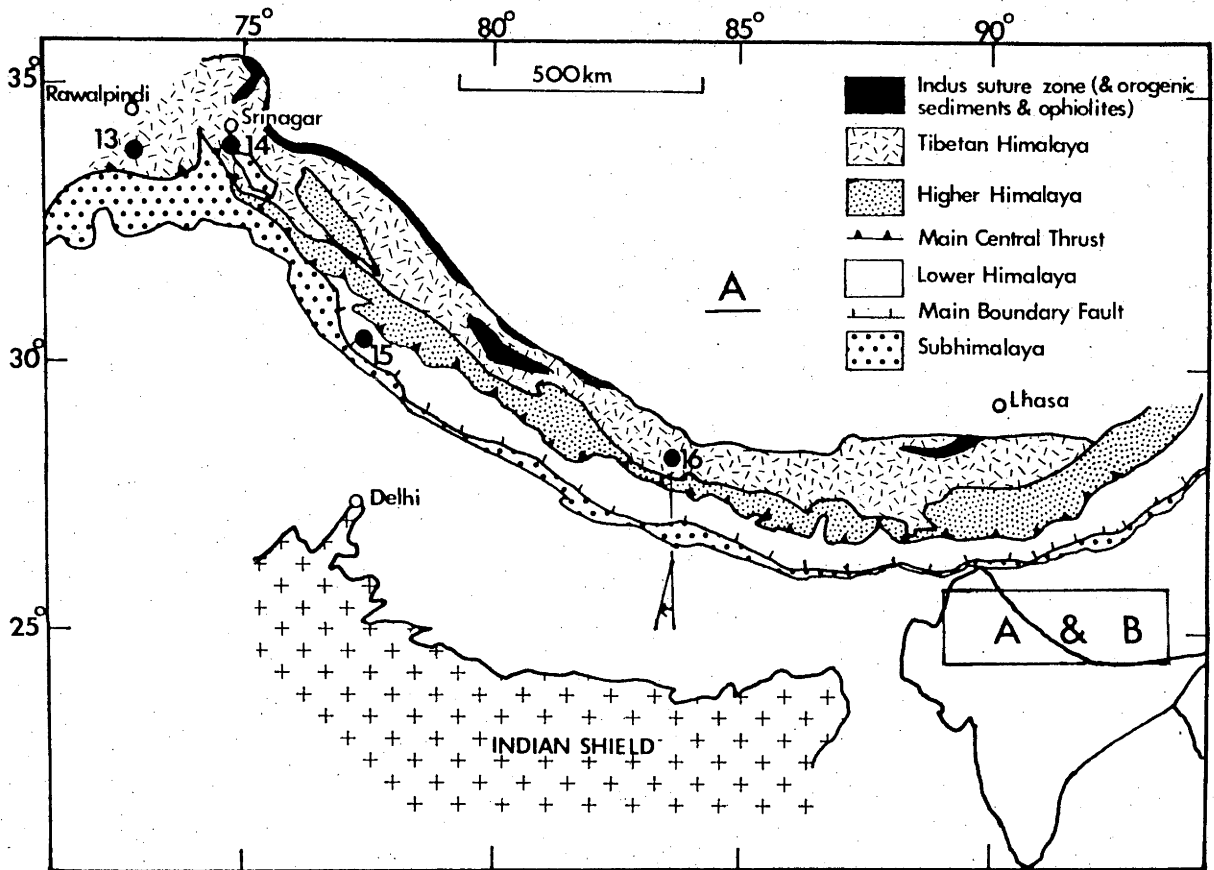
Figure 1.4a. Main structural zones of the Extra-Peninsular Indo-Pakistan
(Himalayan belt), after Gansser 1964, 1977. Showing the positions of the
palaeomagnetic sampled localities in solid circles. The numbers correspond
with results listed in Table 1.1 and shown in Figure 1.2b.

rotations if they are to be used for refining the Indo-Pakistan APWP. To determine such rotations Klootwijk (1979b) has compared the observed directions for extrapeninsular Indo-Pakistan either with the expected directions for peninsular Indo-Pakistan or with the results obtained from the DSDP cores (section 1.3). If no corresponding primary magnetic data were avaliable from peninsular Indo-Pakistan, rotation corrections were assumed to be similar to those deduced from the Tertiary remagnetization components (if any). Rotations so obtained at most of the studied localities are shown in Figs. 1.4a and 1.4b. These local rotations and applied rotational corrections can be summarized as follows :

1. The rotational movement of the allochthonous Salt Range -Potwar Plateau structural unit (Fig. 1.4b, Loc.No.13) has not yet been established (Klootwijk, 1979b). Results from the Early Permian Warchha Sandstones of this structural unit (Fig. 1.2, Pole Nos. 15A, B) are therefore to some extent ambiguous in detailing the Indo-Pakistan APWP.

2. Results from the Permo-Carboniferous Blaini Formation and from the Permo-Triassic Krol Limestones of the Krol Belt (Fig. 1.4b, Loc.No. 15; Fig. 1.2, Pole Nos. 17, 18 and 19) have been tentatively corrected for a 40 degrees clockwise rotation. This rotation was determined using observed early Tertiary secondary directions deduced from the DSDP results.

3. Permian to Early Cretaceous results from the Thakkhola region, Nepal Himalaya (Fig. 1.4a, Loc.No. 16; Fig. 1.2, Pole Nos. 20 to 27) have been corrected for a 15 degrees clockwise rotation with respect to the Indian Shield. This correction results from the comparison of observed primary directions and may be considered as the best documented.

4. Results from the Loralai Range i.e. the Loralai Limestones (M-U

Figure 1.4b. Generalized tectonic map of South Central Asia, taken from Klootwijk (1979b), after Gansser (1964). Map showing the tectonic corrections applied to the palaeomagnetic sampled localities (Fig. 1.4a). Solid circles representing the sampled localities considered for drawing Extrapeninsular Indo-Pakistan APWP. Legend: 1 = Ophiolitics; 2 = Metamorphics in general; 3 = Krol Belt and older sediments in the lower Himalaya; 4 = Palaeozoic-Mesozoic sediments; 5 = Tertiary sediments.
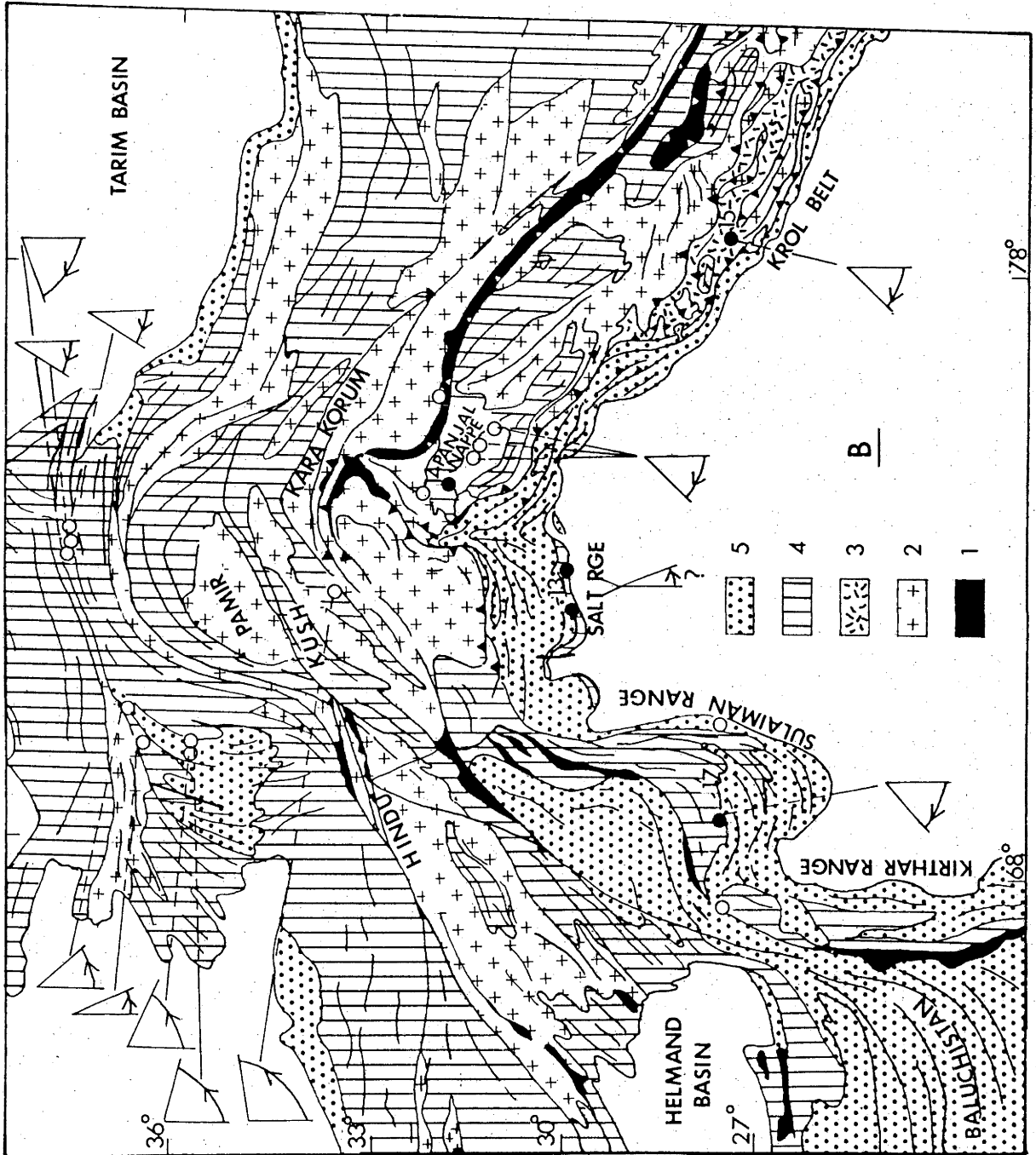
Jurassic) and the Goru Formation-Parh Limestones (Aptian to Coniacian) from northeastern Baluchistan, Pakistan (Fig. 1.4b, Loc. No. 17; Fig. 1.2, Pole Nos. 28 and 29) have been corrected for a 50 degrees clockwise rotation. These pole positions and results from the Kirthar Range (Klootwijk 1979b) further define the Jurassic-Early Cretaceous APWP of Indo-Pakistan.

1.5   A Review of the Indo-Pakistan Apparent Polar Wander Path

The tentative Indo-Pakistan APWP as given by Klootwijk and Bingham (1980), based on results from both the peninsular and extrapeninsular regions, is shown in Fig. 1.2. Poles which possibly represent secondary magnetic directions are also plotted on this path. In the following discussion all results have been subdivided into seven periods, i.e. Siluro-Devonian, Permo-Carboniferous, Permo-Triassic, Late Triassic, Jurassic, Early Cretaceous and Tertiary (Table 1.1).

1   Silurian-Devonian:

A brief discussion of Silurian-Devonian pole positions is presented here as they are relevant to the interpretation of the new results. The latest Precambrian to Middle Cambrian part of the APWP of Indo-Pakistan is reasonably well defined (Klootwijk, 1979a), but the middle Palaeozoic trajectory is very poorly defined. The Silurian-Devonian pole position for the Rudraprayag Volcanics (Athavale et al., 1979, Fig.1.2, Pole no AT, pole. post. 67°S , 25°E , E 95=12°), whose sampled locality is near to locality no 15, falls near to the expected Palaeozoic part of the Indo-Pakistan APWP, when a correction is made for a clockwise rotation of the sampled locality similar to the correction applied for the Krol Belt samples, Locality no 15 (Jain et al., 1979). This Palaeozoic trajectory is based on transferred Devonian pole positions from SE.

Australia (Goleby, 1980, Fig.1.2, Pole no's BG1 ,BG2 ., pole. posts. 67°S, 104°E, E95=28° and 69°S, 84°E, E95=9° respectively).

2   Permo-Carboniferous

   Permo-Carboniferous poles show a considerable scatter (Fig. 1.2). There are only two poles available from the peninsular region. One is from the well dated Talchir beds (Fig. 1.1, Loc. No. 1; Fig. 1.2, Pole No. 2). The other result is from the Taroba beds. The age of these beds is, however, not very well established. They may be Late Permian to Early Triassic or possibly late Precambrian. Other Permo-Carboniferous poles come from the extrapeninsular region. Results from the Warchha Sandstones of the Salt Range, Pakistan (Fig. 1.1 Loc. No. 13, Pole Nos. 15a and 15b) have not been corrected for any local rotation, but results from the Blaini Formation of the Krol Belt (Fig. 1.1 Loc. No. 15, Pole Nos. 17 and 18) have been corrected for a 40 degrees clockwise rotation. A Permo-Carboniferous to possibly Late Triassic pole position obtained from the Pir-Panjal Traps, Kashmir (Loc.No. 14, Pole No. 16) is in very close agreement with the Deccan Traps (60-65 My.) pole position (Pole No. 14). Although the results has a positive fold test , an early Tertiary secondary origin is considered likely (McElhinny et al. 1978).

   3   Permo-Triassic:

      Elaborate thermal demagnetization studies were carried out on the Mangli beds and Kamthi beds from the Wardha Valley and on Panchet clays from the Damodar Valley (Fig. 1.1, Loc. Nos. 2,5 and 6 respectively). Results show good internal agreement (Fig 1.2, Pole Nos. 3,4,7 and 8). In contrast, results obtained from mainly AF demagnetization studies for red beds of the Kamthi Formation and from the Himgir beds (Fig. 1.1,

Loc. Nos. 3 and 4) show a streaking of the pole positions (Fig. 1.2, Pole Nos. 5 and 6) towards the Triassic and Deccan Trap poles. This has been interpreted as the result of incomplete separation of a secondary Deccan Trap component (Klootwijk, 1974). In addition to these poles from the peninsular region, there is a single Permo-Triassic pole available from extrapeninsular Indo-Pakistan i.e. from the Krol-A Limestones of the Krol Belt (Fig. 1.4b, Loc.No. 15: Fig. 1.2, Pole No. 19). This pole position falls far off the main grouping of the pole positions obtained from the peninsular studies. This casts some doubt to the rotation correction applied to the results from this locality. Alternatively uncertainties in the age of the formation may be advanced as a possible explanation.

4   Late Triassic:

  There are only two poles available from peninsular India i.e. from the Pachmarhi beds and from the Parsora beds (Fig. 1.1, Loc.Nos. 7 and 8: Fig. 1.2, Pole Nos. 9 and 10 respectively). Originally, Klootwijk (1976) interpreted these poles as being not completely cleaned and having a Deccan Trap overprint , because of the streaking of pole positions towards the Deccan Trap pole position (Pole No. 14). This interpretation however, has now been superseded (Klootwijk and Bingham, 1980) on the basis of recently obtained Triassic and Jurassic results from the Thinigaon Limestones and the Jomosom Quartzites of the Nepal Himalaya (Fig. 1.4a, Loc.No. 16: Fig. 1.2, Pole Nos. 21,22 and 23). It is now thought that these poles may represent a primary magnetization and may delineate a Triassic-Jurassic loop in the Indo-Pakistan APWP.

5   Jurassic Poles:

  There are no Jurassic poles available as yet from peninsular India.

Several poles (Fig. 1.2, Pole Nos. 24,25 and 28) are available from the extrapeninsular region, namely from the Jomosom Limestones and the Lumachelle Formation from the Nepal Himalayas (Fig. 1.4a, Loc. No. 16) and from the Loralai Limestones from northeastern Baluchistan, Pakistan (Fig. 1.4b, Loc. No. 17). These Jurassic pole positions further delineate the Triassic-Jurassic loop in the Indo-Pakistan APWP.

6   Early Cretaceous

There are three Cretaceous pole positions available from peninsular Indo-Pakistan. A precisely determined pole position (Fig. 1.2, Pole No. 11) from the Rajmahal Traps (100-105 My., McDougall and McElhinny, 1970) and two other pole positions (Fig. 1.2, Pole Nos. 12 and 13) from the Satyavedu Sandstones and Tirupati beds (Fig. 1.1, Loc. Nos. 10 and 11) respectively. The pole positions from the Satyavedu Sandstones and the Tirupati beds falls very close to the early Tertiary Deccan Trap pole position (Fig. 1.2, Pole No. 14), indicating possibly a younger magnetic age than their Early Cretaceous formation age. In addition there are three poles available from the extrapeninsular region namely from the Kagbeni Sandstones (Wealden) and the Dzong Sandstones (late Aptian) from the Nepal Himalaya (Fig. 1.4a, Loc. No. 16: Fig. 1.2, Pole Nos. 26 and 27) and also from the Goru Formation-Parh Limestones (Aptian to Coniacian) from northeastern Baluchistan, Pakistan (Fig. 1.4b, Loc. No. 17: Fig. 1.2, Pole No. 29). These pole positions when corrected for best documented local rotations (Klootwijk, 1979b), are in agreement with poles from peninsular Indo-Pakistan.

7   Tertiary:

Precisely determined pole positions are available from the Deccan Traps (60-65 My.) of west-central India (Fig. 1.2, Mean Pole Pos. 14).

The Tertiary APWP is based, however, mainly on simulated pole positions obtained from DSDP core results from the Ninety East Ridge and from the Arabian Sea.

Summary

In summary, it should be noted from the above discussion that the Indo-Pakistan APWP possibly suffers from two major deficiencies.

A. Biased results due to incompletely eliminated Deccan Trap remagnetization components in the peninsular results.

B. Uncertainty in the rotational corrections applied to results from the extrapeninsular region.

For these reasons, it is very necessary to update the present tentative Indo-Pakistan APWP as follows :

1. The shape of the Permo-Carboniferous trajectory of the Indo-Pakistan APWP.

2. The suspected secondary nature of some of the Permo-Triassic poles.

3. The reality and possible shape of the Triassic-Jurassic loop in the Indo-Pakistan APWP, which may reflect the opening of the Neotethys at Gondwanaland's northern rim (Stoneley, 1972: Stocklin, 1977: Bordet, 1978: Sengor, 1979).

Clearly the Indo-Pakistan APWP has to be established first as a reliable frame before it can be used to establish whether parts of present day Asia once formed part of Gondwanaland.

For this purpose, a palaeomagnetic study of the more basal part of the Gondwana System (Permo-Carboniferous to Late Triassic) of peninsular India was considered to be of great importance. An extensive sampling expedition was carried out through north-eastern India in regions far away from the present exposures of Deccan Traps (along the Koel-Damodar

Valley and the Son Valley, Figure 1.1) by Dr. C. Klootwijk and myself,

from September to December, 1976, in collaboration with the Geological

Survey of India. Geologists of the Geological Survey of India guided us

in the field around favourable sampling localities and provided detailed

information on the successions sampled.

Chapter 2

GEOLOGY OF THE SAMPLED REGIONS

2.1   Introduction

Sampling for the present study was carried out in five major coal fields in north-eastern India, namely the Hutar and the Auranga coalfields in the Koel Valley, the Raniganj and the North Karanpura coalfields in the Damodar Valley and the Johilla coalfield in the Son Valley (Fig. 2.1). The ages of the samples collected range from Permo-Carboniferous to Late Triassic and cover a wide range of lithologies such as red clays, shales, siltstones and red sandstones.

The geology of the sampled coalfields in the Koel -Damodar Valley and the Son Valley is summarised below with particular reference to the stratigraphy and structure of the sampled localities.

2.2   Summary Geology of the Peninsular Gondwana Basins

The Gondwana System in the various Gondwana basins of peninsular India can be subdivided into three divisions based on floral evidence (Sastry et al., 1977). The Lower Permian period is characterised by the Glossopteris flora, the Middle Triassic period is characterised by the Lepidopteris-Dicroidium flora and the Jurassic-Early Cretaceous period is characterised by the Ptilophylum flora (Table 2.1). The depositional history of the Gondwana System started in the Permo-Carboniferous and lasted till the Early Cretaceous. Sedimentation was predominantly of continental type, with marine incursions during the Permian, as seen in the Umaria, Manandragarh (Ghosh, 1954) and the Daltonganj coalfield (Dutt, 1965, Fig. 2.1, No. 6). Also marine deposits of Early Cretaceous age occur along the east coast (Fig. 2.1). The

Figure 2.1   Geological setting of sampled coalfields (redrawn from Sastry et al., 1977). Sampled coalfields are designated by solid circles.   1 = Raniganj Coalfield; 2 = N.Karanpura Coalfield; 3 = Auranga Coalfield; 4 = Hutar Coalfield; 5 = Jharia (unsampled); 6 = Daltonganj (unsampled); Tiki and Parsora are two localities shown, sampled in Johilla Coalfield.
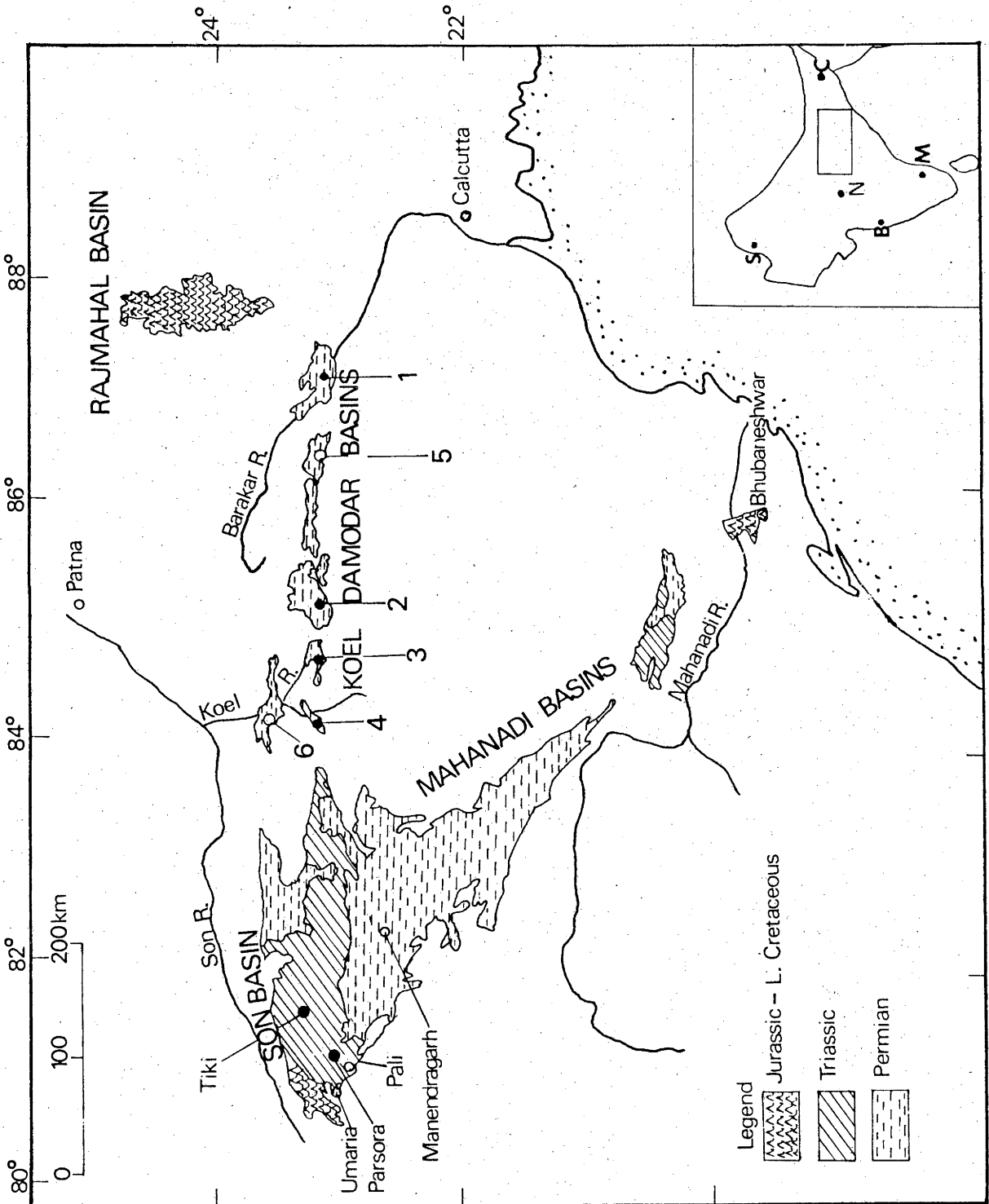
continental type deposits are not easily correlated between far apart basins, and this has led to the establishment of different local formation names and different type localities. The Gondwana sediments are preserved in a number of down faulted basins in central India (Satpura Basin) and in eastern India (basins along the Koel-Damodar Valley, the Son-Mahanadi Valley and the Wardha-Godavari Valley) (Fig1.1). Gondwana sedimentation on the Indian Shield was interrupted by a period of volcanic activity, the Rajmahal Traps (100-105 My.) in NE India covering a relatively restricted surface outcrop. These flood basalts are very similar in petrography to the younger Deccan Traps (60-65 My.) which cover a considerable part of western and central India (Fig. 1.1).

2.3 General Stratigraphy of the Sampled Coalfields, NE India

A general lithostratigraphy of the NE India coalfields is shown in Fig. 2.2, Table 2.1. This figure also shows ideal stratigraphic columns for some of the Gondwana formations collected for this study (Table 2.2).

The Gondwana System can be divided lithologically into three distinct assemblages.

a) The glacials at the base, believed to be of Permo-Carboniferous age.

b) A prolonged sequence of continental fluviatile deposits ranging in age from late Sakmarian /Artinskian to Late Jurassic.

c) Paralic to marine deposits of Early Cretaceous age which are confined to the east coast.

A brief description of these lithological assemblages and their age ranges follows below. Samples were collected only from the basal glacials (a), and the continental fluviatile deposits (b).
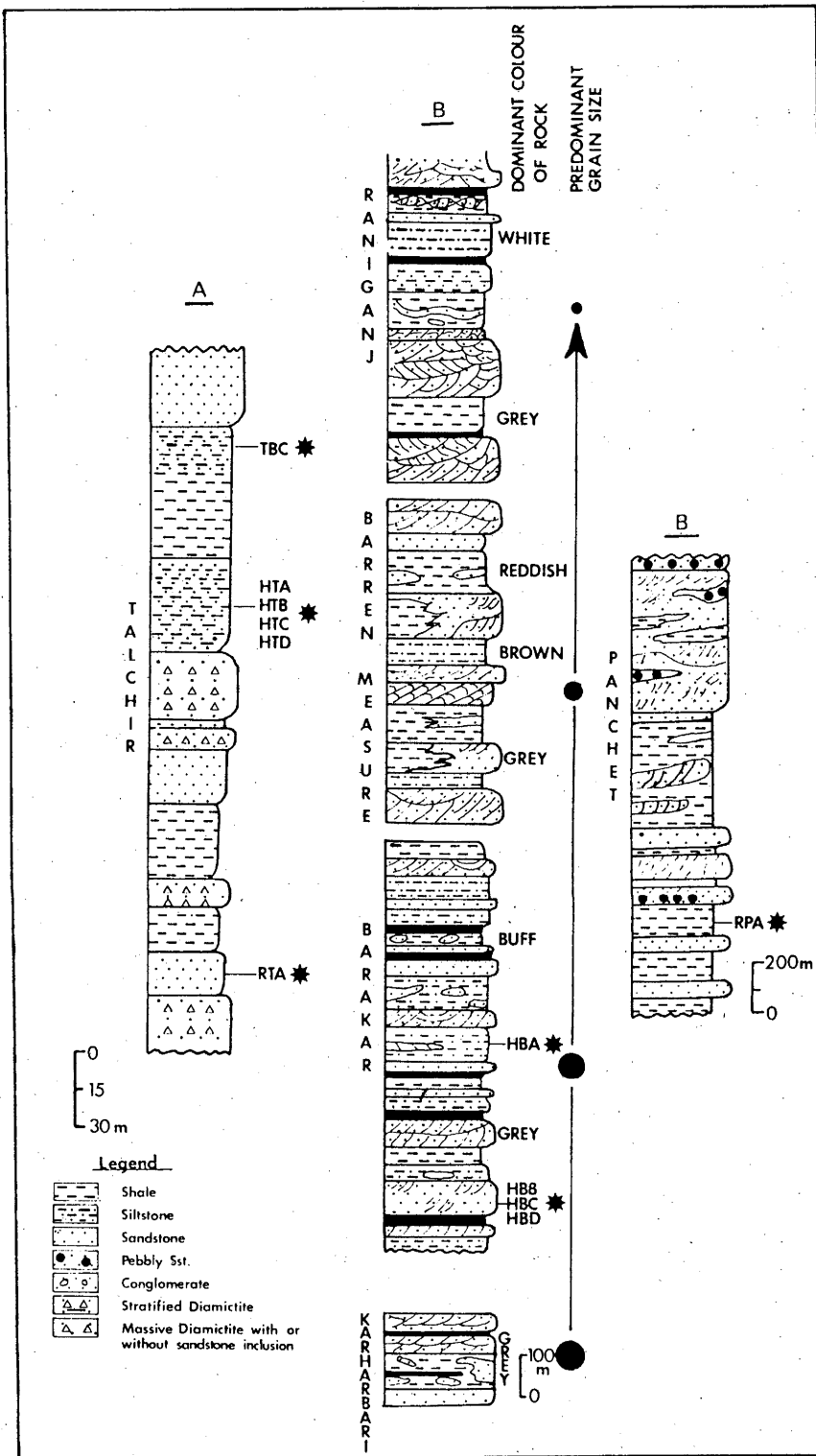
Figure 2.2   General vertical distribution of lithofacie observed in various Gondwana formations of the coalfields, exposed along Koel-Damodar Valley (redrawn from Cashyap, 1977).

A)   Vertical distribution in glacial deposits (Talchir Formation).
B)   Vertical distribution in the continental fluviatile deposits
     (Karharbari Formation to Panchet Formation).

Some Gondwana Formations collected from these coalfields are shown in their stratigraphical order with reference to Table 2.2.

a) Basal Glacials

TALCHIR FORMATION: Glacial deposition is mainly confined to the basal part of the Talchir Formation (Fig. 2.2a). According to Casshyap (1977) three types of tillites occur in general in the glacigene Talchir deposits. In stratigraphic order these are :

1. Massive tillites which are considered to be of continental origin.

2. Tillites with inclusions of sandstone bodies which can be regarded as reworked tillites.

3. Stratified tillites of subaqueous origin.

A complete sequence of these glacial stages has not been observed in all the studied coalfields, but the various tillite types present can be distinguished according to Casshyap's scheme.

The glacials are interbedded with coarse and fine clastic strata, including conglomerates and varve-like laminated siltstones and shales. In the present study the Talchir Formation was sampled in three different coalfields, i.e. the Raniganj coalfield, (RTA); the North Karanpura coalfield,(TBC); both in the Damodar Valley, and the Hutar coafield (HTA-HTD),in the Koel Valley (Fig. 2.1). The figure shows the various stratigraphical successions of the Talchir Formations collected from these coalfields. The lithologies sampled varied from fine to coarse grained sandstones, siltstones and varved shales.

Two marine incursions occurred during deposition of the Talchir beds, as evidenced in the Manendragarh beds and in the Daltonganj coalfield (Fig. 2.1, No. 6). In the Manendragarh beds, a marine intercalation occurs at the base of the Talchir Formation. On faunal evidence an Asselian age has been suggested for these beds (Shah and Sastry, 1973). The marine beds of the Daltonganj coalfield, although faunistically similar to the Manendragarh beds, are located near to the top of the

Table 2.1 A comparison of ideal stratigraphical columns of Gondwana Formations exposed along Koel-Damodar and the Son Valley, NE-India

Age	Area		Damodar Valley	Koel Valley	Son Valley
Cretaceous-Early		Ptilophylum Assemblage Zone			Bansa Beds
Jurassic	Late				
	Middle		Durgapur Beds		
	Early		Hiatus		↑
Triassic	Late	Lepidopteris-Dicroidium Zone	Mahadeva Formation Supra-Panchet	Mahadeva Formation	Parsora Formation ∿∿∿ Unconformity ∿∿∿ ↑ Tiki (Pali) Formation
	Middle		? ∿∿∿∿∿ Unconformity ∿∿∿∿∿		
	Early		Panchet Formation	Panchet Formation	↓
Permian	Late	Glossopteris Zone	Raniganj Formation Barren Measures	Raniganj Formation ?Barren Measures	?
	Early		Barakar Formation Karharbari Formation Talchir Formation	Barakar Formation Karharbari Formation Talchir Formation	Barakar Formation Karharbari Formation ∿∿ disconformity ∿∿ Talchir Formation
Precambrian			∿∿∿∿∿∿∿∿∿∿ Unconformity ∿∿∿∿∿∿∿∿∿∿∿∿		

Table 2.2   A sampling detail of various Gondwana formations collected from the coal fields of NE India.

Formation	Age	Coal Field Site Coordinates	Sa.(spec.) site[1]	Sampled Stratigraphic Interval (mtr.)	Bedding Strike (°)	Dip (°)
PARSORA	Rhaetic	Johilla 23°22'N 81°6'E	27 (40) JPB	0.6	78	9SSE
			32 (70) JPA	3.0	75	18SSE
			13 (30) JPC	0.5	80	9SSE
			14 (29) JPD	1.0	77	9SSE
TIKI	Carnian to early Norian	Johilla 23°25'N 81°02'E	50 (120) TPA	4.0	235	7NW
			20 (45) TPB	0.5	270	10N
MAHADEVA	late Early-Triassic to ? Early Jurassic	Auranga 23°45'N 84°35'E	19 (40) AMA	8.5	110	19SSW
PANCHET	Late Permian to Early Triassic	Raniganj 23°35'N 86°58'E	31 (90) RPA	1.5	100	55SSW
BARAKAR	late Early-Permian	Hutar 23°48'N 84°06'E	32 (80) HBA	1.2	176	16W
			18 (60) HBB	1.0	85	10S
			20 (20) HBC	0.1	180	16W
			13 (30) HBD	0.2	180	16W
TALCHIR	Permo-Carboniferous	N.Karanpura 23°41'N 85°06'E	50 (200) TBC	7.5	280	10N
TALCHIR	Permo-Carboniferous	Hutar 23°49'N 84°06E	13 (30) HTA	2.0	95	12S
			30 (120) HTB	1.8	95	12S
			9 (20) HTC	0.5	220	16WNW
			11 (25) HTD	0.5	240	15NW
TALCHIR	Permo-Carboniferous	Raniganj 23°50'N 86°58'E	28 (110) RTA	7.0	120	14SW

[1] Sa.: Samples; spec.: specimens.

Talchir Formation, and a lower Sakmarian age has been suggested (Sastry and Shah, 1964) The Talchir Formation may thus range in age from Asselian to lower Sakmarian age.

b) Continental Fluviatile Deposits

These deposits of late Sakmarian/Artinskian to Late Jurassic age have been subdivided into different formations in the Koel-Damodar Valley and in the Son Valley. Along the Koel-Damodar Valley, fluviatile deposits are subdivided into the Karharbari Formation, the Barakar Formation, the Barren Measures, the Raniganj Formation, and the Mahadeva Formation. Along the Son Valley, fluviatile deposits are subdivided into the Karharbari Formation, the Barakar Formation, the Tiki (Pali) Formation and the Parsora Formation (Table 2.1).

There is evidence that sedimentation in the Koel-Damodar Valley went on almost uninterrupted from the Karharbari Formation to the Raniganj Formation (Casshyap, 1977). The Karharbari Formation is made up of pebbly arkosic sandy beds. The Barakar Formation was deposited largely in channels of braided-streams (Fig. 2.2b). Meandering river systems replaced the braided-channel pattern, as may be concluded from the fining upward cycles which replaced the noncyclic to poorly cyclic braided-river sequences. These fining upward cycles grade from coarse to medium feldspathic sandstones to fine clastics which are rich in coal in the Barakar Formation, but are devoid of workable coal and rich in red shale in the succeeding Barren Measures (Fig. 2.2b). Coal forming environments prevailed again during deposition of the Raniganj Formation when sedimentation occurred largely on the flood plains of meandering rivers. Similar fluviatile conditions characterise the early Mesozoic beds of the Panchet Formation which are made up of red and brown coarse to medium sandstone and shale alternations. The succeeding assemblage

of the Mahadeva Formation and its probable time equivalents of the Tiki and the Parsora Formations in the Son Valley, are also considered to result from typical flood plain sedimentation on a cratonic basin.

In these fluviatile deposits, samples were collected from the Barakar Formation of the Hutar coalfield, from the Panchet Formation of the Raniganj coalfield, from the Mahadeva Formation of the Auranga coalfield, and from the Tiki and Parsora Formations of the Johilla coalfield. For the Barakar Formation (HBA-HBD) and the Panchet Formation (RPA), sampled horizons are indicated on the idealized stratigraphic column (Fig. 2.2b).

BARAKAR FORMATION: The Talchir Formation-Karharbari Formation has been dated as early Early Permian on the basis of marine fauna. The Karharbari Formation is overlain by the Barakar Formation, generally in a conformably fashion but at a few localities only with an unconformity. A late Early Permian age has been suggested for the Barakar Formation on floral evidence, i.e. Glossopteris and Gangamopteris findings, and on vertebrate evidence (Shah et al. 1971).

PANCHET FORMATION: The Panchet Formation is very rich in fossil assemblages. It has yielded megaflora, mioflora and vertebrates (Lystrosaurus) , together with freshwater invertebrates. These assemblages are quite different from the underlying Raniganj Formation and also from the overlying Mahadeva Formation (Sastry et al., 1977). On these floral and faunal evidences, an Early Triassic age has been assigned to the Panchet Formation.

MAHADEVA FORMATION: In the Koel-Damodar Valley, the Mahadeva Formation unconformably overlies the Panchet Formation. On the basis of the lithology and miospore content, the Mahadeva Formation of the

Raniganj coalfield has been tentatively correlated with the Durgapur beds which are Jurassic in age (Table 2.1). The age of the Mahadeva Formation of the Koel-Damodar Valley basins is however, poorly restraint between the late Early Triassic and the Early Jurassic.

TIKI (PALI ?) FORMATION: Profound differences of opinion exist (Lele, 1964; Chatterjee and Ray, 1974) regarding the mutual correlation and age of rocks around Pali and Tiki (Figure 2.1). These outcrops may or may not represent lateral equivalents exposed in different limbs of a large synclinal structure. Plant fossils collected from the Pali area are solely from the basal part of this formation. Much of the upper part of the Pali sequence is missing in the type section due to faulting. This assemblage shows an Early Triassic affinity. In contrast, vertebrate fossils collected from the Tiki area are mainly from the topmost horizon of this formation and indicate a Carnian-early Norian age. The present sampling was restricted to the Tiki area, so the age of the samples collected can be taken as Carnian-early Norian.

PARSORA FORMATION: There is no report of faunal evidence so far from the Parsora Formation but it contains a variety of plant fossils. Plant fossils so far reported (Lele, 1965; Gopal Singh, 1975) are referred to as the Dicroidium assemblage zone, which is a typical Triassic flora. The stratigraphic inter-relationship of the Parsora Formation, the Tiki Formation and the Pali Formation remains controversial, though Dutta and Ghosh (1972) have convincingly suggested on the basis of field relationship and detailed laboratory studies that the Pali Formation and the Tiki Formation represent lateral equivalents exposed on the southern and northern limb respectively of a broad syncline. The Parsora Formation is exposed in the more central part of the syncline, and is regarded as Rhaetic in age.

c) Paralic to Marine Deposits

These represent the youngest Early Cretaceous, Gondwana beds in the Indian Shield region. These deposits have not been reported so far for the coalfields in the Koel-Damodar Valley, but isolated outcrops occur in the other coalfields of the Son-Mahanadi Valley, the Wardha -Godavari Valley and the Satpura basin. These beds were not sampled in the present study and will not be discussed for that reason.

2.4   General structure of the sampled coalfields

In most coalfields, the Gondwana rocks show a gentle dip southwards .Where effected by faults or folds the dip direction and amount of dip varies locally. The coalfields are mainly characterised by numerous faults within and along the basins, where dolerite dykes and lamprophyre dykes may occur. Chatterji and Ghosh (1967) have broadly classified the faults in the Gondwana coal fields into three categories, on their spatial relationship within and between the various basins.

a. Boundary faults,

b. Basin marginal cross faults, and

c. Interbasinal faults.

There is a controversy about the age of these faults , about their influence on the sedimentation pattern and about their relationship with the igneous intrusions. Ghosh and Mitra (1975) suggest that the initial phase of the Talchir sedimentation in the various coalfields was largely restricted to a few erosional depressions, peripheral to the important relief features which existed at that time and which exercised dominant control on the transportation and supply of detritus in the different coalfields. From this initial stage onwards, the various Gondwana coalfields assumed their present shape as a result of progressive subsidence during post-Talchir sedimentation. In contrast, others (e.g.

Ahmad, 1964, 1966; Ahmad and Ahmad, 1977) believe that the Gondwana strata originally formed a sedimentary blanket covering nearly the entire shield area, and were eroded away apart from the down faulted Gondwana fields.

The concept of Ghosh and Mitra (1975) seems less plausible, because the faults are limited in most basins to one flank or part of a flank and many basins are accordingly considered to be half grabens. There is a controversy about the syn- or post- sedimentary activity of these faults. Attempts have been made to establish the age relationship of these faults with the basic and ultrabasic intrusives (dolerite and lamprophyres dykes) present in various fields but it is found that such age relationships vary from field to field. There is no generalized picture, whether faulting predated or postdated the intrusions. Ahmad et al. (1977) have postulated, particularly in reference to the coalfields exposed along the Damodar Valley, that the entire tectonic-igneous activcity is related with the extrusion of the Rajmahal Traps (100-105 My.) and the Deccan Traps (60-65 My.). According to Ahmad et al., the Damodar Valley sequence of events can be established as:

a. Strong faulting in a general EW direction recognized now as the southern boundary faults at about 100-110 My. ago.

b. Faulting in oblique directions.

c. Intrusion of ultrabasic dykes (lamprophyres etc.).

d. Intrusion of dolerite dykes, 65 My. ago.

e. Further movement along some of the existing faults.

In addition to the above mentioned tectonic-igneous activity stages recognised in the Damodar Valley, there is a possibility of an earlier period of faulting and possibly even igneous activity which can be

correlated with epiorogenic movements observed in the Gondwana coalfields exposed along the Koel-Damodar Valley, the Son-Mahanadi Valley, the Wardha-Godavari Valley and the Sutpura basin, Fig. 1.1 (Casshyap, 1977). According to Casshyap, at the onset of the Gondwana sedimentation, the regional palaeoslope and palaeodrainage in peninsular India was dominantly northerly directed. At the termination of the Talchir glaciation, the river system established across the shield area flowed dominantly from a SE to a NW direction. This direction of palaeoslope remained persistent up to the Middle Triassic sedimentation. Subsequently, in Late Triassic and Middle-Late Jurassic times the river drainage and palaeoslope changed to a SW to W direction in the Satpura basin (Figure 1.1) and to a westerly drainage for the Wardha-Godavari Valley. Also to a northerly drainage into the Tethyan shore zone for the other two basins i.e. Koel-Damodar Valley and Son-Mahanadi Valley. During Late Jurassic to Early Cretaceous times, the palaeoslope of the cratonic block between the Godavari Valley and Mahanadi Valley underwent a complete reversal to a SE direction. The above mentioned changes in palaeoslopes in the Gondwana basins during late Triassic to Early Cretaceous times, may reflect in a wider perspective:

a) Initial breakup of Gondwanaland and the formation of the Neotethys during the Permo-Triassic . According to Sengor (1979) the Permo-Triassic Palaeo-Tethys closed between the Late Triassic and Middle Jurassic. This closure was caused by the collision with Eurasia of a Cimmerian continent breaking away from northern Gondwanaland during the Triassic.

b) Break-up of Greater India from Antarctica during the Late Jurassic and Early Cretaceous.

There are various conceptual models for Greater India:

a) In some models, the Tibetan plateau is considered as an integral

part of greater Gondwanaland with a Permian to Jurassic opening to the mantle at the site of the present Indus-Tsangpo suture zone, Figure 1.4a (Crawford, 1974).

b) Powell and Conaghan's (1973) model explains the far thicker than normal sialic crust beneath the Tibetan Plateau by postulating a formerly far greater northern extent of Indian subcontinent i.e. the Greater India of Veevers et al. (1975), now underthrust beneath the Tibetan Plateau and possibly extending as far north as the Kunlun Nan Shan zone.

c) In a more recent study Powell (1979) reduced this estimate considerably. In the more widely accepted class of models however, the Indus-Tsangpo suture zone is seen as the site of initial collision between southern Asia (Tibetan Plateau is seen as an integral part of southern Asia, although island arc accretion might have occurred) and the Indian subcontinent. Only moderate subduction of continental crust took place and southward progradation of fracture zones has occurred (Le Fort, 1975; Gansser, 1977). The Indus-Tsangpo suture zone became choked off after initial collision (pre-middle Eocene) with a subsequently renewed convergence during the main Himalayan orogenic phase (Neogene) at the site of the Main Central Thrust zone (Fig. 1.4a, MCT). From late Miocene time onwards subduction may have shifted to the Main Boundary Fault zone (Fig.1.4a, MBF). Taking into account the underthrusted portion of the Indian plate and crustal shortening within the Himlayan zone, the proposed northern extent of Greater India fits within the adapted (Griffiths, 1974; Norton and Molnar, 1977) Smith and Hallam reconstruction (1970) and with facies constraints from the western Australia continental margin (Veevers and Cotterill 1978, Klootwijk and Bingham 1980).

To summarize the general tectonic-igneous activity stages in the

Gondwana basins, it can be said that possibly the main faulting and folding of Gondwana strata took place during the Triassic-Jurassic, during the Early Cretaceous and during the early Tertiary. The wide spread early Tertiary Deccan Trap activity has been related to doleritic and lamprophyric intrusions in different coalfields. The lamprophyre dykes possibly may be related to the Early Cretaceous extrusion of the Rajmahal Traps. No igneous activity has been reported so far for the Triassic-Jurassic.

2.5 Local Geology of the Sampled Coalfields

A broad stratigraphical subdivision of the sampled coalfields (Hutar, Auranga, Raniganj, N-Karanpura and Johilla) is given in Table 2.1 and their localities are shown in Fig. 2.1. The main geological features of these coalfields are summarised below.

2.51 Hutar Coalfield

This coalfield is elongated in a NE-SW direction and covers about 200 square kilometers (Figure 2.3). The surface outcrop of the Talchir Formation is about 20 square kilometers. Surface outcrop of the Barakar Formation is about 100 square kilometers and the Mahadeva Formation exposed in the western part of the field covers about 30 square kilometers in outcrop. Faulting in this coalfield is post-depositional as all the formations have been affected by the faults (Rizvi, 1972). According to Rizvi, two phases of faulting occurred in this field as the faults show displacement amongst themselves, but the dating of these faults is uncertain. Two dolerite dykes (probably early Tertiary in age) have been mapped. One dyke passes near the Barwadih area (Fig.2.1, approx. 1 km north of the sampled Talchir locality) and the other NE of Tiharo (Fig. 2.3). The dolerite dyke of Tiharo has been found to be

Figure 2.3 Geological map of Hutar Coalfield, along Koel Valley (redrawn from Rizvi, 1972). Sampling localities are shown with solid circles. See Table 2.2.

displaced by a fault, thus the dolerite activity predates the faulting. Two formations, the Talchir and the Barakar, were sampled from this coalfield.

1. TALCHIR FORMATION: An extensive Talchir section is exposed in the Deori Nala directly west of Barwadih Village (Fig. 2.3). Samples were taken in this section at four sites (HTA-HTD, Table 2.2), stratigraphically HTA site is the youngest and HTD the oldest. From site HTA, 13 samples were collected over a 2 meter thick section of medium to coarse grained sandstones, probably representing a tillite outwash. At site HTB, 30 samples were collected from an almost 1.8 meter thick varved clay section.

Sites HTC and HTD were sampled at opposite limbs of a small undulated structure, which may represent part of an olistostrom. For both of these sites, sampling was carried out in a section of greenish sandstones about 1 meter thick. A total of 20 samples was collected. The dip of the beds at sites HTA and HTB was approximately 12 degrees S, whereas at sites HTC and HTD the dip was approximately 15 degrees WNW.

2. BARAKAR FORMATION: The Barakar Formation was sampled at four sites (HBA-HBD, going stratigraphically from young to old Fig. 2.3, Table 2.2). Sampling at site HBA was performed in a clayey to coarse sandy section approximately 1.2 meter thick. A total of 32 samples was collected. At the other sites, mainly red sandstones were sampled. The sampled section at sites HBB, HBC and HBD was approximately 1.3 meters thick and a total of 41 samples was collected. Beds at sites HBA, HBC, and HBD dip about 16 degrees to the West, whereas the site HBB beds showed a dip of 10 degrees to the south.

2.52 Auranga Coalfield

This coalfield lies about 20 km east of the Hutar coalfield and encompasses about 220 square kilometers (Fig. 2.4). Exposures of the Talchir rocks in this field are limited and cover an area of 10 square kilometers only. Rocks of the Barakar Formation are well developed and cover an area of about 210 square kilometers. The rocks of the Raniganj Formation, the Panchet Formation and the Mahadeva Formation occur in isolated patches which may represent sub-basins. Faults in this coalfield represent two different phases. A first phase of faulting possibly affected all the formations of the field and a second phase of faulting resulted in displacements between the faults (Rizvi, 1972). Igneous activity has not been recorded so far in this field.

Only the Mahadeva Formation (AMA) was sampled from this coalfield (Table 2.2). Sampling was carried out in a section of Mahadeva beds which were well exposed in the Jharna Nala, east of Latehar village (Fig. 2.4). Samples were collected from a section about 8.5 meter thick . The lithology varying from medium to coarse grained ferruginous and feldspathic pale-brownish to red sandstones. The ferruginisation of the samples is probably of a secondary origin, as it was confined generally to the top of the current-bedded layers. A total of 19 samples was collected in beds dipping 19 degrees S.

2.53   Raniganj Coalfield

This eastern most field in the Damodar Valley covers an area of about 1550 square kilometers (Fig. 2.5). This coalfield is structurally the most complex and shows two types of igneous activities, namely lamprophyres intrusions and dolerite intrusions. The southern boundary fault is well developed and oblique faults existing within the field have affected almost all the exposed formations . Ahmad et al. (1977) have tentatively dated the sequence of events affecting this basin as
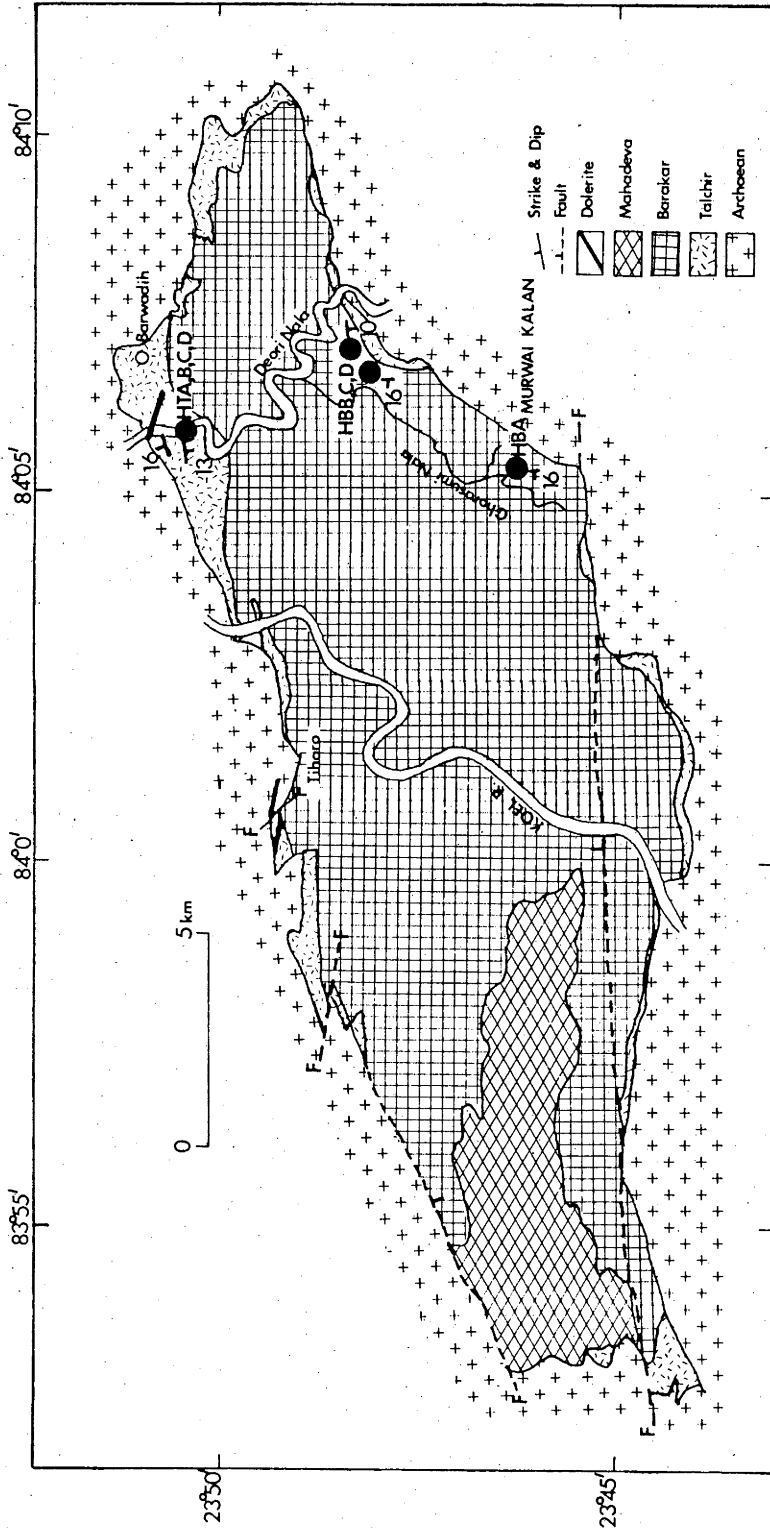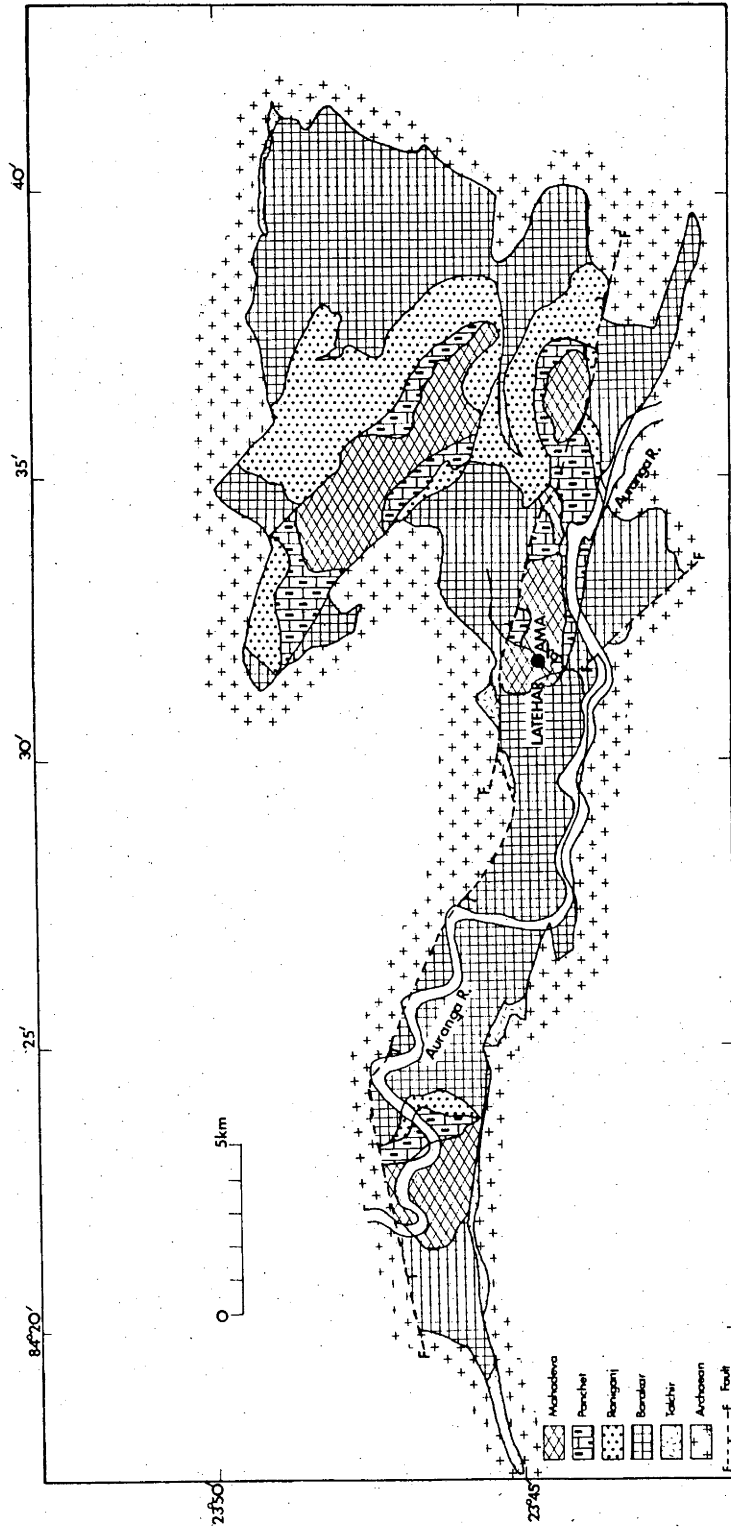
Figure 2.4 Geological map of Auranga Coalfield, along Koel Valley (redrawn from Rizvi, 1972).
Sampled locality is shown with solid circles. See Table 2.2.

follows:

1. Strong faulting in a general EW direction recognised now as the southern boundary faults at about 100-110 My. ago.

2. Faulting in other oblique directions whose age is uncertain.

3. Intrusion of lamprophyre dykes.

4. Intrusion of dolerite dykes at about 65 My. ago.

5. Further movement along some of the existing faults.

Two formations, the Talchir Formation and the Panchet Formation were collected from this coalfield (Table 2.2).

a. Talchir Formation: Sampling was performed in a 7 meter thick section dominated by silty shales and sandstones, exposed along a Nala which is a tributary to the Azay River (Fig. 2.5). A total of 28 samples was collected in beds dipping 14 degrees SW. Around 600 meters south of the sampled locality two intrusions , a SE trending lamprophyre dyke and a dolerite dyke were noticed. They were expected to have a negligible direct heating effect on the sampled rocks.

b. Panchet Formation: The samples were collected SSW of Sonori from a 1.5 m thick red clay zone. A total of 31 samples was collected. The dip of the beds was about 55 degrees SSW.

2.54 North-Karanpura Coalfield

This coalfield is exposed in the extreme western portion of the Damodar Valley (Figure 2.6). It shows a good exposure of all formations of the the more basal part of the Gondwana System (up to the Mahadeva Formation). The structural development of this coal field is regarded as being very similar to the Raniganj coalfield (Section 2.5.3), but with considerably less abundant igneous activity. Only the Talchir Formation, (TBC) was sampled from this field (Table 2.2). Despite the wide areal extent of the Gondwana sediments in this basin, the Talchir
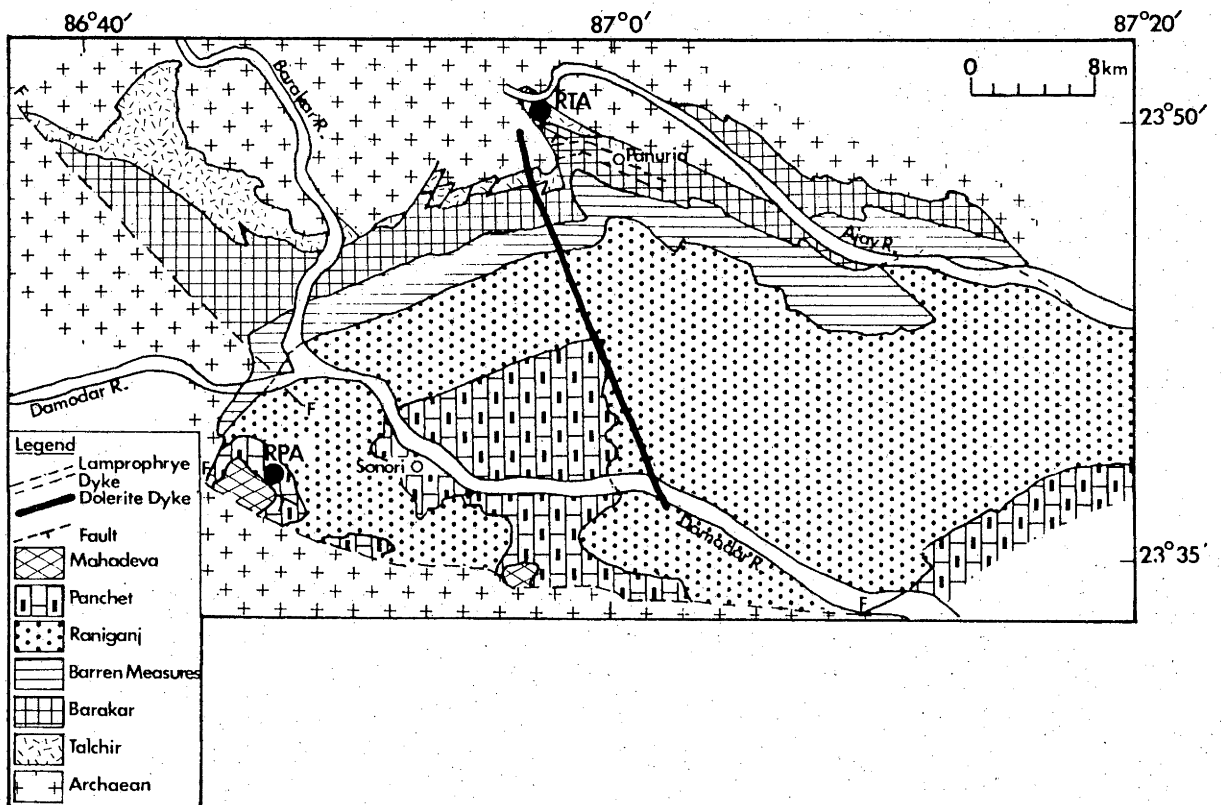
Figure 2.5 Geological map of Raniganj Coalfield, along the Damodar
Valley (after Krishnan, 1968). Sampled localities are shown with solid
circles.

Formation is exposed only in discontinuous patches along the periphery of the basin. Sampling was carried out along a Nala, very near to the Bachra colliary (Fig. 2.6) where an approximately 7.5 meter thick section of varied lithology such as coarse grained sandstones, siltstones and varved clays was sampled. The sampled beds had a northward dip of about 10 degrees.

2.55 Johilla Coalfield (Son Valley)

This coalfield is the nearest to the present Deccan Trap outliers (which are about 8 km away in southern direction). The various Gondwana formations exposed in this field are the Talchir Formation, the Karharbari Formation, the Barakar Formation, the Tiki (Pali ?) Formation, the Parsora Formation and the Bansa Formation (Table 2.1). The Tiki and Parsora Formations were sampled from this coalfield (Table 2.2). A detailed geological map of this field was not available, so the sampled localities are shown on a general geological map of the Son Valley coalfields (Fig. 2.1).

a. Tiki Formation: This formation was sampled at two sites (TPA, TPB) near the Tiki village, the only locality where the formation has been described. At site TPA, sampling was carried out over a 4 meter thick section of medium grained red soft feldspathic sandstones, whereas at site TPB, sampling was made in an approximately 0.5 meter thick section of silicified red clays. In total 70 samples were collected from both of these sites. The sampled beds were dipping NW to N at about 10 degrees.

b. Parsora Formation: This formation was sampled at four sites (JPA-JPD, Table 2.2) about five kilometers NW of Pali, where a railway bridge crosses the Johilla River. Stratigraphically site JPB was the youngest, with sites JPD, JPC and JPA being of increasingly older age.
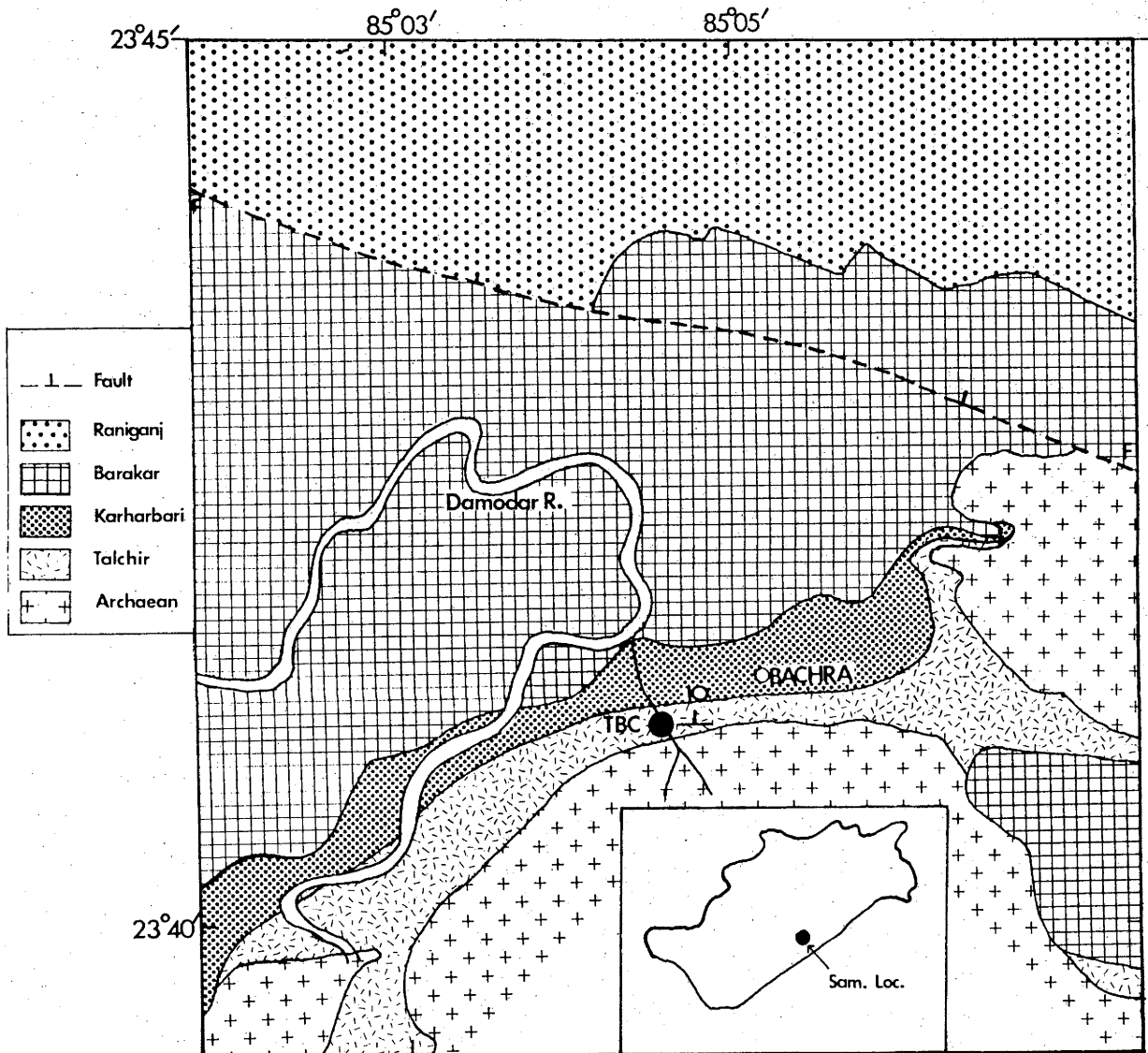
Figure 2.6   A part of the geological map of North-Karanpura Coalfield, along the Damodar Valley. Sampled locality is shown with solid circles.

A 3 meter thick band of reddish to purple silty clays was sampled at site JPA and an 0.6 meter thick band of siliceous to ferruginous sandstones was sampleds at site JPB. At site JPC, a medium to coarse grained sandstone about 0.5 meter thick with occasional occurrences of siliceous ferruginous bands was sampled. At site JPD, a section of red silty clays about 1 meter thick was sampled. A total samples collected from sites JPA-JPD was 90. At site JPA, beds dipped 18 degrees SSE whereas the beds at the other sites dipped gently in a SSE direction at about 9 degrees.

CHAPTER   3

MAGNETIC PROPERTIES OF ROCKS

3.1   Introduction

The samples collected for this study were all sedimentary rocks and consisted almost exclusively of fluvio-glacial varve-like deposits and continental red beds. In this chapter, the rock magnetic properties of sediments will be summarized briefly with respect to their mineralogy, particulary of red beds and types of remanence. Although no specific rock magnetic studies have been carried out, a general overview is thought to be relevant for the results obtained. For a more extensive discussion of palaeomagnetism and rock magnetism, see Nagata (1961), Irving (1964), Stacey and Banerjee (1974) and McElhinny (1973). The main points are summarized below.

1. In sedimentary rocks, haematite is one of the most stable magnetic phase under oxidising conditions (O'Reilly, 1976) and can be of both syn- and post-depositional origin in red beds. Other types of sedimentary rocks such as varved clays may more directly reflect mineralogy related to the source material in the bed rock terrain and can be expected to contain both haematite and magnetite as detrital minerals.

2. The total Natural Remanent Magnetization (NRM) of rocks is commonly a vector sum of several different types of remanent magnetization. The magnetization may be acquired at the time of formation of the rock or at a later stage. In sedimentary rocks possible types of remanence are a.) Depositional Remanent Magnetization, DRM, or Post-Depositional Remanent Magnetization, PDRM, b.) Chemical Remanent Magnetization, CRM, c.) Thermal Remanent Magnetization, TRM and

Viscous Partial Thermal Remanent Magnetization, VPTRM, and d.) Isothermal Remanent Magnetization, IRM.

3.2   Magnetic Mineralogy of Sediments

Sedimentary rocks generally contain magnetic minerals or their alteration products. Such alterations can occur in sedimentary rocks at the time of their formation or later. The most stable mineral in the iron-titanium-oxide system under oxidizing conditions is haematite. It may be of primary origin or may have resulted from syn- or post-depositional alterations (Fig. 3.1). The formation of haematite is discussed below with particular reference to red beds.

3.21   Red Beds

The term red beds covers a variety of sediments with colours ranging from brown to purple. The common characteristic of red beds is their pigmentation due to finely divided haematite or ferric oxyhydroxide. This secondary haematite may form in several ways.

a.) During and directly after deposition by chemical alteration upon consolidation of sediments, through processes like dehydration of iron oxyhydroxide $2FeOOH \rightarrow Fe_2O_3 + H_2O$, as described by Hedley (1968) and Strangway (1968).

b.) Upon burial and particularly in arid and warm humid climatic conditions, haematite may form upon breakdown of iron bearing silicates and clays (Walker, 1976).

Apart from its occurrence as finely divided red pigment, haematite can also be present in red beds as black specularite grains (O'Reilly, 1976). According to O'Reilly these grains appear to have been formed upon in situ oxidation of magnetite particles. Unaltered magnetite is sometimes present but becomes less abundant with increasing age of the
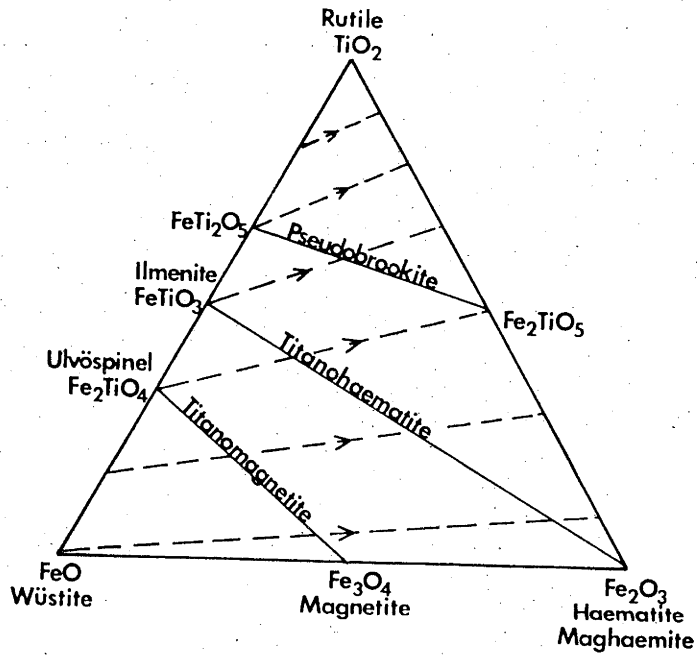
Figure 3.1   Ternary composition diagram for FeO-Fe$_2$O$_3$-TiO$_2$.   The solid lines representing the principal solid solution series and the dashed lines are some lines of constant Fe:Ti ratio along with oxidation may proceed in the direction of the arrows.   From McElhinny (1973).

sediments.

3.3   Types of Remanence

The total magnetization of a rock sample is termed the Natural remanent magnetization (NRM) and is commonly the vector sum of several components. The components can have different origins and can have formed at different times in the rock's history. The acquisition of such components is briefly describrd below.

A. Depositional and Post-Depositional Remanent Magnetization

(DRM and PDRM)

The magnetization of sedimentary rocks is most commonly of this type (Griffiths et al. 1960, Irving and Major 1964). It often results from thermo-remanence already present in the magnetic grains at the time of their deposition. The assumption made for DRM in sedimentary rocks is that magnetic grains can align themselves in the direction of the applied field upon deposition or that such grains can rotate into the field direction when they are in the water filled interstitial holes of a wet sediment. This latter process is known as PDRM.

B. Chemical Remanent Magnetization (CRM)

Chemical remanent magnetization in sedimentary rocks may form in magnetic grains at low temperatures by chemical or phase changes in the presence of the ambient gomagnetic field. Collison (1965) concluded that CRM is the predominant magnetization in sedimentary formations, particularly in red beds. Chemical changes in rocks may occur throughout their history and a CRM may therefore develop. CRM in sedimentary rocks can develop in various ways:

1. Dehydration of iron-oxyhydroxides to haematite.

2. Breakdown of iron-bearing silicate minerals with formation of haematite.

3. Reduction of haematite to magnetite at temperatures around 300 degrees centigrade.

Acquisition of CRM in rocks generally occurs through a nucleation process. Originally the grains are very fine particles with superparamagnetic properties. During growth the spontaneous magnetization lines up with the applied field. When the grains pass through their critical blocking diameters, d_B the relaxation time τ increases very rapidly (Definition of τ is given below). The equilibrium magnetization becomes frozen in and subsequent changes in the field direction as the grains grow further have no effect upon the direction of magnetization.

A magnetic grain **whose** initial magnetic moment is M_o decays exponentially to zero, in the absence of any external field, according to the following equation:

$$M_r = M_o \exp(-t/r) \qquad (1)$$, where M_r = moment left after time t and τ relaxation time of the grain. The initial moment will reduce to one half that is $M_r = M_o/2$ after time t = 0.693τ , which is defined as the half life of the initial remanence.

Furthermore, the relaxation time of the grain is related to the ratio of two energies $E_r = vK$ and $E_t = kT$ and is given by the following equation:

$$t \ \tau = \frac{1}{C} \exp(E_r/E_t) = \frac{1}{C} \exp(\frac{vK}{kT}) \qquad (2)$$, where E_r = internal magnetization energy, v = volume of the grain, K = anisotropy energy of the grain, E_t = thermal fluctuations energy, k = Boltzmann's constant, T = absolute temperature and C = frequency factor equal to

about $10^{10} s^{-1}$.

It is clear from equation 2 that if the volume of the grain v is sufficently small at a given temperature so that $E_r \ll E_t$ (thermal energy overcomes the internal magnetization energy), then the relaxation time τ becomes very small. This results in the magnetic moment of the grain decaying spontaneously according to relation 1 and therefore no remanent magnetization can be acquired.

Now, since the anisotropy energy of the grain K can arise from three factors such as magnetocrystalline anisotropy, shape anisotropy and magnetostrictive anisotropy and is given by $\dfrac{H_c J_s}{2}$. Where H_c and J_s are Bulk coercivity and saturation magnetization respectively. Substituting in equation 2 gives

$$\tau = \frac{1}{C} \exp\left(\frac{v H_c J_s}{2kT}\right) \tag{3}$$

It is evident from this that for a particular composition of the magnetic grains, in absence of any external field, the relaxation time is dependent on two factors, v and T. It becomes small when T is large (that is at higher temperature) and also when v is small (small grain size). For each grain of volume v there is thus a critical blocking temperature T_B at which τ becomes small (say 100 to 1000 sec.) but which might also be below the Curie temperature. Similarly at any given temperature T there is a critical blocking diameter d_B (corresponding to a sphere of volume v) at which τ becomes small.

C. Thermal Remanent Magnetization (TRM) and Viscous Partial Thermal Remanent Magnetization (VPTRM)

Sedimentary rocks may acquire a TRM upon heating and subsequent cooling. Consider an extreme case where sedimentary rocks containing haematite grains are heated up to say, 700 degrees centigrade. The remanence acquired by such rocks during cooling from the Curie

temperature (T_C = 675 degrees centigrade for haematite) to room temperature is called the total TRM. Upon cooling from a high temperature, spontaneous magnetization appears at the Curie temperature T_C and assumes an equilibrium magnetization in the presence of an applied field. Grains of different volume v will each have different blocking temperatures T_B. As the temperature drops below T and goes through the T_B of a specific grain, the relaxation time 'τ' of such a grain increases rapidly. The equilibrium magnetization stabilizes in the grains and subsequent changes in the field direction, undergone at temperatures below T_B, have no effect on changing the direction of magnetization. The TRM is thus acquired over a range of blocking temperatures T_B from the Curie temperature to room temperature (Fig. 3.2). The total TRM can be considered to have been acquired in steps within successive temperature intervals, i.e. (T_C - T_1), (T_1 - T_2) and so on. The part of the total TRM acquired in a particular temperature interval is called a partial thermoremanent magnetization (PTRM). The PTRM acquired in any temperature interval depends only on the field applied during that interval and is not effected by the field applied at subsequent intervals on cooling.

When sedimentary rocks undergo a long period of deep burial and thus elevation to temperatures of say 100 to 200 °C or are heated to such temperatures because of prolonged igneous activity in the nearby region, then they will acquire a viscous PTRM on cooling from this temperature to 0°C say. For example, In the old Red sandstone (Chamalaun and Creer, 1964) the secondary component (Permo-Carboniferous) was found to be dominant and a much smaller, more stable component was detected only after thermal demagnetization to at least 600°C. They ascribed the secondary component to a rapid increase in the relaxation time of the grains as a consequence of fall in
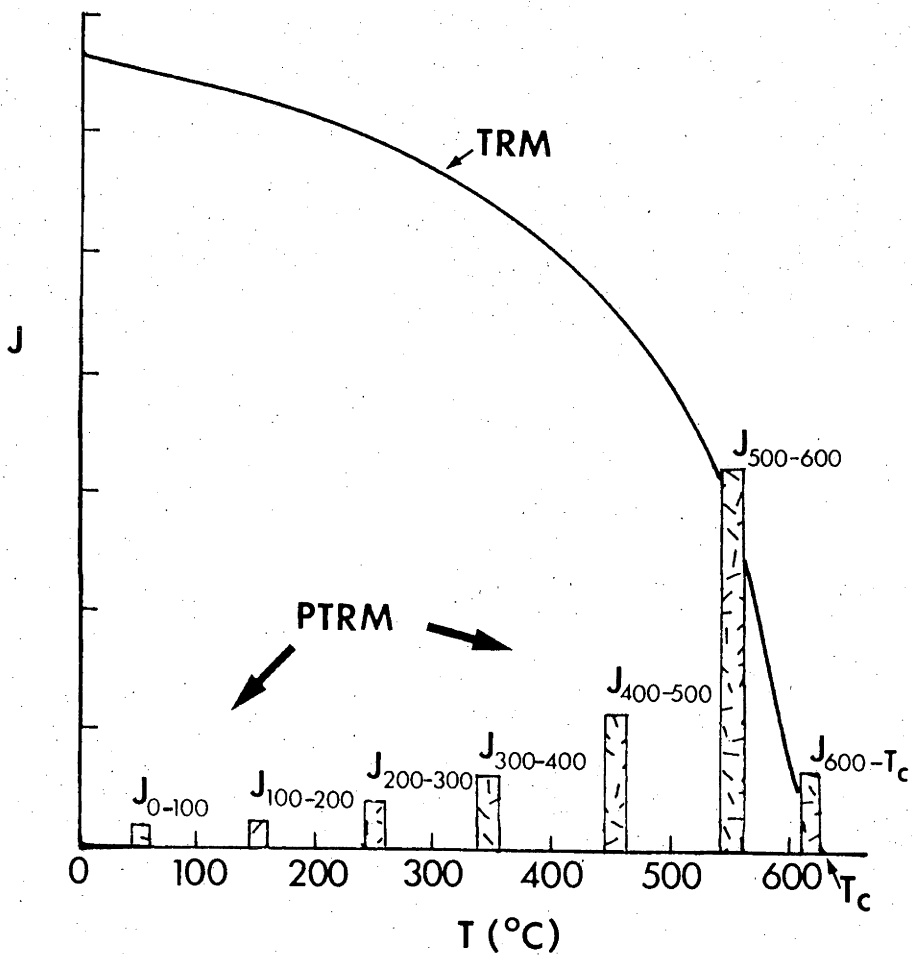
Figure 3.2   The acquisition of TRM.   The PRTMs acquired over successive temperature intervals add up to give the total TRM curve.   From McElhinny (1973).

temperature during uplift and folding. Also, In the Bloomsberg red beds (Irving and Opdyke, 1965) identified a secondary component of Permain age which was of comparable magnitude to a more stable component that is believed to be of the same age, Silurian,as the Bloomsburg Formation itself. They suggested that the secondary magnetization was a moderate temperature viscous remanent magnetization acquired when the beds were buried beneath a thick sedimentary pile or that it could be a chemical effect due to increase in grain size. These examples suggest that a similar conditions -Long burial of rocks and eventually their uplift or their prolonged heating due to Deccan Trap magmatic activity -could have prevailed for the presently studied sedimentary formations, in acquisition of viscous PTRM. To recognise these types of ancient orogenic effects it is necessary to investigate the complete blocking temperature spectrum up to the Curie temperature during thermal demagnetization experiments (section 4.4).

D. Isothermal Remanent Magnetization (IRM)

IRM in sedimentary rocks can be produced by lightning strikes. These often cause rocks containing magnetite grains to acquire an IRM of large intensity, but of soft magnetic characteristics.

CHAPTER 4

SAMPLING, MEASUREMENT AND INTERPRETATION TECHNIQUES

4.1   Introduction

Block- and core- samples were oriented in the field with a magnetic and solar compass using an orientation device similar to that described by Embleton and Edwards, (1973, Fig. 4.1).

Remanence measurements were carried out mainly on a two-axis cryogenic magnetometer (3CT) with a 3.6 cm access opening and a 30 litre liquid helium dewar (Fig. 4.2). Bulk susceptibility measurements were carried out on a Digico susceptibility bridge (Fig. 4.3).

Two demagnetization techniques were used to study the magnetic stability of the rocks.
  A)   Thermal demagnetization (Fig. 4.4); and
  B)   Chemical demagnetization (Fig. 4.5).

Reduction and analysis of the directional data was carried out on a UNIVAC 1108 and more recently on a UNIVAC 1142 computer at the Computer Sciences Centre, Australian National University, Canberra. Programs developed by Klootwijk , Kirschvink (1979) and Morgan (1976) were used for data reduction and analysis.

4.2   Sampling Techniques

As discussed in Chapter 2, geological formations were sampled over stratigraphic intervals at different sites. The stratigraphic thickness sampled at any particular site ranged from a minimum of half a meter to 8.5 m (Table 2.2). The intensity of remanent magnetization of the

Gondwana sediments was in general too low to deflect a magnetic compass, but bearings from both the sun and magnetic compasses were taken as an extra check. The samples were oriented and collected in three ways according to field conditions.

A. Block Samples with Flat Surfaces

The strike and dip lines were marked on a suitably flat surface (Fig. 4.1a). The azimuth of the strike direction was measured with both a sun and magnetic compass. The dip was measured with a clinometer.

B. Block Samples with Uneven Surfaces

Such block samples were oriented using a sun compass device mounted on an isosoles tripod (Fig. 4.1b) and a magnetic compass. The lower plate of the sun compass mounted immediately on the legs of the tripod creates an artificial plane, whereas the upper plate is hinged to the lower along the strike direction. For the required orientation plane the position of the legs is adjusted until the upper surface is horizontal. In this position, the azimuth of the strike line is measured both with a sun and a magnetic compass. The dip is measured as the angle between the horizontal and the dipping plane.

C. Core Samples

Core samples were oriented with an apparatus similar to that used for block samples with uneven surfaces, but now mounted on a tube, which is inserted and oriented in the bore hole (Fig. 4.1c). A fiducial mark is made on the core through a slit 90 degrees counterclockwise from the dip direction, this mark indicates the strike direction. The strike and dip of the orientation plane are measured in a manner similar to that described for block samples with uneven surfaces.

In the laboratory, the block samples were cored perpendicular to the

Figure 4.1a   Orientation of block sample with flat surface, showing
the sun compass reading for the azimuth.

Figure 4.1b.   Orientation of block sample with uneven surface.   The
tripod arrangement is shown for the sun compass azimuth and the inclination
of the plane is read from the clinometer scale, shown at the side of
the instrument.

Figure 4.1c.   Orientation of cored sampled. Sun compass azimuth and inclination of the plane is recorded as in Figure 4.1b. The fiducial mark position, i.e. antistrike direction on the core is 90° counter clockwise from the dip direction.

orientation plane marked in the field. At least 4 cores were drilled from each block sample, each generally sliced into 8 specimens of approximately 2.5 cm diameter and 2.2 cm length. Core samples drilled in the field were sliced in general into 3 specimens.

4.3   Measurement Techniques

Remanence measurements were made mainly on a two-axis cryogenic magnetometer (SCT). A practical lower intensity limit for remanence measurements on the cryogenic magnetometer was about 2×10^{-2} m.A/m. The magnetometer was interfaced initially with a Digico mini-computer, and later on a HP 2116B for on line data reduction.

Bulk susceptibility measurements were made with a Digico susceptibility bridge during all steps of a pilot progressive thermal demagnetization series (Section 4.4). Paper tape output obtained from both sets of measurements was further processed at the ANU UNIVAC 1142 computer. A brief discussion of the operation mode of both the above instruments is given below.

A. Cryogenic Magnetometer:

External and sectional views of the SCT cryogenic magnetometer are shown in Figs. 4.2a and 4.2b. The sectional view of the cryogenic magnetometer shows one set of measurement coils only, though the magnetometer used in the present study had two sets of mesurement coils, which could measure two magnetic components of a specimen simultaneously, one horizontal component and the vertical component. The superconducting shield reduces the ambient field to less than 10γ at the position of the measurement coils. When a sample is inserted into the superconducting pick-up coils, a current is induced in the pick up coils due to changes in the magnetic flux linked to the coils. Since

the coils are superconducting, this induced current does not decay with time.The strength of the induced current is then a direct measure of the magnetic moment of the sample along the axis of the pick up coils. The response curve of the non-axial magnetic component vs. distance with respect to the measurement coils is shown in Fig. 4.2b. The analogue signal produced is also shown on a digital voltmeter, which is interfaced to the mini computer for on line data reduction. Directional and intensity information is thus obtained more or less instantaneously. Measurement of the various components and processing of a full measurement series takes about half a minute.

Operation Mode:

Initially the cryogenic magnetometer is to be calibrated for both the horizontal and the vertical component. This is achieved by inserting an artificial sample made of uniaxially magnetized tape into both the direction of the vertical and of the horizontal measurement axis. In this way the sample holder is also aligned with respect to the instrument fixed orientation system. The software allows adjustment of parameters such as volume of the specimens measured, normal and inverse modes with correspondingly measured components as shown in Fig. 4.2c. In a normal measurement series, 4 measurements are obtained for each horizontal component (X and Y) and 8 measurements for the vertical component (Z). The mean resultant magnetic components and directions and intensity of magnetization are punched on paper tape for further processing on the ANU UNIVAC 1142 computer.

B. Bulk Susceptibility Unit:

Magnetic susceptibilities were measured on a Digico bulk susceptibility bridge (Fig. 4.3). It was found difficult to get reproducible results for susceptibilities below 0.2×10^{-6}. The unit

Figure 4.2a. A general view of the cryogenic magnetometer with part of attached electronics.

Figure 4.3   An external view of the Bulk Susceptibility Unit (details in text).
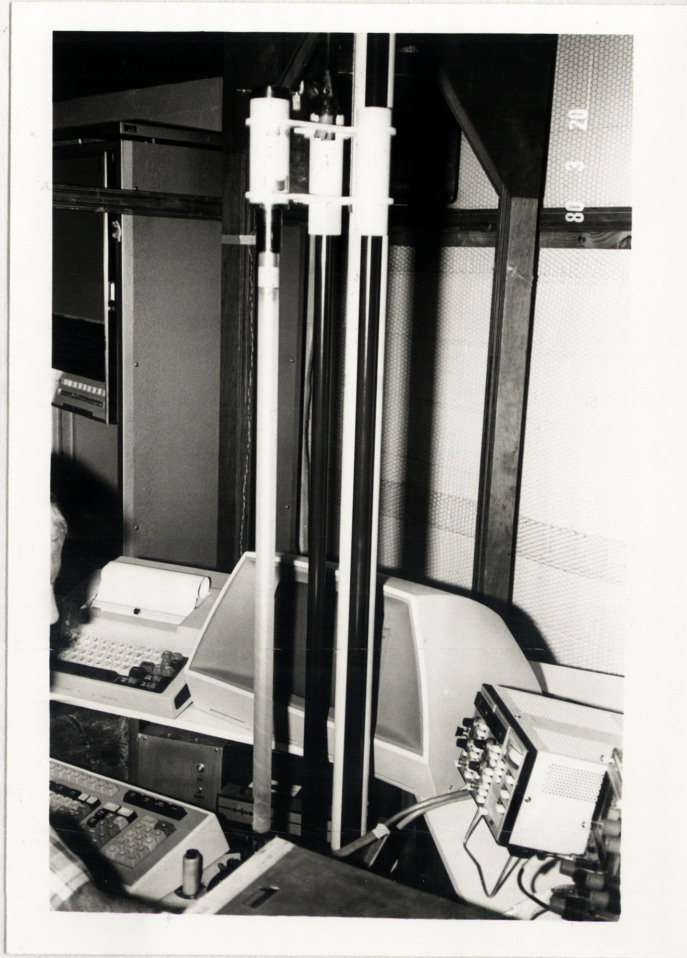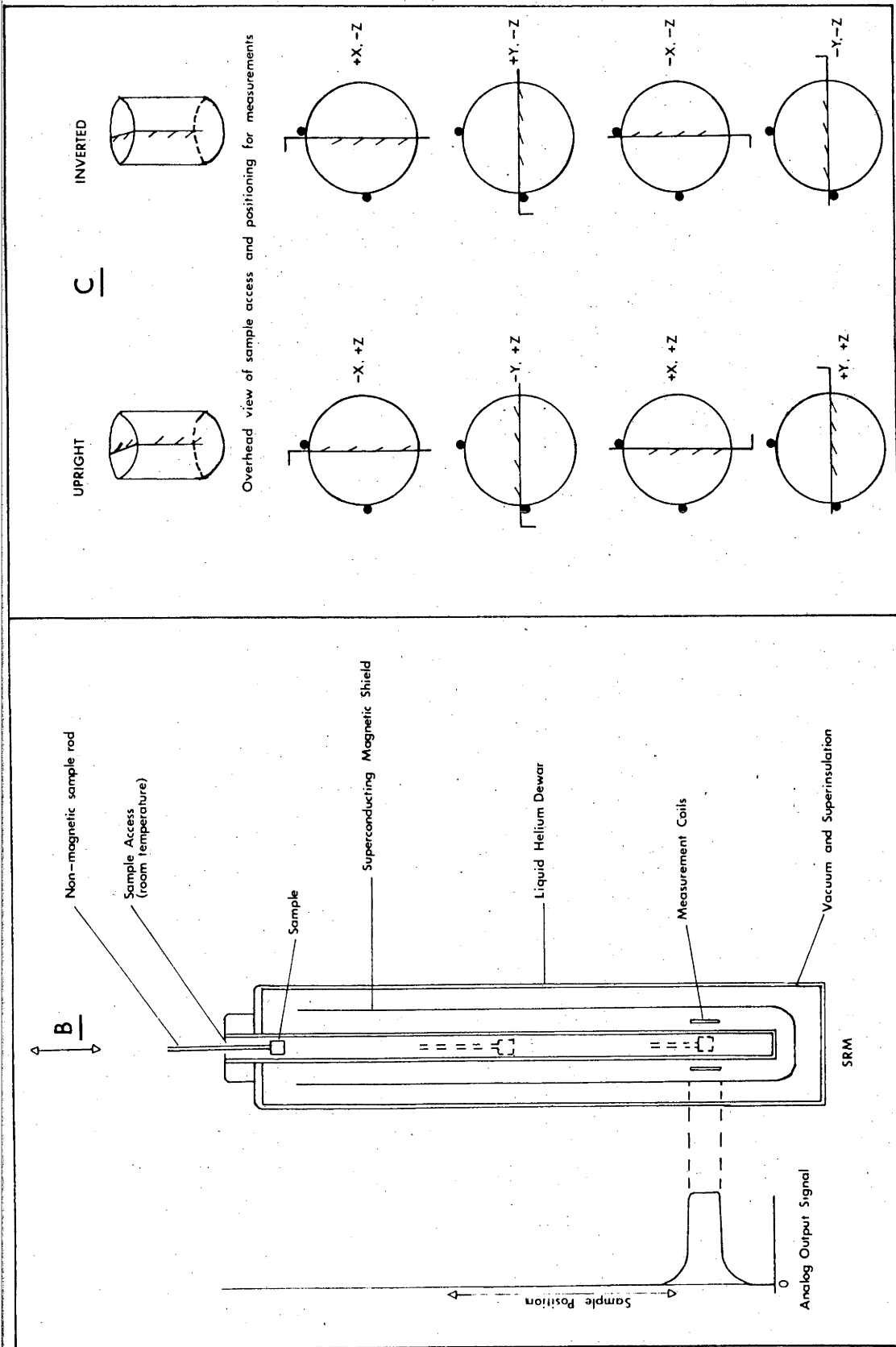
Figure 4.2b. A sectional view of the Cryogenic Magnetometer (one axis system) showing on the left an analogue signal of the nox-axial magnetic component vs. distance with respect to the pick up coils.

Figure 4.2c. Mode of operation under normal and reverse positions of the specimen.

works on an electrical bridge principle and has resistive and inductive balance controls. There are two signal wires, one of which is connected to the electronics unit and the other one is connected to an oscilloscope (Fig. 4.3). Before measurement the bridge is to be brought into equilibrium by making use of resistive and inductive controls. The unit is now to be calibrated with a sample of known susceptibility. After calibration, susceptibility of the specimens can be measured. For this the sample is placed in a wooden box holder and is brought into the coil. The susceptibility change can be visualized on the oscilloscope unit. Digital read out is available in print form or on paper tape for further processing at the ANU Computer Centre.

4.4   Demagnetization Techniques

Sedimentary rocks may possess various secondary magnetizations (Section 3.4) in addition to a primary magnetization (if present). The difference in stability of the various magnetic components forms the basis for their separation upon magnetic cleaning and may be explained according to Neel's single domain theory (Section 3.3).

If anisotropy changes with temperature 'T' are neglected, then the relaxation time τ_1 at temperature T_1 is simply related to the relaxation time 'τ_2' at temperature T_2, as follows

$$T_1 \; \log C \, \tau_1 = T_2 \; \log C \tau_2$$

This means that for a set of uniformly magnetized grains the same effect upon the remanence is obained either by maintaining them at temperature T_1 for sufficient time τ_1 (geological condition) or by raising to a higher temperature T_2 and maintaining them at some shorter time 'τ_2' (laboratory condition). Thermal demagnetization was mainly applied in the course of this study for separation of components with distinctly

different temperature spectra. Chemical demagnetization appeared most useful to study any post-depositional chemical changes in the rocks. Further thermal demagnetization after chemical demagnetization gave no satisfactory results. Earlier to this project, I had some experience with Alternating field demagnetization - statically along three axes according to Utrecht university convention - which was carried out on rocks from foot-hills of the Himalaya region and from the western portion of Indian Shield region. The lithologies of these sections were very similar to the presently studied Gondwana formations. But the demagnetization technique met with little success in separating the various magnetic components. This was suspected because of two reasons.

   1) Noise of the A.F.demagnetization machine at A.N.U. may be much stronger than the remanence intensity of the rocks.

   2) Rock magnetic properties could have been complex.

   Realising these diffculties, this technique was not pursued further for this project.

   The normal operation mode upon thermal and chemical demagnetization is described below. After every demagnetization step, the samples were kept in mu-metal shields to minimize the acquisition of viscous magnetic components.

A.   Thermal Demagnetization:

   Detailed thermal demagnetization experiments (up to 675 degrees centrigrade) were carried out in argon gas (to reduce oxidation during heating) in non-magnetic furnaces described by McElhinny et al. (1971). The furnaces are capable of attaining temperature in excess of 700 degrees centigrade, and are surrounded by a 10 coil feed-back controlled field cancellation system (Fig. 4.4). The ambient magnetic field within the furnace was kept below $\pm$ 5γ during the heating and cooling cycle

Figure 4.4   An external view of the thermal demagnetization apparatus (details in text).

Figure 4.5b. A set up of the chemical apparatus (details in text).
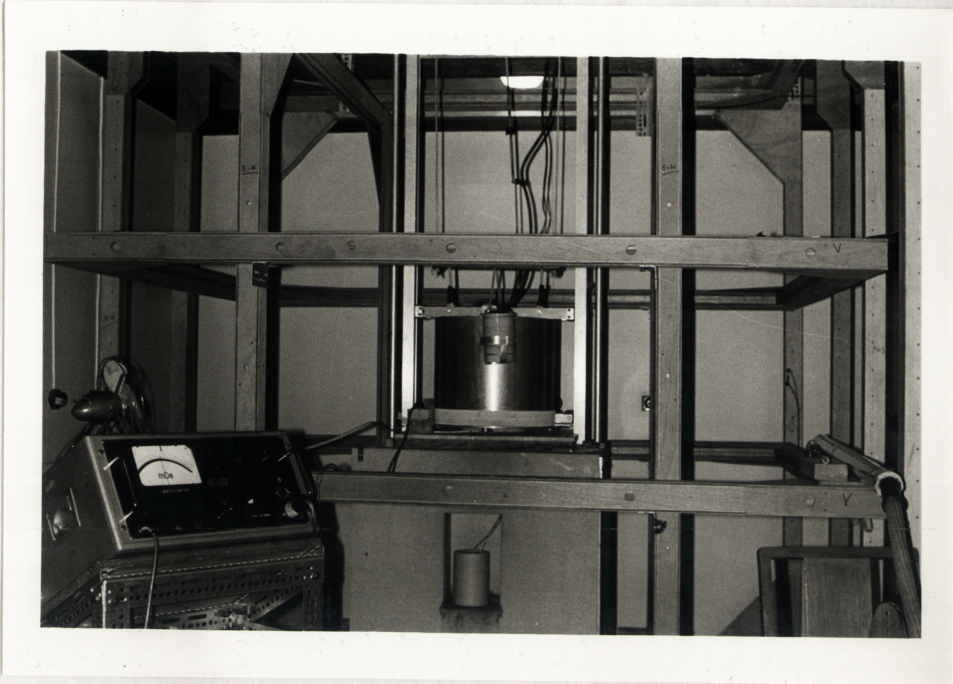
which lasted approximately 2 hours. To reduce the possibility of mutual remagnetization of the specimens in their demagnetizing fields, the specimens were positioned with appropriate spacing and only specimens of roughly the same NRM intensity were heated together. The position of the specimens within the furnace was reversed upon every successive heating cycle to prevent a systematic directional bias (if any) due to a possible non-perfect field cancellation. For pilot progressive thermal demagnetization studies, in general the following peak temperatures were reached at successive steps.

STEPS: 100,200,300,350,400,450,475,500,525,550,575,

600,620,640,660,675 degrees centigrade.

B. Chemical Demagnetization:

Chemical demagnetization was carried out within a Parry coil system made up of 3 pairs of coils, about 1 meter across. The ambient field at the centre of this set could be cancelled to about $\pm$ 100-200γ. Specimens were serrated perpendicular to their axis in the lower and upper part of the sample (Fig.4.5a) to facilitate more rapid penetration with HCl. The specimens were demagnetized in the apparatus shown in Figure 4.5b, the inside beaker containing specimens in acid was covered on top with a second beaker which neutralized the acid fumes through an alkali solution present in a wider outer beaker. Remanence measurements were taken after 1, 2 and 6 days of leaching in a 6N-HCl solution. Further leaching was carried out at 12N-HCl and measurements were taken after the 10th and 14th day. Specimens were checked for removal of their red coating, by cutting them in half. In most of the specimens, the red coating remained present for maximum of 14 days. After every leaching step and before remanence measurements, the specimens were thoroughly rinsed in water for at least half an hour and then heated to a temperature of 150 degrees centigrade and cooled in zero field as
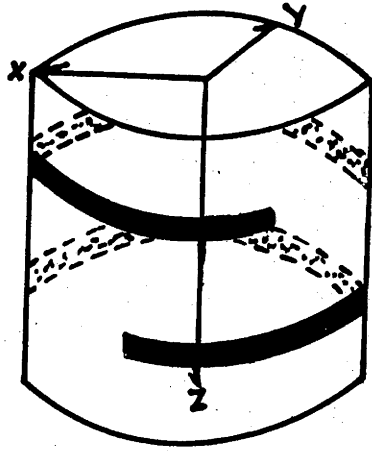
Figure 4.5a. A serrated specimen.
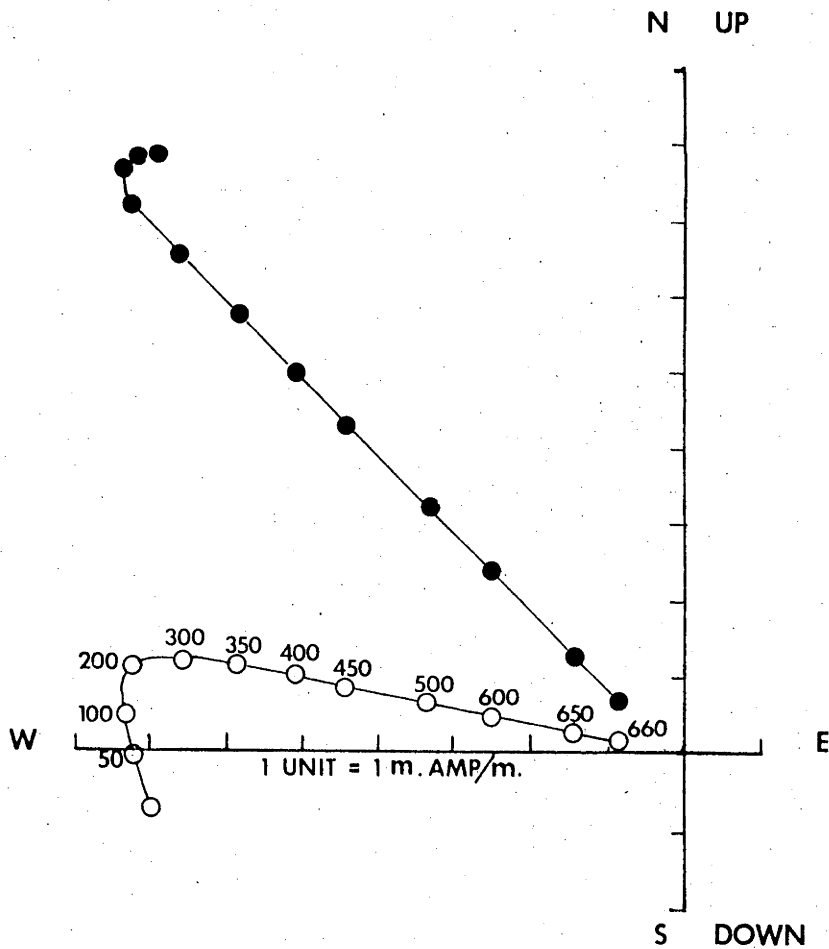
Figure 4.6   Orthogonal projection for a thermally demagnetized
specimen.   Solid circles denote the projections of the end point of
the changing resultant magnetization vector on the horizontal plane,
open circles denote the projections of these end points on the vertical
plane with E-W axis in common.

described in section 4.4a. The specimens were kept in barbecue bags during the heating which prevented HCl vapours from corroding the furnace. This removal of aggressive vapours through heating was thought necessary to prevent corrosion of the cryogenic magnetometer during subsequent measurements.

After removal of the red coating, the specimens were subjected to progressive thermal demagnetization up to a temperature of 675 degrees centigrade. The specimens however behaved erratically and no additional magnetic component could be conclusively identified.

4.5 Interpretation Techniques

The run stream followed for data reduction is described below.

A. Reduction of Sun Compass Data:

Sun compass data were checked against magnetic compass data for possible errors. If sun compass data were not available, the magnetic measurements were corrected for the magnetic deviation at the sampling locality.

B. NRM Directions:

NRM directions were measured on the cryogenic magnetometer, or on a Digico magnetometer at the time when the cryogenic magnetometer was not yet in operation (before january 1978). The directional data obtained in sample coordinates were transferred to field coordinates. The field-corrected directions were plotted on equal area projection. Pilot specimens for progressive thermal demagnetization were selected by inspection of the NRM results on a basis of their directions, grouping and intensities.

C. Orthogonal Projections, Analysis and Determination of

Magnetic Components:

Pilot specimens selected from NRM data were demagnetized thermally or chemically. Remanence measurements and bulk susceptibility measurements were made after every heating step. Susceptibility measurements were not carried out in the case of chemical demagnetization. The variation of remanence direction upon progressive demagnetization was studied on the basis of orthogonal projection figures and also from normalized intensity decay graphs. The bulk susceptibility graphs, however, did not show any substantial changes upon progressive thermal demagnetization other than a slight decrease (10-20%). This indicates that no significant chemical alterations occurred in the specimens during thermal demagnetization . Orthogonal projection figures were studied in separation of various magnetic components and determination of their directions. This method is thought to be superior to conventional analysis techniques such as equal area projection or equal angle projection, which show only changes in direction of the resultant magnetic vector and do not show changes in intensity. Orthogonal projection figures show changes in the end point of the resultant magnetic vector during progressive demagnetization. These vectors are projected on a horizontal and a vertical plane. Both projections are combined into one figure with one horizontal axis in common. For illustration, an example is shown in Fig. 4.6. The resultant magnetization vector moves during thermal demagnetization in an upward direction with an initial slight increase in intensity followed by a later steady decrease towards the origin. Clearly this specimen contains two magnetizations: a soft component with a NE declination and steep positive inclination, and a harder component with a SW declination and a small negative inclination.

Individual magnetic components were interpreted and determined from

these projections on the basis of straight trajectories, based on at least three measurements. The directions of these observed components were determined with a principal component analysis program adapted after Kirschvink (1979).

D. Estimation of Mean Directions:

The field corrected magnetic components, determined from orthogonal plots were grouped on the basis of their characteristic temperature ranges and on the basis of their directions. Mean specimen directions of such components were calculated by giving unit weight to individual specimens. A correction for bedding was made and the pre-, or post-folding origin of the magnetic component under study was determined from changes in the precision parameter 'K' upon application of the fold test (McElhinny, 1964),

E. Palaeomagnetic Poles:

Pole positions were computed from the mean directions, either corrected or not corrected for bedding. Since the mean directions were obtained from the specimens sampled from a stratigraphic section sufficiently extensive to average out palaeo-secular variation (Table 2.2), the poles may be interpreted as palaeomagnetic poles rather than virtual geomagnetic poles. All pole positions presented in this study are given as south poles, following the established convention. These calculated palaeomagnetic poles have been compared with the previously available APWP for Indo-Pakistan (Klootwijk and Bingham 1980).

CHAPTER 5

PALAEOMAGNETIC RESULTS

5.1   Introduction

    Palaeomagnetic results for the   Gondwana Formations studied are
presented in Table 5.2.   Some of the more relevant results are
summarized below.

 A.   Although similar type of lithologies for example silty shales
,sandstones and silicified red clays, were usually found to exhibit
consistent directions sometimes an erratic directional behaviour was
noticed.   Note this behaviour in the Talchir Formation collected from
Raniganj coalfield and the Tiki Formation collected from Johilla
coalfield, in contrast to lithologies of other Formations (Table 5.2).
This may however, be directly linked with the distribution of types of
magnetic grains (SP, SD or MD grains) in the rocks.

 B. Individual magnetic components observed in the specimens at various
sites are interpreted as characteristic components (Zijderveld, 1967).
Information relevant to the different characteristic components observed
upon Thermal and Chemical demagnetizations are listed in Tables 5.1a to
5.1e.   In general, there was a good agreement between these results .
Chemical demagnetization was very successful in separating the various
magnetic components present in the rocks, and of prime importance in
establishing the primary or secondary nature of the NRM in the rocks
(Table 5.1 d).

    5.2   Palaeomagnetic Results of the Talchir Formation

    5.2.1   General

The Talchir Formation was sampled from three different coal fields
i.e. from the Hutar coalfield (sites HTA, HTB, HTC, HTD), from the
Raniganj coalfield (RTA), and from the North-Karanpura coalfield (TBC).
The total number of samples (specimens) collected has been tabulated per
site in Table 2.2. The remanent magnetization of the samples collected
was studied only through thermal demagnetization .Consistent directions
could only be obtained from two sections sampled in the Hutar
coalfield- from a 2 metre thick section of medium to coarse grained
sandstones (HTA) and from a 1.8 metre thick section of varved clays
(HTB). In the North Karanpura coalfield (TBC), results from an upper
section of siltstones and varved clays showed consistent directions,
whereas its lower section made up of medium to coarse grained sandstones
showed random directions. The other two sites of the Hutar coalfield
(HTC and HTD, 8 and 11 samples resp.) which were collected from a band
of greenish sandstones exhibited only random directions. This possibly
may be attributed to the olistostromic nature of these beds (Section
2.51). There was an intrusion of early Tertiary dolerite dykes about 1
km north of the sampled localities (HTA, HTB, HTC, HTD, Figure 2.3), but
no apparent direct heating effect has been noticed in the palaeomagnetic
directions. A random directional behaviour was also noticed in a
section of silty shales and sandstones (26 samples) from the Talchir
Formation of the Raniganj coalfield (RTA). This, however, could be due
to the weak initial intensity (0.05 - 0.1 mA/m) of the samples.
Fold-tests for the characteristic components observed in specimens from
sites (HTA, HTB, TBC) of the Talchir Formation remained inconclusive.
The characteristic components were all of reversed polarity. A detailed
description of the characteristic components observed in the Talchir
Formation at sites HTA, HTB and TBC is given below. Information about
the characteristic components and their Fisherian statistics is

Table 5.1a . Hutar, Talchir and Karanpura Talchir: Mean Directions of characteristic component after thermal demagnetization

Before Structural Correction

Site	Initial NRM Intensity Range mA.m⁻¹	N(n)	N'(n')	D_m (°)	I_m (°)	K	α_{95} (°)	R	S.Pole Position Lat.S (°)	Long.E (°)	d_p (°)	d_m (°)
HTA	1-20	9(9)	20(11)	120.7	60.3	46.3	7.6	8.8	5.0	124.4	8.8	11.6
HTB	1-20	27(26)	40(28)	138.4	57.4	30.7	5.1	26.1	16.9	117.1	5.4	7.4
TBC	0.2-200	13(12)	52(25)	133.6	54.5	28.4	7.9	12.5	16.6	123.2	7.8	11.1

After Structural Correction

Site	Initial NRM Intensity Range mA.m⁻¹	D_m' (°)	I_m' (°)	K'	α_{95} (°)	R	S.Pole Position Lat.S (°)	Long.E (°)	d_p (°)	d_m (°)
HTA	1-20	136.3	53.6	46.3	7.6	8.8	18.8	121.1	7.4	10.6
HTB	1-20	149.4	47.6	30.1	5.1	26.1	29.8	114.9	4.3	6.6
TBC	0.2-200	125.8	55.7	29.5	7.7	12.5	11.2	126.7	7.9	11.1

Table 5.2 Summary of Palaeomagnetic Results

Formation (Coal Field)	Site	Dominant Lithology	Demag.Tech.	Characteristic Comp.Range (General)	Polarity (CH.comp.)	Fold Test
	JPB	Siliceous to ferruginous sandstone	Thermal & Chemical		N	
Parsora (Johilla)	JPA	Reddish to purple silty clays	Thermal & Chemical	230°C - 675°C	N	Positive but insignificant
	JPC	Medium to coarse grained slicified ferruginous sandstones	Thermal & Chemical	2 - 14 days &	N	
	JPD	Red silty clays	Thermal & Chemical		R	
	TPB	Slicified red clays	Thermal	Random	-	-
Tiki (Johilla)	TPA	Medium grained red sandstones	Thermal / Chemical	200°C - 675°C {1 - 6 days / 6 - 14 days	N	NA
Mahadeva (Auranga)	AMA	Coarse to medium grained ferruginous and feldspathic red sandstones	Thermal	220°C - 675°C	N	NA
Panchet (Raniganj)	RPA	Red clays	Thermal	200°C - 675°C	R	NA
Barakar (Hutar)	HBA	Clayey to coarse sandstones	Thermal & Chemical	545°C - 675°C / 6 - 14 days	R	Inconclusive
	HBB	Red sandstones	Thermal / Chemical	200°C -675°C / Unsuccessful	N & R	Inconclusive
	HBC	Red sandstones	Thermal / Chemical	Recent field	-	-
	HBD	Red sandstones	Thermal / Chemical	Recent field	-	-
Talchir (North-Karanpura)	TBC	Siltstones and varved clays	Thermal	200°C - 675°C	R	Inconclusive
Talchir (Hutar)	HTA	Medium to coarse grained sandstones	Thermal	550°C - 675°C	R	Inconclusive
	HTB	Varved clays	Thermal	200°C - 675°C	R	Inconclusive
	HTC	Greenish sandstones	Thermal	Random	-	-
	HTD	Greenish sandstones	Thermal	Random	-	-
Talchir (Raniganj)	RTA	Silty shales and sandstones	Thermal	Random	-	-

tabulated in Tables 5.1a and 5.2.

5.2.2   The Natural Remanent Magnetization of Sites HTA, HTB and TBC

NRM intensities of the specimens at sites HTA and HTB ranged between 1 and 20 mA/m. Site TBC specimens showed somewhat higher intensities between 0.2 and 200 mA/m . NRM directions of site HTA were quite dispersed, streaking from the present field direction (D = 359 degrees, I = + 30 degrees) to downward pointing ESE direction (Fig. 5.1a). Sites HTB and TBC specimens showed nicely grouped directions, downward pointing in the SE quadrant (Figures 5.1b and c).

On progressive thermal demagnetization, HTB and TBC site specimens showed a very similar directional pattern in blocking temperature spectra and normalized intensity decay plots (Figs. 5.2b, 5.2c, 5.2d). The higher blocking temperature directions of site HTA specimens were in agreement with directional information from the above mentioned sites but their low blocking temperature directions were found to be scattered (Fig. 5.2a).

Site HTA specimen revealed the presence of two magnetic components, a soft NE directed and upward pointing component which was removed at 110 degrees C and a harder characteristic component SE directed downward pointing component with a blocking temperature range of 530 to 675 degrees C. Between 210 and 550 degrees C both the soft and hard components were removed simultaneously.

In specimens from sites HTB and TBC a soft downward pointing component was removed at 175 degrees C and a well grouped characteristic component direction could be separated between 175 degrees C to 675 degrees C. The harder component showed a SE and a downward direction in specimens from site HTB, and ESE and downward for site TBC specimen.

Figure 5.1   Directions of the natural remanent magnetizations in specimens
of the Talchir Formation sampled in the Hutar Coalfield and the Karanpura
Coalfield. Symbols: Open circles (4) denote directions pointing upwards;
Solid circles (3) denote directions pointing downwards; Diamonds (2) denote
local direction of the present axial geocentric dipole field; Solid
triangle (1) denotes present local field direction at sampling locality,
dipping 30° downward. No tectonic correction is applied to specimen
directions denoted in Figures A-G.

(A)   Site HTA initial specimen directions.
(B)   Site HTB initial specimen directions.
(C)   Site TBC initial specimen directions.
(D)   Thermally cleaned specimen directions from site HTA.
(E)   Thermally cleaned specimen directions from site HTB.
(F)   Thermally cleaned specimen directions from site TBC.
(G) & (H)   Checking of fold test in specimen directions from sites HTB, HTA
      and TBC before and after bedding correction respectively.
(I)   Site mean directions from site HTA (6) before and after bedding
      correction, from site HTB (5) before and after bedding correction,
      and site TBC (circles) before and after bedding correction.
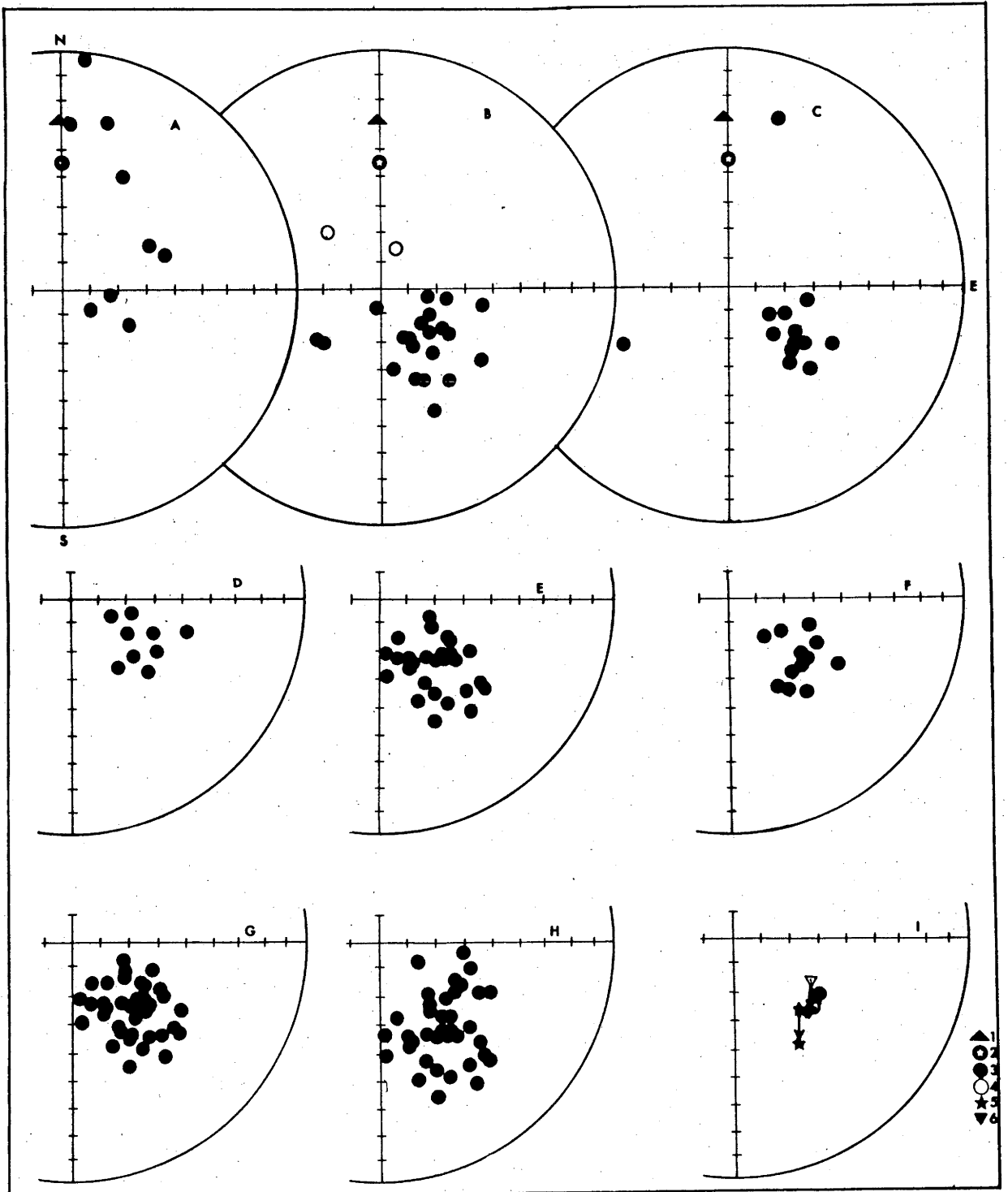
Figure 5.2   Demagnetization diagrams of specimens of the Talchir Formation cleaned with thermal demagnetization.

Demagnetization diagrams are used throughout with the following convention. The plotted points represent successive positions in orthogonal projection of the end of the resultant NRM vector during progressive demagnetization. Solid circles denote the projection of the end points of the changing resultant magnetic vector on the horizontal plane, open circles denote the projection of these end points on the vertical plane with EW line in common. All demagnetization diagrams are drawn with respect to the present horizontal i.e. without applying any bedding correction. The demagnetization temperatures or chemically leached intervals, in days, are mentioned at the vertical projection only.

(A)   Thermally cleaned specimen from site HTA.
(B)   Specimen from site HTB.
(C)   Specimen from site TBC.
(D)   A normalized intensity decay curve of total remanent magnetization during thermal cleaning.

The squares represent site HTA specimen; circles represent site HTB specimen and triangles represent site TBC specimen.
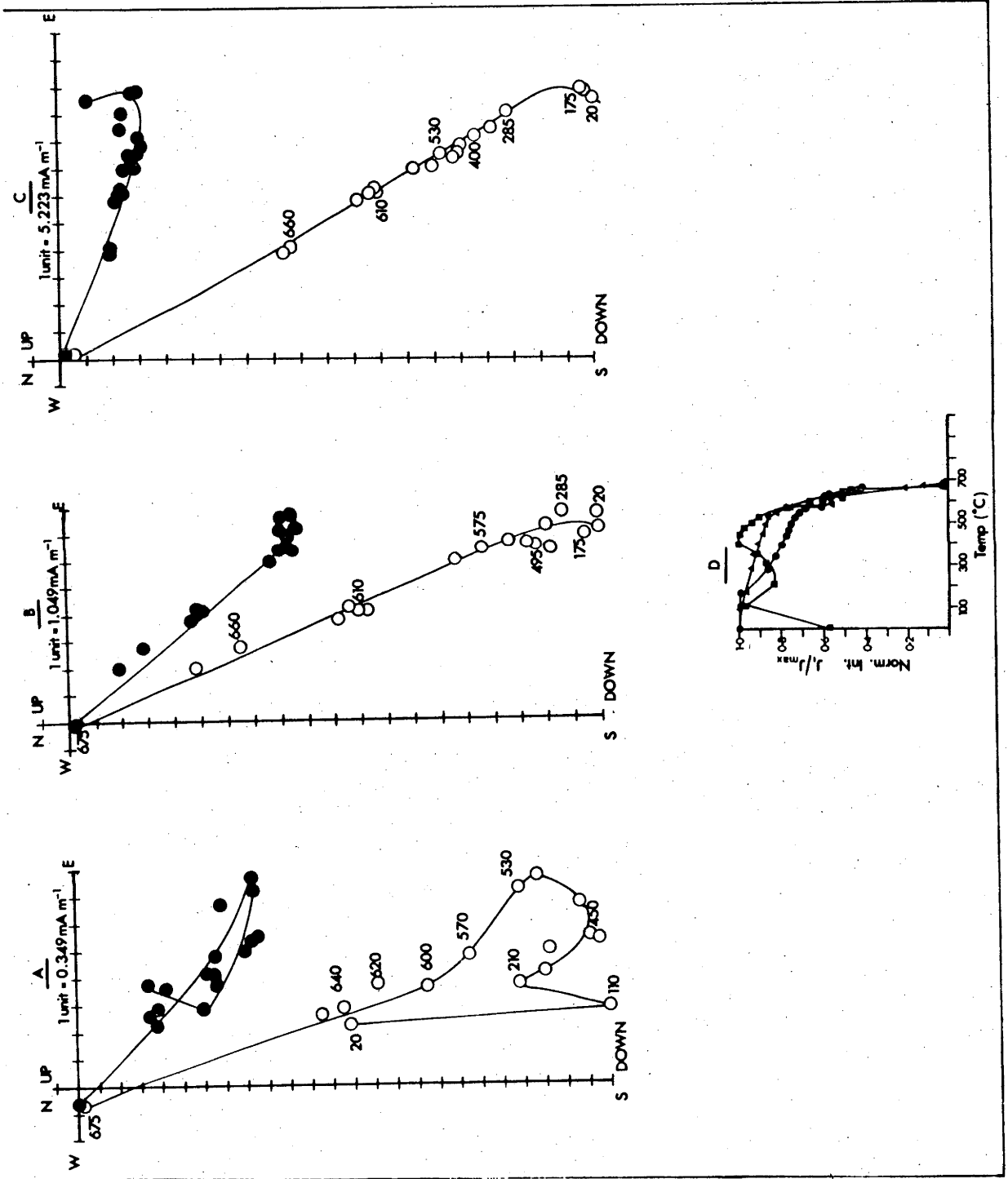
The remanent intensity decay curves at all these sites were very similar in pattern (Fig. 5.2d). A steady decay in intensity up to the blocking temperature of 575 degrees (Curie point of magnetite), followed thereafter by a rapid drop in intensity up to the blocking temperature of 675 degrees C (Curie point of haematite). This possibly indicates that the remanent magnetization of the rocks resides both in magnetite and haematite grains.

Characteristic directions for sites HTB and TBC specimens, before bedding correction (Figs. 5.1e and f) showed a minor directional change when compared with their NRM directions (Figs. 5.1b and c), whereas the originally scattered NRM directions at site HTA specimens (Fig. 5.1a) showed a marked improvement (Fig. 5.1d).

Application of a fold test to the characteristic directions from sites HTA, HTB and TBC gives a negative result (Figs 5.1g, 5.1h). The precision parameter K, before and after bedding correction decreased from 840.8 to 47.6. These sites come from two different coalfields - Hutar and North Karanpura coalfields and their is appreciable chronostratigraphical difference between them (Fig. 2.2 a). Under these conditions, the negative fold test is open to two different interpretations, depending on the as yet uncertain established magnitude of apparent polar wandering during Permo-Carboniferous time.

A. In case of limited polar wandering, the components from both the coalfields are comparable and the negative fold test represents their secondary nature of post folding age.

B. In case of appreciable polar wandering, the components from both the coalfields are incomparable and the negative fold test is meaningless. For this case, the characteristic mean directions for sites HTA, HTB and TBC both before and after bedding correction are shown in

Fig. 5.1i. Note that the dispersed directional pattern before bedding correction lines up after bedding correction in accordance with their stratigraphical order (Site HTB to TBC in decreasing age order). Further discussion about the magnetic nature of the component is deferred to the next chapter on interpretation.

5.3   Palaeomagnetic Results of the Barakar Formation

5.3.1   General

The Barakar Formation from the Hutar coalfield (Fig. 2.3) was collected at four sites HBA, HBB, HBC, and HBD with site HBA the youngest and site HTD the oldest stratigraphically (Table 2.2). The magnetic remanence content of the rocks was analysed by thermal demagnetization and also by chemical demagnetization techniques. Chemical demagnetization of the specimens was followed by thermal demagnetization.

The thermal demagnetization and the chemical demagnetization result showed good agreement in directions but continued thermal demagnetization after chemical demagnetization showed only random directions which may be the result of the very low remaining remanent magnetic intensity (about 0.05 mA/m). Site HBA samples, collected over a section of approximately 1.2 metre thick, dominated by clayey to coarse red sandstones, revealed the presence of only one characteristic component, both upon thermal and chemical demagnetization. Site HBB samples, collected from a section about 1 metre thick composed mainly of red sandstones, also revealed the presence of only one characteristic component upon thermal demagnetization. Chemical demagnetization however, was not successful for this site (10 samples) as most of the samples broke apart upon chemical treatment. Sites HBC and HBD samples

80.

Table 5.1b Hutar Barakar: Mean directions of characteristic component after thermal and chemical work

Before Structural Correction

Site (Tech.)	Initial NRM Intensity Range mA.m^-1	N(n)[*1]	N'(n')[*8]	D_m[*2] (°)	I_m[*3] (°)	K[*4]	α95[*5] (°)	R[*6]	S.Pole Position Lat. (°)	Long. (°)	d_p[*7] (°)	d_m (°)
HBA (Thermal)	3-50	20(18)	36(30)	99.2	56.2	36.4	5.4	19.4	7.0N	136.8E	5.6	7.8
HBA (Chemical)	3-50	10(9)	15(14)	106.1	62.6	16.4	12.2	9.4	5.5N	127.9E	14.9	19.0
HBB (Thermal)	3-50	9(9)	19(16)	118.9	44.8	24.8	17.2	8.7	12.5S	137.4E	13.7	21.7

After Structural Correction

Site (Tech.)	Initial NRM Intensity Range mA.m^-1			D_m' (°)	I_m' (°)	K'	α95 (°)	R	S.Pole Position Lat. (°)	Long. (°)	d_p (°)	d_m (°)
HBA (Thermal)	3-50			111.0	74.3	35.1	5.5	19.4	10.9N	111.7E	9.1	10.1
HBA (Chemical)	3-50			135.9	79.5	16.5	12.2	9.4	8.6N	98.0E	22.2	23.2
HBB (Thermal)	3-50			124.3	40.4	26.3	16.7	8.7	18.5S	137.2E	12.1	20.1

Table 5.1c Raniganj Panchet Formation and Auranga Mahadeva Formation: Mean directions of characteristic component after thermal demagnetization

Before Structural Correction

Site	Initial NRM Intensity Range mA.m^-1	N(n)	N'(n')	D_m (°)	I_m (°)	K	α95 (°)	R	S.Pole Position Lat. (°)	Long. (°)	d_p	d_m
RPA	3-10	18(16)	20(17)	52.0	37.3	28.2	6.6	17.4	42.0N	169.4E	4.5	7.7
AMA	1-1000	9(9)	20(16)	329.8	-53.3	82.1	10.5	8.8	25.6S	112.1E	10.1	14.5

After Structural Correction

Site	Initial NRM Intensity Range mA.m^-1			D_m' (°)	I_m' (°)	K'	α95 (°)	R	S.Pole Position Lat. (°)	Long. (°)	d_p (°)	d_m (°)
RPA	3-10			115.3	55.6	31.2	6.2	17.4	4.6S	134.0E	6.4	9.0
AMA	1-1000			343.6	-39.2	81.2	10.5	8.8	41.4S	104.9E	7.5	12.5

(13 & 9 resp.) which were collected from a section 0.6 metre thick of red silicified siltstone, showed the presence of only a recent field component, both upon thermal and chemical demagnetization. The fold-test was inconclusive for the characteristic components observed in specimens from sites HBA and HBB. Relevant palaeomagnetic results obtained from sites HBA and HBB are listed under Table 5.1b and will be discussed briefly below.

5.3.2   Natural Remanent Intensities of Sites HBA, HBB, HBC and HBD

The initial intensity range for samples belonging to sites HBA and HBB varied from about 3 mA/m to 50 mA/m, whereas the intensity of the samples from sites HBC and HBD ranged from as low as 30 mA/m to about 700 mA/m. The NRM directions of site HBA specimens were quite dispersed, downward pointing and mainly confined to the NE and SE quadrants (Fig. 5.3a), whereas directions obtained from site HBB specimens streaked from the present field direction (D = 359 , I = +30) towards the NE quadrant upward pointing (Fig. 5.3b). In contrast to these NRM directions from site HBA and HBB specimens, specimen directions from sites HBC and HBD showed results grouped around the recent field direction only.

Specimens from site HBA, on thermal demagnetization revealed mainly two magnetic components. A soft recent field component of about 5% to 10% of the NRM intensity which was removed at about 200 degrees C (Fig. 5.4a, 5.4c), and another hard easterly directed and downward pointing characteristic component with a blocking temperature range from 545 degrees C to 675 degrees C. Between 200 degrees C and 545 degrees C, a simultaneous breakdown of the recent field component and the harder component was observed, which mainly resulted in a progressive change in declination. A similar directional pattern was also observed for the
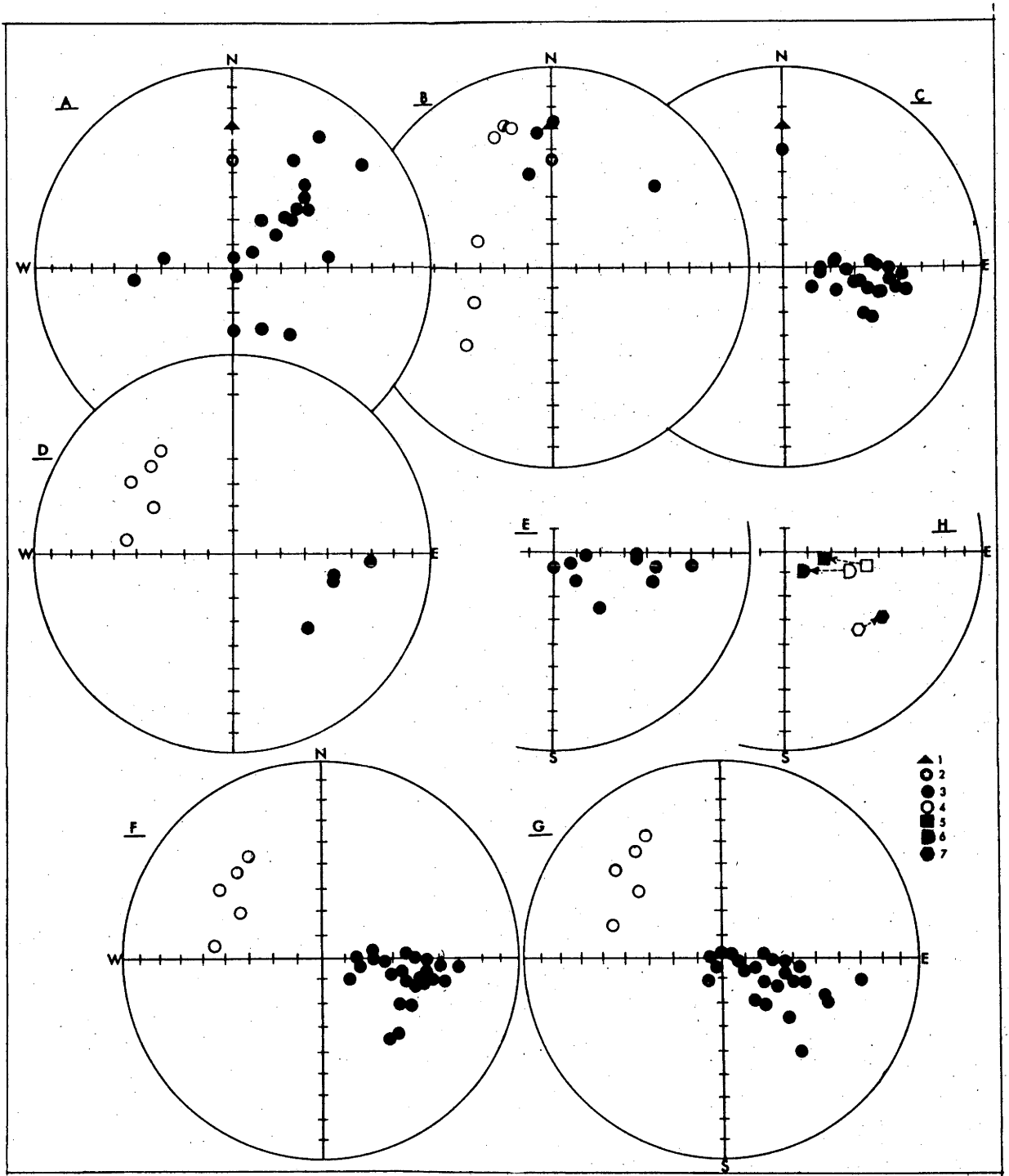
Figure 5.3 Directions of the natural remanent magnetizations in specimens of the Barakar Formation sampled in the Hutar Coalfield. For explanation of symbols 1-4, refer to Figure 5.1 No tectonic correction is applied to specimen directions denoted in Figures A-F.

(A) Site HBA intial specimen directions. (B) Site HBB initial specimen directions. (C) Thermally cleaned specimen directions from site HBA. (D) Thermally cleaned specimen directions from site HBB. (E) Chemically cleaned specimen directions from site HBA. (F) & (G) Checking of fold test in specimen directions from sites HBA and HBB (C & D) representing before and after bedding correction respectively (note the directional spread after bedding correction). (H) Site mean directions; site HBA thermally (5) before and after bedding correction; site HBA chemically (6) before and after bedding correction; site HBB thermally (7) before and after bedding correction.

chemical demagnetization results (Fig. 5.4b). Specimens from site HBB, after removal at about 200 degrees C of a soft recent field component, representing about 50% of NRM intensity, showed a magnetically hard ESE directed and downward pointing characteristic component, whose blocking temperature ranged from 200 degrees C to 675 degrees C. The remanent intensity decay for the characteristic components observed at higher blocking temperatures in specimens from sites HBA and HBB, was found to be gradual up to the Curie point of haematite at 675 degrees C (Fig. 5.4d). This possibly indicates the presence of a remanent magnetization in haematite grains.

Characteristic directions of specimens from sites HBA and HBB before and after bedding correction obtained by thermal and chemical demagnetizations are shown in Fig. 5.3h. However, when the fold-test was applied to the thermally obtained characteristic directions from sites HBA and HBB it came out negatively (Figs. 5.3f, 5.3g), with a precision parameter K value of 46.4 before bedding correction decreasing to 11.1 after bedding correction. Further discussion is deferred to the next interpretation chapter. The characteristic directions in specimens from sties HBA and HBB were dominantly of reversed polarity. A few specimens from site HBB also showed normal polarity directions.

In contrast to sites HBA and HBB, specimens from sites HBC and HBD showed only a recent field component both upon thermal and chemical demagnetization. A representative progressive thermal demagnetization "Zijderveld" plot for a site HBC specimen and a representative progressive chemical demagnetization plot for a site HBD specimen and their intensity decay plots, clearly indicate the dominant presence of this recent field component in the rocks (Figs. 5.5a,b,c).

5.4   Palaeomagnetic results of the Panchet Formation

Figure 5.4   Demagnetization diagrams of specimens of the Barakar Formation cleaned with both thermal and chemical demagnetization.

(A) Thermally cleaned specimen from site HBA.   (B) Chemically cleaned specimen from site HBA.   (C) Thermally cleaned specimen from site HBB. (D) Normalized intensity decay curves of total remanent magnetization during thermal cleaning and chemical cleaning.   Open circles represent thermal cleaned site HBA specimen; squares represent chemically cleaned site HBA specimen; solid circles represent thermally cleaned site HBB specimen.

Figure 5.5   Demagnetization diagrams of specimens of the Barakar Formation cleaned with both thermal and chemical demagnetization.

(A) Thermally cleaned specimen for site HBC.   (B) Chemically cleaned specimen from site HBD.   (C) Normalized intensity decay curves.   Solid circles represent thermally cleaned site HBC specimen; squares represent chemically cleaned site HBD specimen.

A

B

C

D

1 UNIT: 0·698 mA·m⁻¹

1 UNIT: 0·366 mA·m⁻¹

1 UNIT: 3·178 mA·m⁻¹

A

B

C

1 UNIT: 64·306 mA·m⁻¹

1 UNIT = 10·494 mA·m⁻¹

5.4.1   General

The Panchet Formation was collected at one site (RPA) from the
Raniganj coalfield (Fig. 2.5).   The sampling was carried out in a
section   about   1.5 metre of red clays which were steeply SSW dipping at
55 degrees (Table 2.2).   The magnetic content of the samples was
analysed through thermal demagnetization.   One characteristic component
with a blocking temperatures range from 370 degrees C to 675   degrees   C
was   noticed.   The   direction of the characteristic component before
bedding correction showed no correlation with   earlier   available
palaeomagnetic results from Gondwana rocks.   After bedding correction
this result shows a good agreement with earlier results for the   Panchet
Formation (Klootwijk, 1974) and comes much closer to the directional
results described previously for the Talchir and Barakar Formations
(Table 5.1c).   The characteristic component direction was of reversed
polarity (Table 5.2).

5.4.2   The Natural Remanent Magnetization of Site RPA

NRM intensities of the specimens varied from 3 mA/m to 10 mA/m   .
NRM directions were all downwards pointing and showed a streaking from
the recent field direction to the NE quadrant (Fig. 5.6a).   On thermal
demagnetization two components could be distinguished, a soft recent
field component (10 to 15% of NRM intensity, Fig. 5.7B) which was
removed after heating up to 200 degrees C (Fig. 5.7a). Another
characteristic component NE ward and downward pointing was observed with
blocking temperatures range from 370 degrees C to 675 degrees C.   The
remanent intensity decay was very gradual throughout this blocking
temperature range (Fig. 5.7b) possibly indicating the presence of
remanent magnetization in haematite grains.

Figure 5.6   Directions of the natural remanent magnetizations in specimens of the Panchet Formation sampled in the Raniganj Coalfield.   For symbols 1-4 refer to Figure 5.1.

(A)   Site RPA initial specimen directions with respect to the present horizontal.   (B) Site RPA thermally cleaned specimen directions with respect to present horizontal.   (C) Site mean directions (5) with respect to present and palaeo horizontal.

Figure 5.7

(A) Demagnetization diagram of specimen of the Panchet Formation (RPA) cleaned with thermal demagnetization.
(B) A normalized intensity decay curve of total remanent magnetization upon thermal demagnetization.

Figure 5.9

(A) Demagnetization diagram of specimen of the Mahadeva Formation (AMA) cleaned with thermal demagnetization.
(B) A normalized intensity decay curve of site AMA specimen during thermal demagnetization.

1 UNIT = 1·146 mA·m⁻¹

1 UNIT = 1·956 mA·m⁻¹
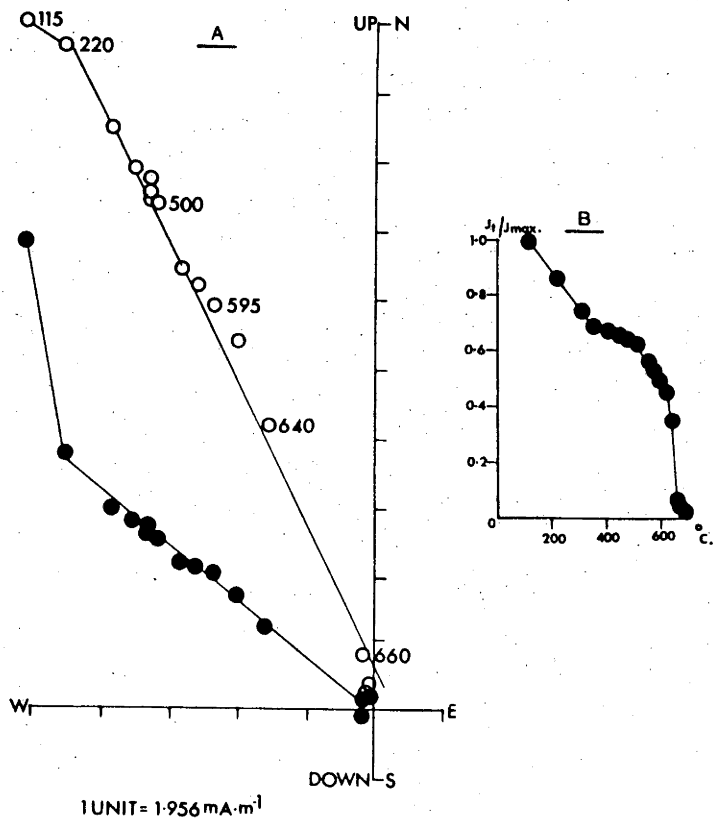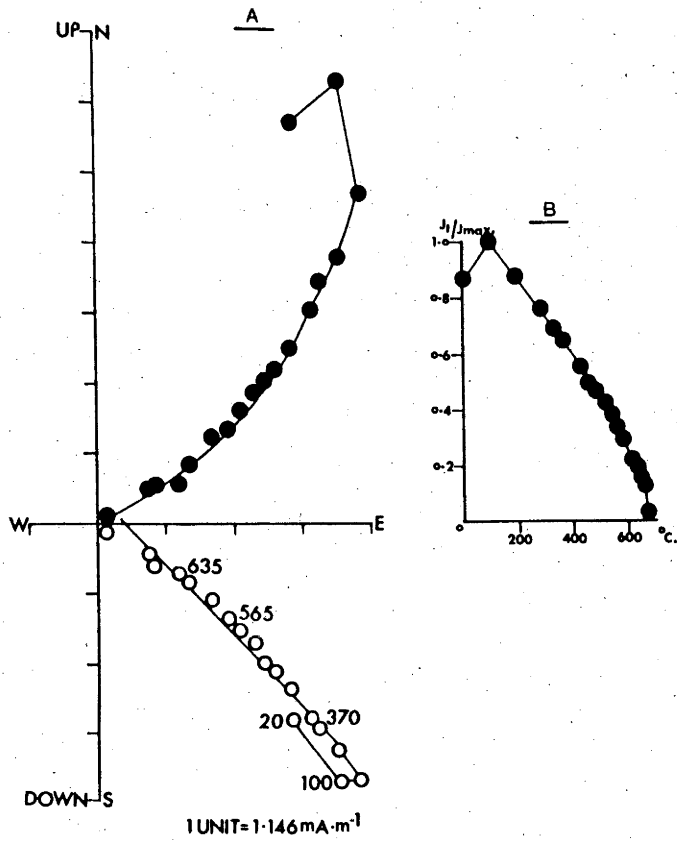
The characteristic component directions before bedding correction (Fig. 5.6b) when compared with the rather scattered NRM directions (Fig. 5.6a) show a marked improvement in grouping. Characteristic mean directions both before and after bedding correction are shown in Fig. 5.6c.

5.5   Palaeomagnetic Results of the Mahadeva Formation

5.5.1   General

The Mahadeva Formation was collected at one site (AMA) from Auranga coalfield (Fig. 2.4). The sampling at this site was carried out in an 8 metre thick section dipping 19 degrees SSW and made up of medium to coarse grained ferruginous and feldspathic pale brownish to reddish sandstones (Table 2.2). The magnetic content of the samples was analysed through thermal demagnetization studies. Only one characteristic component was observed in specimens studied for site AMA, whose blocking temperatures ranged from about 310 degrees C to 675 degrees C (Table 5.1c). The fold-test however, could not be applied because of the uniform dip of the beds. The characteristic component directions were of normal polarity (Table 5.2).

5.5.2   The Natural Remanent Magnetization of Site AMA

The NRM intensity of the specimens varied from 1.0 mA/m to 1000 mA/m. The NRM directions were spread over the NW and the NE quadrant, both downward and upward pointing (Fig. 5.8a). On thermal demagnetization, two components were observed (Fig. 5.9a). A soft recent field compondent (30% of the NRM intensity, Fig. 5.9b) which was removed at 310 degrees C. Subsequently a NW and upward pointing characteristic component was removed with its blocking temperatures ranging from 310 degrees to 695 degrees C. The remanent intensity
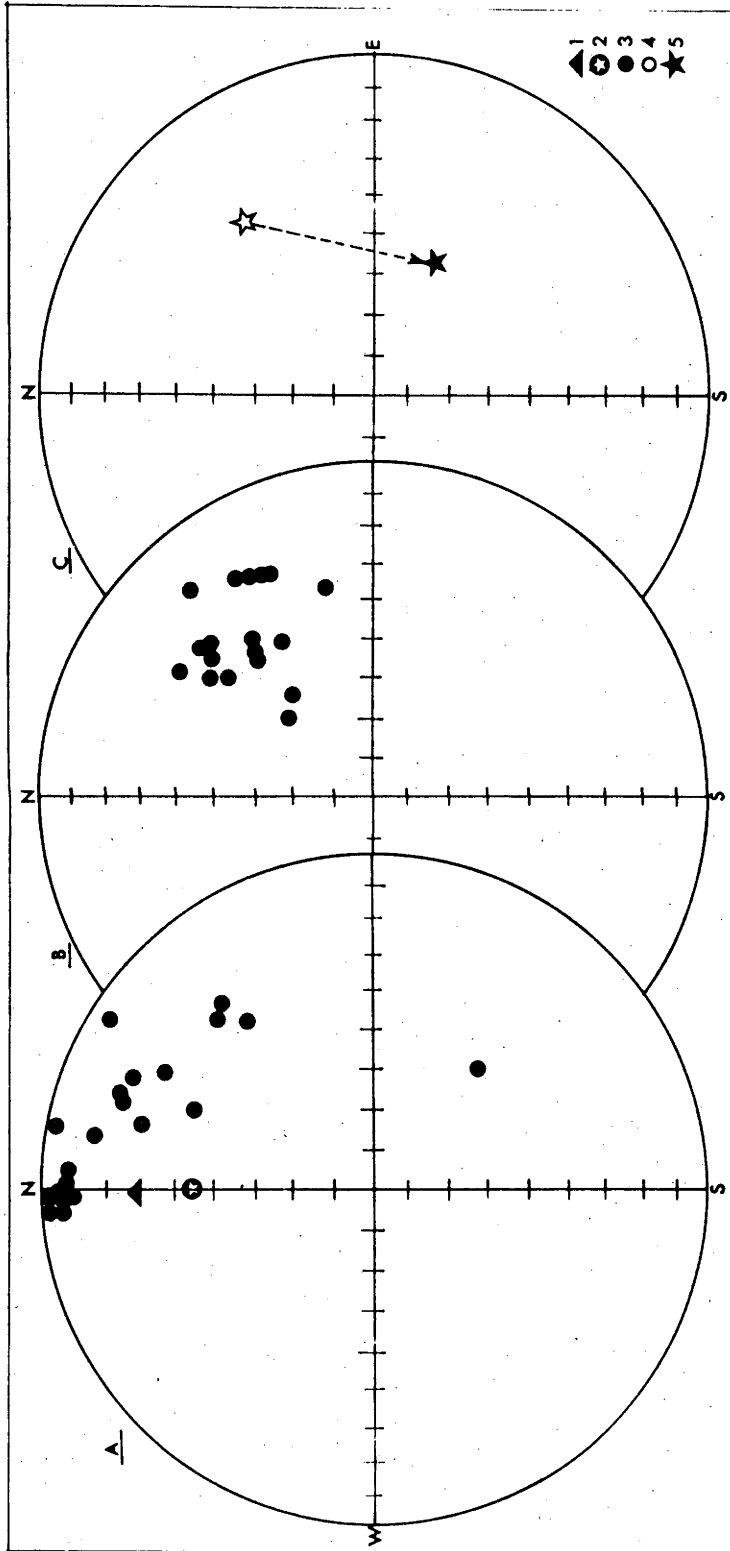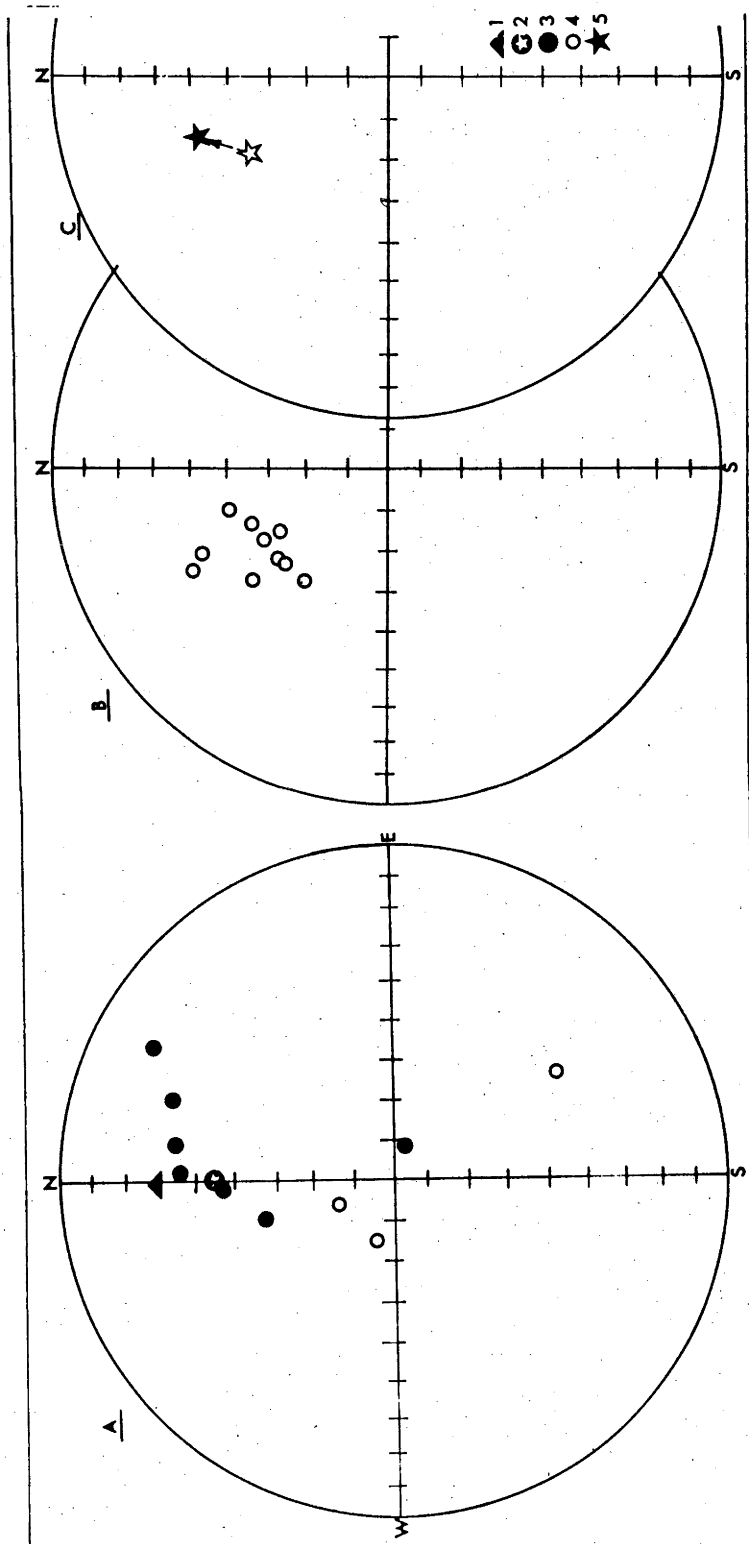
Figure 5.8 Directions of the natural remanent magnetizations in specimens of the Mahadeva Formation sampled in the Auranga Coalfield. For symbols 1-4 refer to Figure 5.1.

(A) Site AMA initial specimen directions with respect to present horizontal. (B) Site RPA thermally cleaned specimen directions with respect to present horizontal. (C) Site mean directions (5) with respect to present and palaeohorizontal.

decreased gradually with temperature (Fig. 5.9b). This gradual decrease up to the Curie point of haematite indicates that part of the remanent magnetization resides in haematite grains.

The characteristic component directions before bedding correction (Fig. 5.8b) group markedly better than their scattered NRM directions (Fig. 5.8a). Characteristic mean directions both before and after bedding correction are shown in Fig. 5.8c.

5.6   Palaeomagnetic Results of the Tiki Formation

5.6.1   General

The Tiki formation was collected at two sites, TPA and TPB from the Johilla coalfield (Fig. 2.1). The sampling at site TPA was carried out through a 4 metre thick section dipping 19 degrees SSE, and made up of medium grained red sandstones. At site TPB, samples were collected from a band 0.5 metre thick of silicified red clays, dipping 10 degrees N (Table 2.2). The magnetic content of the samples at site TPA was analysed both by thermal and chemical demagnetization studies. Chemical demagnetization was followed up with a progressive thermal demagnetization, but this follow-up was not successful and exhibited random directions only, possibly because of the remaining low remanent intensity of the specimens after leaching. The 15 samples from site TPB were thermally demagnetized and exhibited only random directions. Specimens from site TPA revealed the presence of one characteristic component upon thermal demagnetization. This characteristic component however, could be removed at the initial steps of chemical demagnetization. With continued chemical demagnetizations, specimens showed another characteristic component whose direction throughout the site were well grouping. This component was not recognized from the

Table 5.1d   Tiki Formation, Johilla Coal Field: Mean directions of characteristic components after thermal and chemical demagnetization

Before Structural Correction

Site (Tech.)	Initial NRM Intensity Range mA.m^{-1}	N(n)	N'(n')	D_m (°)	I_m (°)	K	α_{95} (°)	R	S.Pole Position Lat.S (°)	Long.E (°)	d_p (°)	d_m (°)
TPA (Thermal)	1-15	23(22)	55(45)	331.3	-40.9	24.0	6.31	22.0	35.4	113.7	4.6	7.6
TPA (Chemical at lower steps)	1-15	29(25)	40(36)	332.9	-41.2	52.8	6.1	28.4	36.0	112.0	4.5	7.4
TPA (Chemical at higher steps)	1-15	13(10)	40(36)	302.0	-22.5	30.8	7.5	12.6	23.2	145.6	4.2	7.9

After Structural Correction

Site	Initial NRM Intensity Range mA.m^{-1}	D_m' (°)	I_m' (°)	K'	α_{95} (°)	R	S.Pole Position Lat.S (°)	Long.E (°)	d_p (°)	d_m (°)
TPA (Thermal)	1-15	331.0	-46.6	22.2	6.58	22.0	31.5	111.0	5.4	8.4
TPA (Chemical at lower steps)	1-15	332.4	-48.2	51.0	6.1	28.4	30.9	109.1	5.2	7.9
TPA (Chemical at higher steps)	1-15	300.2	-28.2	28.9	7.8	12.5	20.0	143.6	4.6	8.5

Table 5.1e   Parsora Formation from Johilla Coal Field: Mean directions of characteristic components after thermal and chemical demagnetization

Before Structural Correction

Site	Initial NRM Intensity Range mA.m^{-1}	N(n)	N'(n')	D_m (°)	I_m (°)	K	α_{95} (°)	R	S.Pole Position Lat.S. (°)	Long.E (°)	d_p (°)	d_m (°)
JPA (Thermal)	1-10	15(14)	35(28)	293.2	-53.7	21.5	8.4	14.3	4.2	130.5	8.2	11.7
JPB (Thermal)	1-10	8(8)	20(20)	317.2	-42.9	18.6	13.2	7.6	26.2	124.3	10.1	16.3
JPC (Thermal)	1-10	11(11)	15(12)	296.1	-48.3	44.8	6.8	10.7	8.9	133.4	5.9	9.0
JPD (Thermal)	1-10	12(10)	14(11)	114.6	45.7	144.9	3.6	11.9	9.0	135.9	2.9	4.6
JPA (Chemical)	1-10	8(7)	12(10)	309.4	-65.4	56.7	7.4	7.8	5.6	112.6	9.7	12.0
JPB (Chemical)	1-10	2(2)	5(5)	300.0	-69.5	148.9	20.6	1.9	2.5N	112.2	30.1	35.2
JPC (Chemical)	1-10	9(8)	10(10)	318.6	-39.0	53.8	7.0	8.8	29.2	125.6	5.0	8.4
JPD (Chemical)	1-10	8(8)	10(9)	115.3	54.2	67.5	6.7	7.9	5.4	129.2	6.7	9.5

Table 5.1e   Parsora Formation from Johilla Coal Field: Mean directions of characteristic components after thermal and chemical demagnetization

Site	Initial NRM Intensity Range $mA.m^{-1}$	D_m (°)	I_m (°)	K	α_{95} (°)	R	S.Pole Position Lat.S (°)	Long.E (°)	d_p (°)	d_m (°)
					After Structural Correction					
JPA (Thermal)	1-10	305.4	-41.7	21.7	8.3	14.3	18.8	132.7	6.2	10.2
JPB (Thermal)	1-10	320.0	-36.0	18.6	13.2	7.6	31.6	126.1	8.9	15.3
JPC (Thermal)	1-10	303.1	-42.6	44.9	6.8	10.7	16.8	133.6	5.2	8.5
JPD (Thermal)	1-10	120.7	40.2	147.5	3.5	11.9	15.9	136.4	2.6	4.3
JPA (Chemical)	1-10	320.2	-52.7	60.1	7.2	7.8	21.7	116.1	6.8	9.9
JPB (Chemical)	1-10	314.0	-62.0	147.3	20.7	1.9	11.0	113.2	24.9	32.1
JPC (Chemical)	1-10	321.7	-31.1	53.9	7.0	8.8	35.0	127.4	4.4	7.9
(JPD (Chemical)	1-10	123.3	48.5	67.4	6.8	7.9	14.0	129.5	5.8	8.9

Table 5.1   Parameters

*1 N(n)	=	Number of specimens (samples) in population used to calculate mean direction.
*2 $D_m(D_m')$	=	Declination with respect to present (palaeo-) horizontal.
*3 $I_m(I_m')$	=	Inclination with respect to present (palaeo-) horizontal.
*4 K (K')	=	Estimate of the precision parameter for a population of directions with respect to present (palaeo-) horizontal.
*5 α_{95}	=	Semi-angle of the cone whose apex lies at the origin and whose axis coincides $Cone$ with the estimated mean direction, calculated from a population of directions and within which the true mean direction lies with 95% probability. The intersection of this core with a surrounding sphere describes the circle of confidence at the 95% probability level (Fisher, 1953).
*6 R	=	The magnitude of the resultant vector of a population of unit vectors (in the present study unit weight has been given in the specimen direction).
*7 d_p, d_m	=	Refer to Table 1.1
*8N'(n')	=	Number of specimens (samples) originally studied.

thermal demagnetization studies, which clearly shows the advantage of combined thermal and chemical demagnetization studies.

The fold-test could not be applied to the characteristic component observed in specimens from from site TPA. The characteristic component directions were of normal polarity. A detailed discussion of these characteristic components is given below. Their mean direction and statistical parameters are listed under Table 5.1d.

5.6.2   The Natural Remanent Magnetization of Site TPA

NRM intensities of specimens from site TPA ranged between 1 mA/m to 15 mA/m . Their upward pointing NRM directions were dispersed over the NW and the NE quadrants (Fig. 5.10a). Upon thermal demagnetization, the specimen revealed two magnetic components (Fig. 5.11a). A soft recent field component which was removed at 155 degrees C at maximum and a characteristic component, NW directed and upward pointing, with blocking temperatures ranging from about 200 degrees to 675 degrees C. Individual specimen directions for this characteristic component (Fig. 5.10b) showed a markedly improved grouping when compared with the scattered NRM directions (Fig. 5.10a). The mean characteristic directions of this component both before (D = 331 degrees, I = -41 degrees) and after (D = 331 degrees, I = -46 degrees) bedding correction for a slight dip of the beds resemble the early Tertiary Deccan Trap direction (D = 340 degrees , I = -44 degrees, Klootwijk, 1974). Chemical demagnetization was carried out therefore, in the hope that the Deccan Trap overprint could be removed and that a primary magnetization could be determined. Upon chemical demagnetization, specimens showed two different magnetic components (Fig. 5.11b). A component removed after leaching with 6N-HCl over 1 to 6 days, was found to be very similar to the characteristic component observed from the thermal

Figure 5.10 Directions of the natural remanent magnetizations in specimens of the Tiki Formation sampled in the Johilla Coalfiled. For symbols 1-3 refer to Figure 5.1. No tectonic correction is applied to specimen directions denoted in figures A-D. (B) Site thermally cleaned specimen directions. (C) Chemically (A) Site AMA initial specimen directions. cleaned specimen directions at lower demagnetization steps. (D) Chemically cleaned specimen directions at higher demagnetization steps. (E) Site mean directions: thermally (5) before and after bedding correction; chemically at lower steps (6) before and after bedding correction; chemically at higher steps (4) before and after bedding correction.
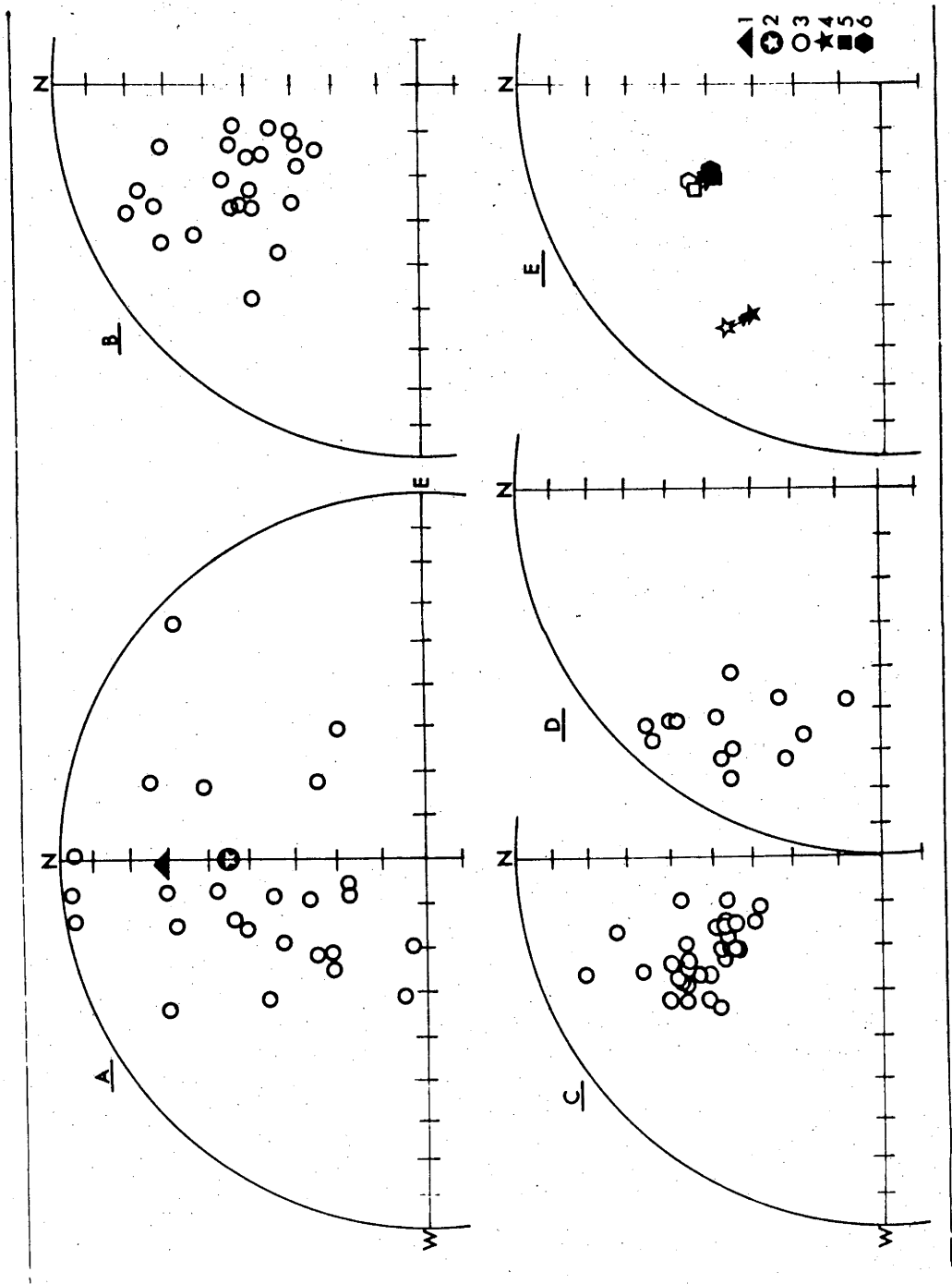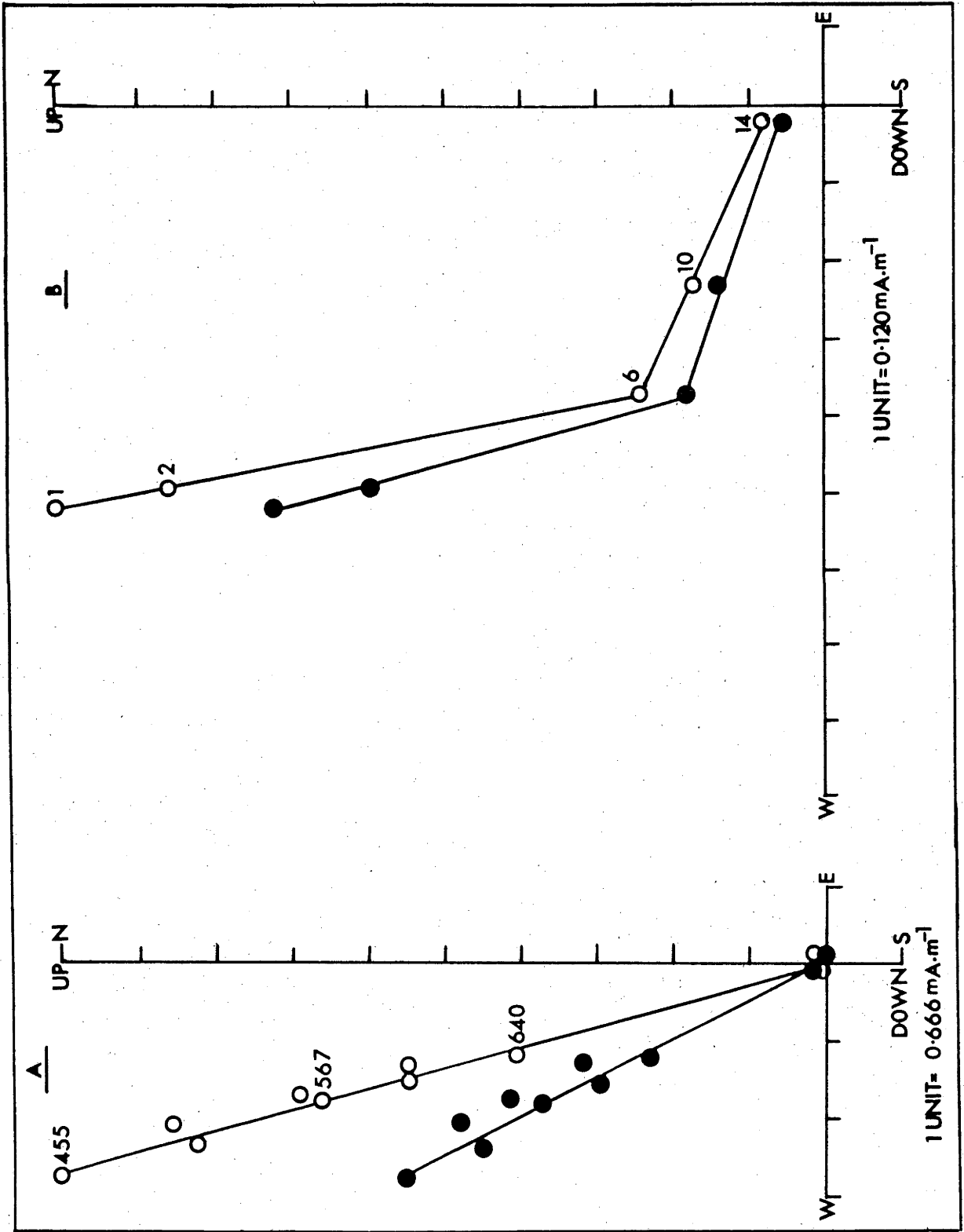
Figure 5.11   Demagnetization diagrams of specimens of the Tiki Formation
(TPA) during thermal demagnetization and chemical demagnetization.

(A) Thermally cleaned specimen.
(B) Chemically cleaned specimen.

magnetization results (Fig. 5.11a). After leaching in 12N-HCl for up to 14 days, after which specimens still showed a slight red colouration, another characteristic component was observed which had directions entirely different from the characteristic components observed from thermal results and chemical results at lower leaching steps. The individual specimen directions of this component before bedding correction are shown in Fig. 5.10d which shows a good grouping in directions when compared with the scattered NRM directions.

The characteristic mean directions of all these three components observed under thermal and chemical demagnetization, both before and after bedding correction are shown in Fig. 5.10e. Note the good agreement of the characteristic component direction between thermal demagnetization results and the results obtained after the lower steps of chemical demagnetization. Results obtained after the higher steps of chemical leaching show entirely different directions.

5.7   Palaeomagnetic Results of the Parsora Formation

5.7.1   General

The Parsora Formation from Johilla coalfield (Fig. 2.1) was sampled at four sites (JPA,JPB,JPC,JPD), stratigraphically site JPB is the youngest whereas, sites JPA, JPC and JPD are of increasingly older age. The sampling at site JPA was carried out in a 3 metre section dominated by reddish to purple silts and mudstones, at site JPB in a 0.6 metre section of siliceous to ferruginous sandstones, at site JPC in a 0.5 metre section of medium to coarse grained red sandstones and at site JPD in a 1 metre thick section dominated by red silty claystones (Table 2.2). Thermal and chemical demagnetizations show the presence of one characteristic component in these sites. Thermal demagnetization

carried out on chemically leached specimens did not reveal any consistency in the directional results. There was a very good agreement between the characteristic directions obtained from thermal and from chemical demagnetization.

The fold-test showed a slight but not significant improvement in grouping of the characteristic component directions. The characteristic directions showed both normal and reversed polarity. Specimens from sites JPA, JPB and JPC showed normal polarity directions, whereas site JPD specimens showed reversed polarity directions. This different polarity pattern was observed both in the thermal and the chemical results.

A detailed description of these characteristic components is given below and their mean directions, corresponding pole positions and other statistical parameters are listed under Table 5.1e.

5.7.2 The Natural Remanent Magnetization of Sites JPA, JPB, JPC, and JPD

NRM intensities observed at all sites ranged from 1 mA/m to 10 mA/m. NRM directions were dispersed over the NE and the NW quadrant with both downward and upward pointing directions (Figs. 5.12a to d). Specimens from all the sites were both thermally and chemically demagnetized. During thermal demagnetization specimens from sites JPA, JPB and JPC showed a recent field component, removed at about 230 degrees C and a characteristic NW directed and upward pointing component with blocking temperatures ranging from about 300 degrees C to 675 degrees C (Figs. 5.13a to D). Site JPD specimens revealed a SW directed downward pointing characteristic component with a blocking temperature range similar to the characteristic components observed in specimens from

Figure 5.12   Directions of the natural remanent magnetizations in specimens of the Parsora Formation sampled in the Johilla Coalfield. For symbols 1-4 refer to Figure 5.1. No tectonic correction is applied to specimen directions denoted in Figures A-K.

(A) Site JPA initial specimen directions.
(B) Site JPB initial specimen directions.
(C) Site JPC initial specimen directions.
(D) Site JDD initial specimen directions.
(E) Thermally cleaned specimen directions from site JPA.
(F) Thermally cleaned specimen directions from site JPB.
(H) Thermally cleaned specimen directions from site JPD.
(I) Chemically cleaned specimen directions from site JPA.
(J) Chemically cleaned specimen directions from site JPC.
(K) Chemically cleaned specimen directions from site JPD.
(J) Sites mean directions both by thermally and chemically demagnetization
     before and after bedding correction: site JPA (5); site JPB (6);
     site JPC (7) and site JPD (8).
(G) Thermally cleaned specimen directions from site JPC.

Figure 5.13   Demagnetization diagrams of specimens of the Parsora Formation (JPA–JPD) during thermal and chemical demagnetizations.
(A) Thermally cleaned specimen from site JPA. (B) Thermally cleaned specimen from site JPB. (C) Thermally cleaned specimen from site JPC. (D) Thermally cleaned specimen from site JPD. (E) Chemically cleaned specimen from site JPA. (F) Chemically cleaned specimen from site JPD. (G) Showing a contrast of normalized intensity decay curves of total remanent magnetization observed during thermal and chemical demagnetizations: solid circles represent a thermally cleaned specimen from site JPA; squares represent chemically cleaned specimen from site JPA.

sites JPA to JPC. This same directional pattern was also observed upon chemical demagnetization. Two chemically demagnetized specimens from sites JPA and JPD (Figs. 5.13e,f) show a consistent directional pattern, similar to thermally demagnetized specimens, over the complete leaching process. Two representative normalized remanent intensity decay curves, one each from the thermal and chemical demagnetization (Fig. 5.13g) show a gradual decay in remanent intensity of the characteristic component, probably indicating the presence of remanent magnetization in haematite grains.

The characteristic component directions as observed in specimens from different sites upon thermal and chemical demagnetizations (Figs. 5.12e to k) show a markedly improved grouping when compared with the NRM directions (Figs. 5a to 5d). The characteristic mean directions of all four sites, both for thermal and chemical demagnetization, are shown in Fig.5.12l before and after bedding correction. A fold-test applied to characteristic mean directions observed upon thermal demagnetization showed an increase in the precision parameter value K from 80.3 to 117.4. Characteristic mean directions observed by chemical demagnetization showed an increase in the precision parameter K from 29.6 to 33.1. This increase in the precision parameter K values, both for thermally and chemically observed characteristic mean directions was, however, insignificant at the 95% level of confidence (McElhinny, 1964). This most probably reflects the only minor difference in dip (around 9 degrees) between site JPA and sites JPB, JPC and JPD (Table 2.2).

5.8   Summary of Results

A summary of the results discussed above is presented in Table 5.2

and some of the relevant points seen are mentioned below:

(a)   Rocks of similar lithological appearance showed widely variable magnetic characteristics.

(b) The magnetic content of different Gondwana Formations studied, upon   thermal   demagnetization   showed   in general a characteristic component with a wide blocking temperature range from 300 degrees C to 675 degrees C, and a soft recent field component removed at about 300 degrees C. For the Talchir Formation, the remanent magnetization probably resides in both magnetite and haematite grains. The red beds studied from the Barakar Formation, from the Panchet Formation, from the Mahadeva Formation, from the Tiki Formation and from the Parsora Formation, the presence of remanent magnetization probably reside in haematite grains. Chemical demagnetization carried out on red beds from the Barakar Formation, the Tiki Formation and the Parsora Formation showed   a   good   agreement   with thermal demagnetization results. Acquisition of this CRM component is therefore supposed   to   be post-depositional, although the time lapse of CRM acquisition with respect to acquisition of the DRM is as yet undetermined.   Thermal demagnetization as a follow-up to chemical demagnetization showed erratic results only.   This probably indicates that the remanent magnetization of red beds was dominantly controlled by haematite grains and less significantly by original specularite grains (DRM, if any). Chemical   demagnetization   revealed   the   presence of two different characteristic components in the Tiki Formation, which could not be separated upon Thermal demagnetization. This emphasises the importance of combined thermal and chemical demagnetizations in distinguishing the magnetic components of red beds.

(c)   The characteristic directions in the different formations were

found to be of both normal and reversed polarities. The Talchir
Formation showed reversed polarity direction. The Barakar Formation
dominantly showed reversed polarity direction with a few samples showed
normal polarity directions. The Panchet Formation also exhibited
reversed polarity directions. The Mahadeva Formation and the Tiki
Formation revealed normal polarity directions. The Parsora Formation
was dominantly of normal polarity with a few samples from its oldest
site JPD also showing reversed polarity directions.

(d) The fold-test on characteristic components from the Talchir and
the Barakar Formations showed an inconclusive result, mainly because of
appreciable chronostratigraphical differences in the sampled sites. The
fold-test could not be applied on results from the Panchet Formation,
the Mahadeva Formation and the Tiki Formation because of the uniform dip
of the beds. The Parsora Formation showed a positive fold-test, which
was not significant however, at the 95% level because of the slight
difference in the dip of the sites.

CHAPTER 6

INTERPRETATION AND DISCUSSION

6.1   Introduction

Interpretation of the various characteristic components observed for the Gondwana formations studied (Table 5.2) is essentially based on;

(a) comparison with the Indo-Pakistan APWP as compiled by Klootwijk and Bingham (1980, see Fig. 1.2, Table 1.1);

(b) the magnetic polarity structure of the observrd directions (Tables 5.1a-e, 5.2);

(c) comparison of directions prior and after correction for tilting of the beds

(d) the possibility of remagnetization due to regional heating and hydrothermal fluids associated with the prolonged period of Deccan Trap magmatism (Pullaiha et al., 1975; Klootwijk, 1975), and

(e) the possibility of an earlier remagnetization event associated with a tensional regime in northern Indo-Pakistan during the late Palaeozoic-early Mesozoic opening of the Neotethys at Gondwanaland's northern rim.

The main conclusions drawn are:

1.   It cannot be decided as yet whether results obtained from the Permo-Carboniferous Talchir Formation and from the upper Lower Permian Barakar Formation (Figs. 6.1a, 6.1c - HTB, HTA, TBC, HBB, HBA) represent a primary magnetization or a secondary magnetization component obtained during Triassic-Jurassic times.

2.   The pole position from the Permo-Triassic Panchet Formation (Fig. 6.1c - RPA) is in good agreement with earlier studies and is interpreted as a primary magnetization.

3.   The pole position for the Mahadeva Formation (Fig. 6.1a, 6.1b
-AMA) of late Early Triassic to Early Jurassic age is very similar to
the Deccan Trap pole position and may reflect a remagnetization
associated with the Deccan Trap magmatism.

4.   The pole positions for the Upper Triassic Tiki and Parsora
Formations (Fig. 6.1c - TPA, JPA-JPD), when compared with the previously
obtained late Triassic and Jurassic pole positions for the Indo-Pakistan
continent, clearly suggest the existence of a Triassic-Jurassic loop in
the Indo-Pakistan APWP.

A detailed account of the interpretation of results from the
various formations studied is given below. It should also be stated
that although the results of both chemical and thermal demagnetization
studies are considered in drawing conclusions (Figs. 6.1a,b), the
thermal demagnetization results are based on much more elaborate studies
than the chemical demagnetization results.

6.2   Talchir and Barakar Formations

The pole positions derived from the characteristic directional
components of the Talchir Formation (HTB, HTA, TBC) and the Barakar
Formation (HBB, HBA) are shown both before and after bedding correction
(Figs. 6.1a, 6.1b). The pole positions before bedding correction are
dispersed quite close to the Triassic-Jurasic trajectory of the APWP as
given   by   Klootwijk and Bingham (1980).   However, After bedding
correction the pole positions show a trend in accord with their
stratigraphic order (Fig. 6.1b). The age of tilting of the Talchir and
the Barakar Formations is not well known. There are two views about
the age of tilting of the beds. Firstly, in about early Tertiary time
(Rizvi, 1972; Section 2.51) and secondly, in about Triassic-Jurassic
times (Casshyap, 1977; Section 2.4). Both of these periods of
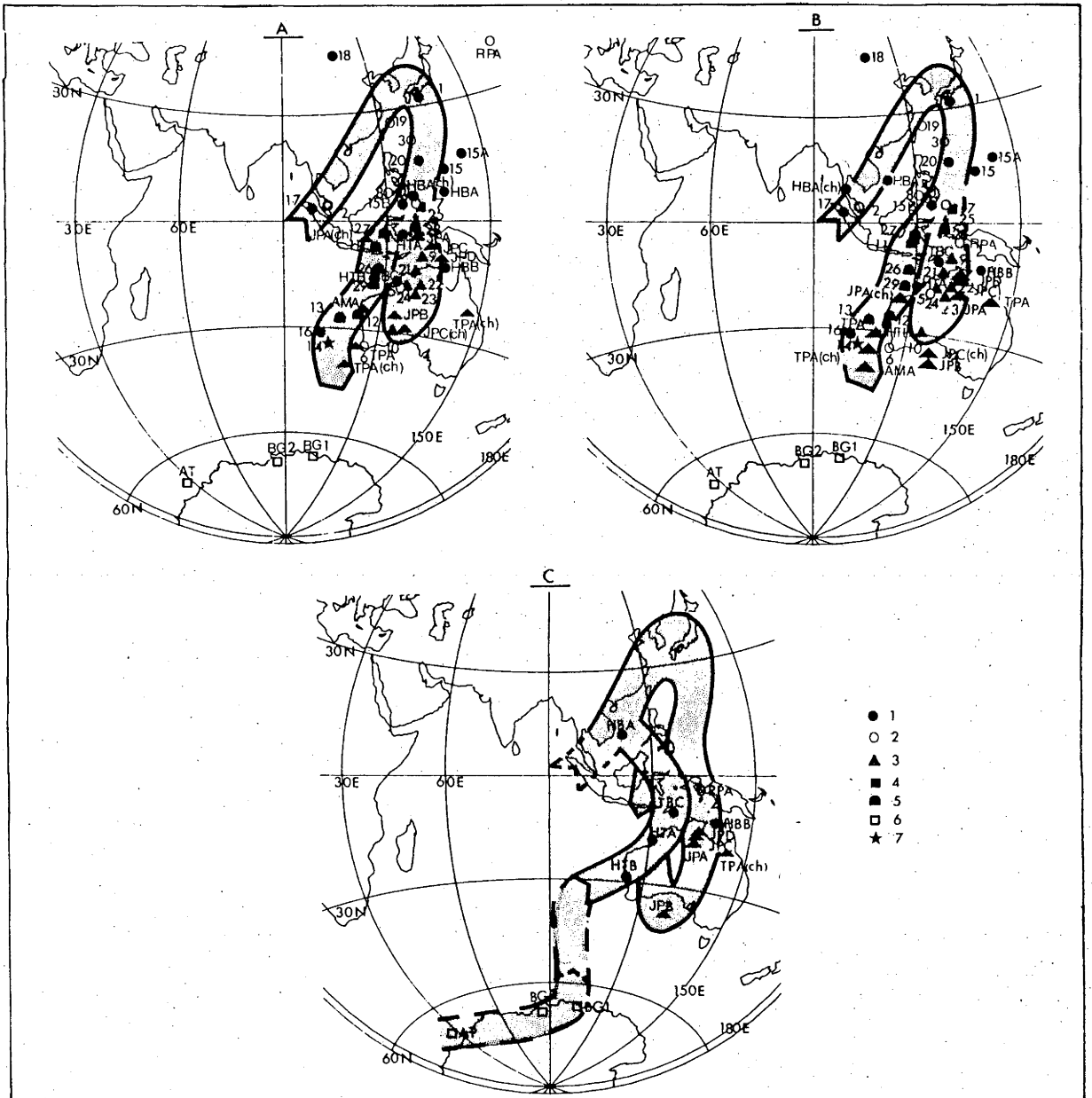
Figure 6.1   Trajectories of the Indo-Pakistan APWP according to the pole positions listed under Table 2.2 with superposition of recently obtained pole positions listed under Tables 5.1a-e.   Swath width = $10°$.

(A)   Superposition of recently obtained pole positions, before bedding correction, a hypothetical case looking for any secondary magnetization of Triassic-Jurassic or early Tertiary times.   (B) Bedding corrected pole positions.   (C) Proposed Indo-Pakistan APW.

For legend refer to Figure 1.2.   Linear polar projection.

Details of Figures 6.1 A,B,C are given on the following pages.

Figure 6.14

Figure 6.1b

Figure 6.1c.

structural activity are suspected to have influenced the formation of secondary magnetization in the rocks. Also, a fold test on the Talchir and the Barakar Formations results, may only be applied with caution because of the appreciable chronostratigraphical difference between the sampled horizons (Fig. 2.2). It is only in the case of limited apparent polar wandering during Permian time that the fold-test may be applied. The implications of (1) limited polar wandering, and (2) appreciable polar wandering in Permian time are now considered.

(1) Assuming limited polar wandering, application of the fold-test gives a negative result (Figs. 5.1, 5.3) which could mean that the acquisition of the magnetic components for the 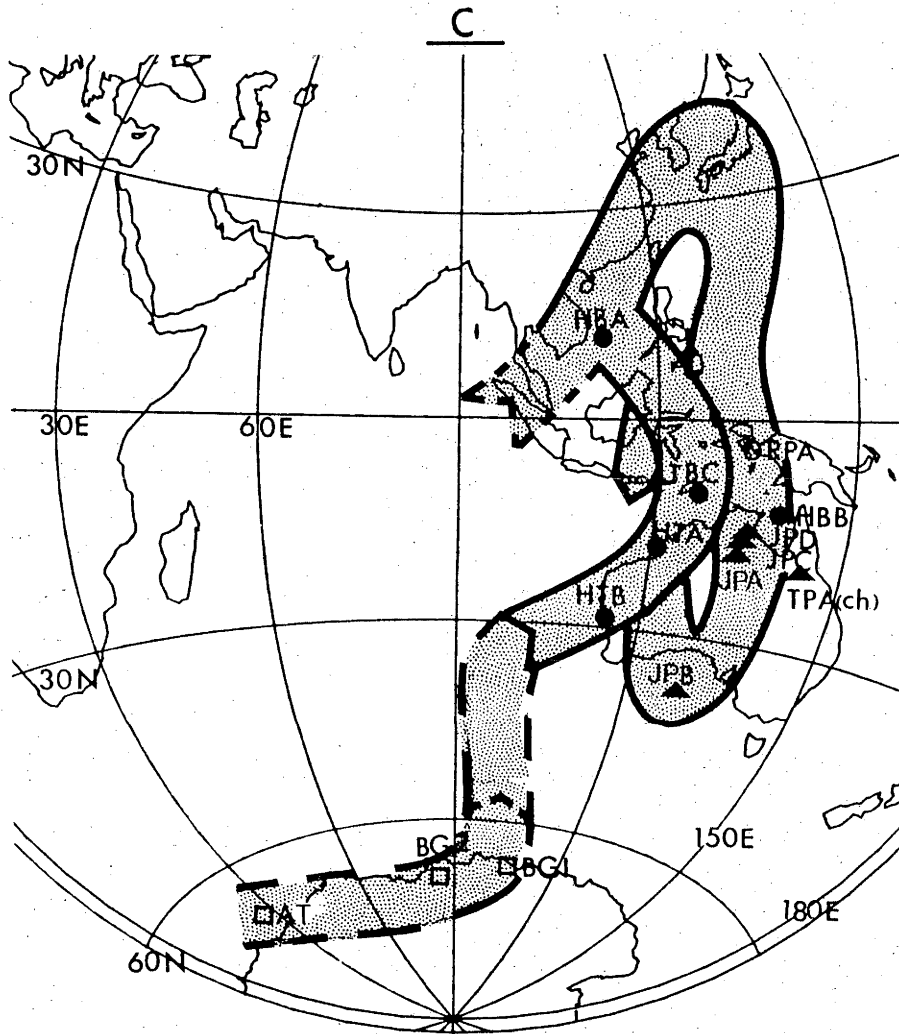Talchir and the Barakar Formations took place after tilting of the beds. The negative outcome of this fold-test is to be ascertained with respect to two possible tilting stages of the beds. In case of an early Tertiary tilting, the pole positions of the Talchir and the Barakar Formations are expected to come close to the pole position suspected for remagnetization during early Tertiary Deccan Trap magmatism (Fig. 6.1a, Pole No. 14), or towards much younger pole positions. This certainly is not the case (Fig. 6.1a), which means that acquisition of the magnetic component after tilting of the beds certainly did not take place during early Tertiary or younger times. The pole positions for the Talchir and the Barakar Formations before bedding correction group loosely in the Triassic-Jurassic trajectory of the APWP given by Klootwijk and Bingham (1980). This may indicate that this magnetic component may have been acquired after tilting of the beds during Triassic-Jurassic times.

(2) In the second case of appreciable polar wandering during Permian time no fold-test can be applied. The pole positions for the Talchir Formation (HTA, HTB and TBC) and the Barakar Formation (HBA and HBB) which are disperse before bedding correction, line up after bedding

correction on the APWP track as indicated by Klootwijk and Bingham (1980), while nicely maintaining the stratigraphical order of the respective sites studied. A suspected remagnetization in the rocks during early Triassic-Jurassic times can be ascertained now after bedding correction for the Talchir and the Barakar pole positions. These results show no correlation with early Tertiary Deccan Trap pole position (Fig. 6.1a, Pole No. 14), and neither good agreement with Triassic -Jurassic pole positions. The so obtained pole positions for the Talchir and the Barakar Formations delineate a polar wander path that is off the above trajectories of the Indo-Pakistan APWP.

The conclusions that can be drawn from both cases discussed above are; that the characteristic directional components in the Talchir and the Barakar Formations in the case of assumed limited polar wander, probably may be interpreted as a secondary component acquired during Triassic-Jurassic times, and in the case of assumed extensive polar wandering may be interpreted as primary magnetizations. The latter interpretation invokes acquisition of the magnetization during the Kiaman reversed polarity epoch (McElhinny, 1973; Fig. 6.2), which is in good agreement with reversed polarity results obtained throughout the Talchir Formation (Fig. 5.1) and predominantly throughout the Barakar Formation (Fig. 5.3). The Barakar Formation site HBB has shown few normal polarity directions as well, which may be difficult to explain in relation to Kiaman magnetic reversed polarity epoch.

Pursuing a primary origin for the magnetization, an additional difficulty in interpretation is encountered as the Talchir and the Barakar Formation pole positions are seemingly in disagreement with earlier available results from peninsular and extrapeninsular Indo-Pakistan. Two results are available from peninsular Indo-Pakistan, namely from the Permo-Carboniferous Talchir beds (Wensink and Klootwijk,
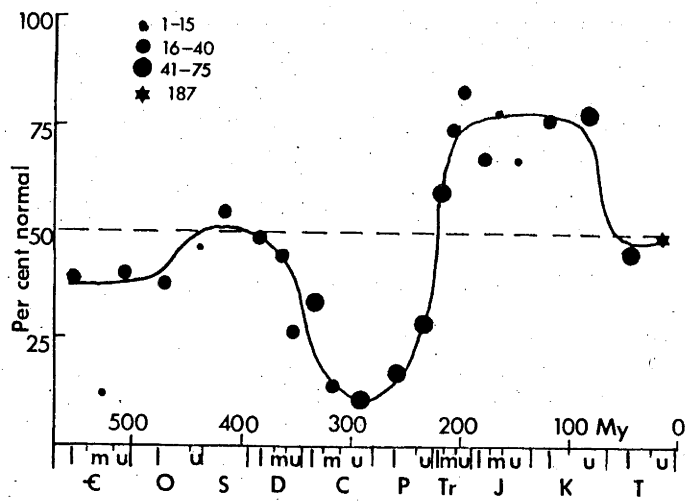
Figure 6.2   Percentage of normal polarity measurements observed in world-wide palaeomagnetic data for the Phanerozoic.   The number of measurements for each period is indicated by the size of the point.   From McElhinny (1973).

1968; Fig. 6.1b, Pole No. 1) and from the Taroba beds (Wensink, 1968; Fig. 6.1b, Pole No. 2) of Late Permian-Early Triassic or may be Precambrian age. Both of these results are in disagreement with the pole positions obtained from the Talchir and the Barakar Formtions. For the Taroba beds a Late Permian-Early Triassic age seems to be doubtful as their pole position falls on the Permo-Carboniferous trajectory of the APWP here obtained. An older, possibly, Precambrian age for the Taroba beds cannot be excluded. The Talchir beds studied by Wensink and Klookwijk (1968) had a positive fold-test. The small scale folding of the sampled varve-like beds was attributed to glacial action which occurred probably shortly after deposition (Klootwijk, 1980 pers. comm.). Interpretation of the Talchir Formation result in terms of a primary magnetization leads to the ambiguity of an inversion in the age of the Barakar site HBA pole position, with respect to the Talchir (Wensink and Klootwijk, 1968) result. This may casts some doubt on (a) the effectiveness of the AF-cleaning applied to the Talchir beds studied, (b) the Talchir age of the studied rocks, or (c) on the correctness of the interpreted APWP as shown in Fig. 6.1b.

Permo-Carboniferous pole positions from extrapeninsular Indo-Pakistan are available from three different structural units (a) the Krol Belt, (b) the Salt Range, and (c) the Kashmir Himalaya.

(a) The results from the Krol Belt i.e. the Permo-Carboniferous Lower Blaini diamictite, the Blaini Limestones and the Permo Triassic Krol-A Limestones (Jain et al, 1979; Pole Nos. 17, 18, 19). These pole positions have been corrected for a 40 degrees clockwise rotation of the Krol Belt with respect to the Indian shield, as deduced from comparison of early Tertiary secondary directions from the Krol Belt with the Indo-Pakistan APWP.

(b) The results from the Early Permian Warchha Sandstones of the Salt

Range (Wensink, 1975   Pole Nos. 15a, b). The Salt Range is an

allochthonous structural unit whose rotational movement is as yet

largely undefined (Klootwijk, 1979b).

(c) The results from the Permo-Carboniferous to may be Late Triassic

Panjal Traps of Kashmir (McElhinny et al., 1978). This pole position

has not been corrected for rotational movement of the Panjal Nappe (Fig.

6.1b, Pole No. 16).

The here obtained pole positions for the Talchir and Barakar

Formations fall off the rotation corrected pole positions from the Krol

Belt (Fig. 6.1b, Pole Nos. 17, 18, 19). It is possible that this

disagreement results from an incorrect rotational correction applied to

the Krol Belt and to the absence of such a rotational correction for the

results of the allochthonous Salt Range structural unit. It is

interesting though that the pole position for site HTB of the Talchir

Formation falls close to the Permo-Carboniferous to may be late Triassic

Pir-Panjal Trap pole position (Fig. 6.1b, Pole No. 16). There is a

positive fold-test on the Panjal Trap results, with folding being of

middle to late Tertiary age. The close agreement of the Panjal Trap

pole position with the Deccan Trap pole position was interpreted

(McElhinny et al., 1978) as indicative for an early Tertiary

remgnetization of the Panjal Traps. The revised Permo-Carboniferous

trajectory for the Indo-Pakistan APWP (Fig. 6.1c) suggests a primary

origin of the Panjal Trap magnetization as an equally plausible

alternative. Newly obtained middle and early palaeozoic pole positions

from SE Australia (Goleby, 1980), when transferred to the Indo-Pakistan

plate, in conjunction with Athavale et al.,(1979) pole position from

ExtraPeninsular Indo-Pakistan(Sec. 1.5.) add further support for such

an interpretation (Fig. 6.1c, Pole Nos.AT, BG1, BG2)

It may thus be concluded from the above discussion that on the presumption of appreciable polar wandering in the Permian, the interpreted smooth trend in the apparent polar wander path, and the observed reversed polarity for the Talchir Formation and the predominantly reversed polarity for the Barakar Formation, that the Talchir and the Barakar Formation results may be interpreted in terms of a primary magnetization. Alternatively, on the presumption of limited polar wandering in the Permian and negative fold test, the internal dispersion of here obtained results and their agreement with the Triassic-Jurassic segment of the Indo-Pakistan APWP may indicate a secondary Triassic-Jurassic origin for the Talchir and the Barakar characteristic magnetization. Clearly more work is to be done to resolve this ambiguity in the interpretation.

6.3 The Panchet Formation

The Upper Permian-Lower Triassic Panchet Formation pole position (RPA) derived from the characteristic directional component, are shown both before and after bedding correction (Figs. 6.1a,6.1b; Table 5.1c). There is no fold-test available for these results and the time of folding of the beds is quite uncertain (Section 2.53). The steep dip of the sampled beds (around 55 degrees southwards) however, allows for a test of a primary or a secondary origin of magnetization. The pole position for the Panchet Formation (RPA) comes only after bedding correction into good agreement with earlier established Permo-Triassic results from peninsular Indo-Pakistan, i.e. with results for the Kamthi Formation and for the Mangli Formation from the Wardha Valley (Wensink, 1968b; Fig. 6.1b, Pole Nos. 3 and 4), for the Kamthi Formation from the Wardha Valley and for the Panchet Formation from the Damodar Valley (Klootwijk, 1974, 1975 Fig. 6.1b, Pole Nos. 7 and 8). The Panchet

Formations pole position however, is in disagreement with the pole position for the Kamthi Formation from the Godavari Valley (Verma and Bhalla, 1968; Fig. 6.1b, Pole No. 5) and for the Himgir beds from the Mahanadi Valley (Athavale et al., 1970; Verma et al., 1973 Fig. 6.1b, Pole No. 6). This disagreement with pole position 6 may be interpreted in support of Klootwijk's (1974) suggestion of incomplete magnetic cleaning of a possibly early Tertiary Deccan Trap overprinting and with pole position 5 may be interpreted in support of its secondary magnetization during Triassic-Jurassic time. For the latter, it may be invoked in view of the new results from the Talchir and the Barakar Formations which are open to two interpretations -. Primary magnetization or acquisition of secondary magnetization during Triassic-Jurassic time.

6.4   The Mahadeva Formation

The pole position derived from the characteristic directional component for the late Early Triassic to Early Jurassic Mahadeva Formation (AMA) is shown both before and after bedding correction (Figs. 6.1a,b; Table 5.1c). There is no fold-test available for the sampled beds. Tilting of the beds possibly occurred during the early Tertiary (Rizvi, 1972; Section 2.52). The pole positions for the Mahadeva Formation both before and after bedding correction are near to the early Tertiary Deccan Trap pole position (Fig. 6.1a,b, Pole No. 14), though the bedding corrected pole position for the Mahadeva Formation is better in agreement with the Deccan Trap pole position than the Mahadeva result before bedding correction. The result is therefore interpreted as an early Tertiary remagnetization during the Deccan Trap magmatic activity with acquisition of magnetization probably preceding tilting of the beds. The normal polarity observed in the specimens studied (Fig. 5.8) supports a secondary Deccan Trap origin, as most Deccan Trap

remagnetization components observed in Gondwana sediments are of normal polarity.

6.5   The Tiki Formation

The pole positions derived from the characteristic directional components observed upon thermal and chemical demagnetization, for the Carnian-early Norian Tiki Formation (TPA) are shown both before and after bedding correction (Figs. 6.1a,b; Table 5.1d). There is no fold-test available for the Tiki Formation site TPA and the time of folding is uncertain (Section 2.55, Table 5.2). The pole positions for the Tiki Formation observed from thermal demagnetization and from the lower steps of chemical demagnetization are in good agreement with the early Tertiary Deccan Trap pole position (Figs. 6.1a,b Pole No. 14). This agreement becomes even better after bedding correction (Fig. 6.1b), and can thus be interpreted as a secondary Deccan Trap magnetization acquired prior to tilting of the beds. The pole position derived from the characteristic directional component observed at higher steps of chemical demagnetization for the Tiki Formation (TPA), agrees after bedding correction with the Late Triassic pole positions for the Parsora Formation (Section 6.6). It also conforms with results from previous Late Triassic studies carried out in peninsular Indo-Pakistan i.e. the Late Triassic Pachmarhi beds (Wensink, 1968; Fig. 6.1b, Pole No. 9), and extrapeninsular Indo-Pakistan i.e. from the Carnian to Norian Thinigaon limestones from Nepal Himalaya (Klootwijk and Bingham, 1980; Fig. 6.1b, Pole Nos 21 and 22). The result from the Tiki Formation is therefore interpreted as a primary magnetization.

6.6   The Parsora Formation

The pole positions derived from the characteristic directional components observed upon thermal demagnetization and chemical demagnetization, for the Parsora Formation of Rhaetic age are shown both before and after bedding correction (Fig.s 6.1a,b; JPA, JPB, JPC, JPD). A fold test applied upon results from site JPA and sites JPB,JPC and JPD is positive but not statistically significant (Section 5.7, Fig. 5.12). The age of the folding of the beds is uncertain. The directions observed for the characteristic components are of normal polarity in sites JPA, JPB and JPC, but are of reversed polarity for site JPD (Fig. 5.12). The pole positions for the Parsora Formation obtained from both thermal and chemical demagnetization, when corrected for bedding come in good agreement with earlier established Late Triassic results from peninsular Indo-Pakistan, i.e. the pole position for the Parsora beds (Bhalla and Verma, 1969; Fig. 6.1b, Pole No. 10) and from extrapeninsular Indo-Pakistan, i.e. the Jomosom Quartzites of Rhaetic age (Klootwijk and Bingham, 1980 ; Fig. 6.1b, Pole No. 23). The predominantly normal polarity directions in the Parsora Formation also substantiate a primary origin of magnetization, as the Late Triassic is a predominantly normal polarity period (McElhinny, 1973; Fig. 6.2).

The obtained results for the Rhaetic Parsora Formation and the Carnian to early Norian Tiki Formation, together with earlier established results from Peninsular and extrapeninsular Indo-Pakistan show a streaking which may be interpreted in terms of a Triassic -Jurassic loop in the Indo-Pakistan APWP. This loop possibly may reflect a Triassic-Jurassic phase of rifting at Gondwanaland's northern rim.

6.7   Discussion

A major aim of the present study was an attempt to clarify some

uncertainties in the Indo-Pakistan APWP, namely:

1. The shape of the Permo-Carboniferous trajectory which was based on only one pole position from the Talchir beds from the Peninsular region and four other pole positions from the extrapeninsular region (Fig. 1.2, Table 1.1).

2. A suspected secondary nature of some of the earlier obtained Permo-Triassic pole positions. (Fig. 1.1, Pole Nos. 5 and 6).

3. The reality and shape of the Triassic-Jurassic loop in the Indo-Pakistan APWP which originally was based on results from the Thakkhola region of the Nepal Himalaya (Klootwijk and Bingham, 1980; Fig. 1.2, Pole Nos. 21, 22 and 23).

The above mentioned problems probably have resulted from two effects.

a). Wide spread early Tertiary Deccan Trap overprinting observed in rocks even at distances up to several hundred kilometers from the present exposures of Deccan Traps. Such secondary acquisition of magnetization has been suggested to result from regional heating and possibly hydrothermal activity associated with the prolonged magmatic activity of the Deccan Traps.

b). Uncertainty about the need to apply rotation corrections for the various formations sampled from the extrapeninsular region.

A reappraisal of these problems on the basis of the results here obtained shows:

a) The results from the Mahadeva Formation (Auranga Coal Field) which is far away (about 300 km) from the present exposures of the Deccan Traps (Fig. 1.1) and from the Tiki Formation (Johilla coal field) which is much closer to the the Deccan Trap exposures (about 20 km), clearly

represent a Deccan Trap remagnetization. Such a component has not been observed in other formations which were sampled near to the locality of the Tiki Formation i.e. the Parsora Formation, or near to the locality of the Mahadeva Formation, i.e. in the Talchir Formation, in the Barakar Formation, and in the Panchet Formation. On the basis of these results, it seems more plausible that hydrothermal agents were mainly responsible for the acquisition of a secondary CRM component in the red beds in contrast to acquisition of a VPTRM component due to prolonged heating of the sediments at the time of Deccan Trap magmatism or deep burial of the rocks for long time. A VPTRM component if prevalent would have been expected to represent a more widespread and rather uniform remagnetization.

b). It is possible that the magnitudes of rotational corrections applied for the extrapeninsular regions may not be correct. I have observed a disagreement between the pole positions obtained from the Talchir Formation and the Barakar Formation (in case of primary magnetization), when compared with the Permo-Carboniferous pole positions from the Blaini Formation of the Krol Belt. This may have to be interpreted as the result of an uncertainty in the rotational correction. On the other hand, the pole positions for the Tiki Formation and the Parsora Formation are in good agreement with the pole position for the late Triassic Thinigaon Limestones and for the Jomosom Quartzites from Thakkhola region of the Nepal Himalaya. These latter pole positions have been obtained after a 15 degrees clockwise rotational correction and this agreement can be seen as support for the correctness of this rotational corection. Further evidence for rotational movements may be obtained from future palaeomagnetic studies in extrapeninsular Indo-Pakistan.

Finally it is important to note that the obtained results clearly have shown the need for the chemical demagnetization in order to remove secondary magnetization components, like the one related to the Deccan Trap magmatism, for instance observed in the Tiki Formation (Fig. 5.10).

6.8   Summary of Interpretation

A summary interpretation of all characteristic components observed in the various Gondwana formations studied (Table 5.2) is listed in Table 6.1. The main conclusions drawn are:

1. The results from the Permo-Carboniferous Talchir Formation and from the upper Lower Permian Barakar Formation are open to two different interpretations A) Primary magnetization B) Alternatively these results may represent a secondary magnetization associated with a late Palaeozoic-early Mesozoic rifting phase in the northern rim of Gondwanaland.

2. The results from the Upper Permian-Lower Triassic Panchet Formation are interpreted as representing a primary magnetization.

3. The results from the upper Lower Triassic to Lower Jurassic Mahadeva Formation probably represent a secondary magnetization, related with the early Tertiary Deccan Trap magmatic activity.

4. The results from the Carnian-lower Norian Tiki Formatioon show two different magnetic components. A secondary magnetic component, observed at the lower steps of chemical demagnetization and also during thermal demagnetization up to 675 degrees C, has been related to the early Tertiary Deccan Trap magmatic activity. Another magnetic component, exclusively observed at the higher steps of chemical demagnetization has been interpreted as a primary component.

5. The results from the Parsora Formation of Rhaetic age has been

118.

Table 6.1   Summary of Interpretation

Formation	Site	Charc. D'_m (°)	Direc.[1] I'_m (°)	Age	Interpretation
Mahadeva	AMA	343.6	-39.2	late Early Triassic-Early Jurassic	Secondary (early Tertiary Deccan Trap?)
Parsora	JPB	320.0	-36.0	Rhaetic	Primary
	JPA	305.4	-41.7		Primary
	JPC	303.1	-42.6		Primary
	JPD	120.7	40.2		Primary
Tiki	TPA	300.2,	-28.2	Carnian-early Norian	Primary[2]
		331.0	-46.6		Secondary (early Tertiary Deccan Trap?)
Panchet	RPA	115.3	55.6	late Permian-Early Triassic	Primary
Barakar	HBA	111.0	74.3	late Early Permian	Primary (?); Secondary (Triassic-Jurassic?)
	HBB	124.3	40.4		Primary (?); Secondary (Triassic-Jurassic?)
Talchir	TBC	125.8	55.7	Permo-Carboniferous	Primary (?); Secondary (Triassic-Jurassic?)
	HTA	136.3	53.6		Primary (?); Secondary (Triassic-Jurassic?)
	HTB	149.4	47.6		Primary (?); Secondary (Triassic-Jurassic?)

*1Characteristic directions observed upon thermal demagnetization.

*2Primary magnetization observed upon chemical demagnetization.

interpreted as a primary magnetization.

The Indo-Pakistan APWP on the basis of the assume primary and secondary magnetization results observed in the various Gondwana Formations is shown (Fig. 6.1c, Table 6.1). Palaeopositions of the Indo-Pakistan continent acording to some selected data are shown in Fig. 6.3 and is discussed below.

6.9   Palaeopositions

The palaeopositions of the Indo-Pakistan continent are derived by rotating palaeomagnetic south poles, (Table 6.1), to the geographical south pole (Fig. 6.3). The northern boundary of Greater India is tentatively drawn, accounting to the magnitude of intracontinental underthrusting along the Main Central Thrust (Klootwijk and Bingham, 1980) and crustal shortening within the Himalayan zone (Gansser 1977).

The oldest palaeomagnetic result obtained during this study is from the Permo-Carboniferous Talchir Formation (Site HTB) and has produced a palaeoposition of Indo-Pakistan within the latitudes 10°S-40°S. The result from the upper Lower Permian Barakar Formation (site HBA) produced a palaeoposition of Indo-Pakistan within the latitudes (35°S-60°S). These two positions suggest a southward and clockwise motion for the Indo-Pakistan continent during the Permo-Carboniferous (in case these represent primary magnetization ?) (Fig. 6.3). From late Early Permian time untill the Late Triassic, Indo-Pakistan drifted in a northward direction while rotating anticlockwise as indicated by the result from the Panchet Formation RPA and the Parsora Formation site JPB (10°S-35°S , Fig. 6.3). In general, the drift of the Indo-Pakistan continent, seems to have been smooth except for some erratic movements as indicated by the results of the Barakar Formation site HBB and the Tiki Formation site TPA. However, It should be noted that the pole
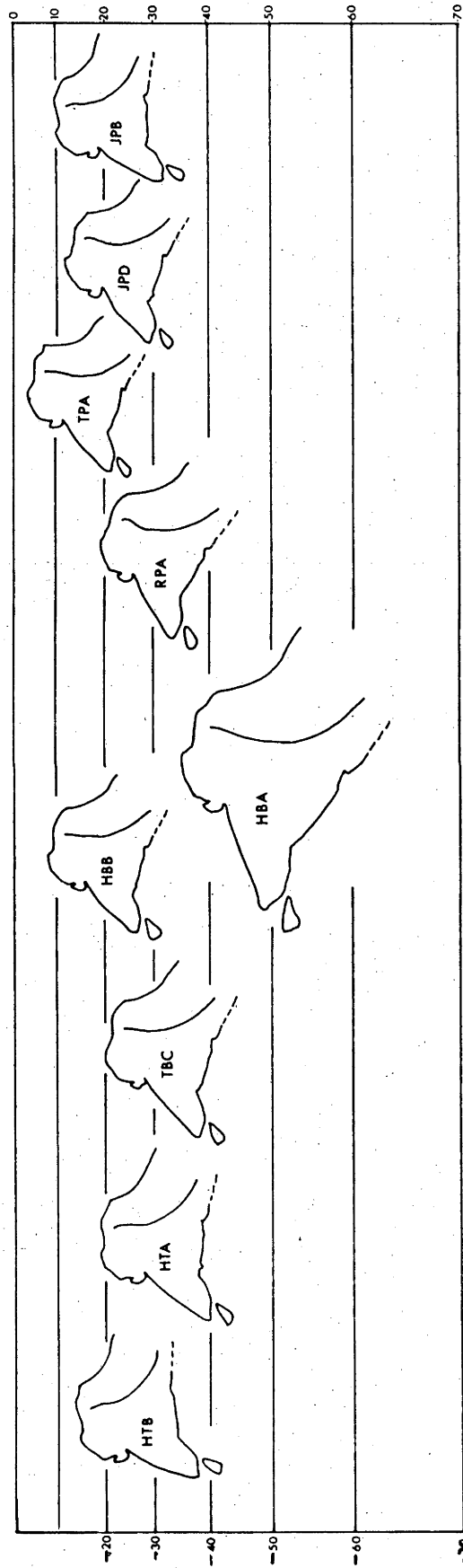
Figure 6.3 Successive palaeopositions of the Indo-Pakistan during Permo-Carboniferous to Late Triassic time, according to the pole positions here obtained, shown in Figure 6.1c and listed under Tables 5.1a-e. The relative longitudinal positions of the diagram are arbitrary. Mercator projection.

positions for these two sites are of rather low accuracy.

CHAPTER 7

COMPARISON OF THE INDO-PAKISTAN APWP WITH THE APWP'S OF

OTHER GONDWANALAND CONTINENTS

7.1   Introduction

A comparison is made of the Indo-Pakistan APWP obtained in this
study with the APWP's of the other Gondwanaland continents.   The   data
for the other Gondwanaland continents has been taken mainly from
Irving's (1964, pp.294-315), and McElhinny's pole lists 8-16 (1968
a,b,69,70,72 a,b,77,78,79).   The data set used in this comparison has
been confined mostly to results with an 95% value of probability level
less than 15 degrees and to results based on at least 10 samples. The
comparison is made with the continents reassembled in the Smith and
Hallam configuration (1970), modified according to Griffiths (1974) and
Norton and Molnar (1977), with Africa held in its present day position.

Particular   attention   is paid to comparing the poorly defined
Permo-Carboniferous loop (In case the Talchir and the Barakar Formations
represent primary magnetizations) and the Triassic-Jurassic loop of the
Indo-Pakistan APWP, with the data from the other Gondwana continents.

The main points noticed in this comparision are as follows:
a).   The Permo-Carboniferous loop as suggested in the Indo-Pakistan
APWP may possibly be recognized in the data from the " stable " Africa
but is not been observed in the data from Morocco, NW Africa, nor is it
distinct in the Australian or the South American APWP.

b).   The Triassic-Jurassic loop in the Indo-Pakistan APWP is in good
agreement with the Triassic-Jurassic loop in the Australian APWP
(Embleton, 1980).   The loop can also be recognised, though on a more
tentative basis in the South American, African and Moroccan APWP's.

7.2   Comparison of Indo-Pakistan's APWP with the Australian APWP

The Indo-Pakistan APWP (Fig. 7.1, Table 1.1,6.1) and Australian APWP (Fig. 7.2, Table 7.1) are shown with the continents reconstructed according to the Smith and Hallam reconstruction (1970), modified according to Griffiths (1974). The pole positions shown range in age from late Carboniferous to Early Cretaceous. The Australian APWP is based on the recent interpretation of Embleton (1980), who has emphasised the effects of a very widespread Late Cretaceous overprinting in rocks of SE Australia. This overprinting is related to a period of burial and raised crustal temperatures prior to initial rifting of the Tasman Sea. The Late Carboniferous to Early Permian pole positions on the Australian APWP (fig. 7.2a, Pole Nos. 1-4) are found to be nicely grouped near to the Late Cretaceous part of the APWP, thus possibly reflecting the above mentioned overprinting. There is only one Early Triassic pole position for Australia (Fig. 7.2a, Pole no. 9), whose position to some extent supports the Permo-Carboniferous loop in the Indo-Pakistan APWP. Late Triassic-Early Jurassic pole positions for Australia are well grouped (Fig. 7.2a, Pole Nos. 9-13, 17 and 18), whereas Middle Jurassic-Late Jurassic pole positions (Fig. 7.2a, Pole Nos. 15, 16 and 20) are more disperse and seem to define part of a loop even more extensive than that interpreted for the Indo-Pakistan APWP.

In summary, the existence of the Permo-Carboniferous loop is uncertain as yet when the Indo-Pakistan APWP is compared with the Australian APWP (Fig. 7.2b). Also, there is convincing agreement between the Triassic-Jurassic loops in both APWP's.

7.3   Comparison of the Indo-Pakistan APWP with the African APWP's

Two African APWP's are considered in this study of African data: (a) The mainland proper ("stable" Africa) and (b) NW Africa, i.e. mainly
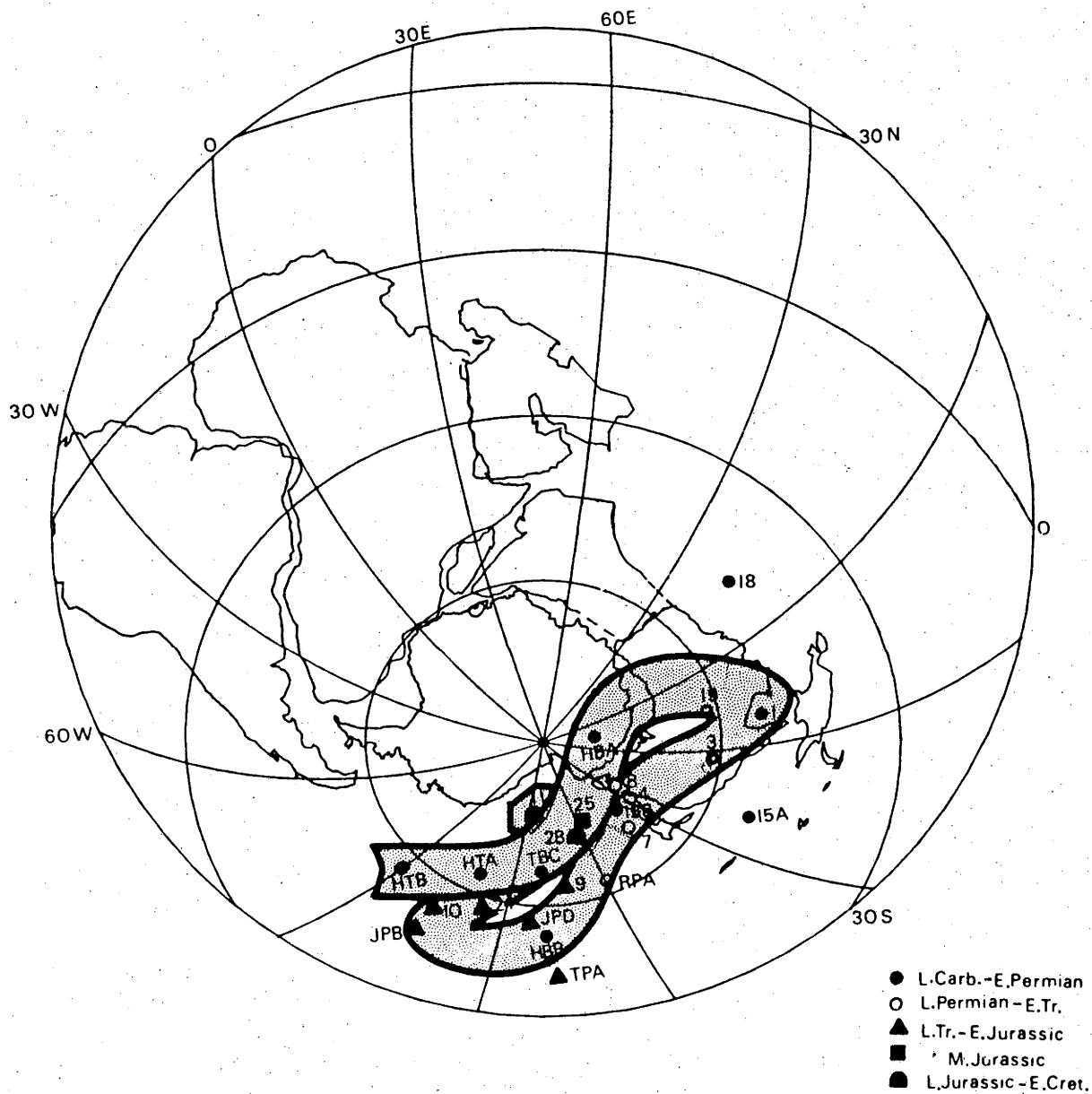
Figure 7.1   Indo-Pakistan APWP from the late Carboniferous–Early Permian
to Early Cretaceous plotted according to the Smith and Hallam reconstruction,
by keeping Africa in its present day position.   The proposed path is on the
basis of established results listed under Table 1.1 and here obtained
results listed under Tables 5.1a–e.   Swath width = 10°.   LInear polar pro-
jection.
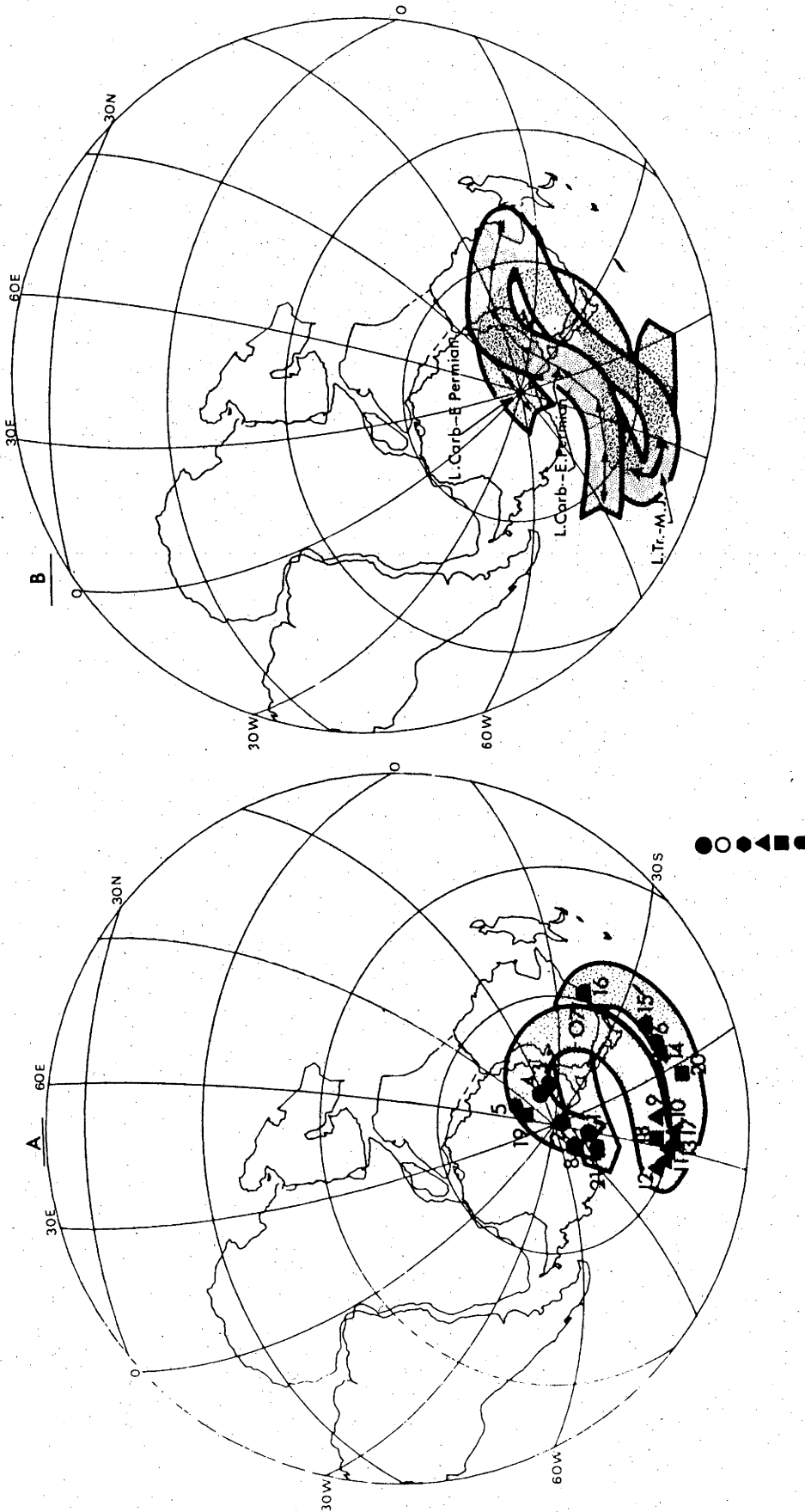
Figure 7.2 (A) Australian APWP from the late Carboniferous-Early Permian to Early Cretaceous (Embleton, 1980) plotted according to the Smith and Hallam reconstruction. (B) A comparison of Indo-Pakistan APWP with Australian APWP from the L.Carboniferous-M.Jurassic, under the Smith and Hallam reconstruction. Note the similarity of Triassic-Jurassic loop but the Permo-Carboniferous loop in Australian APWP is not as extensive as in the Indo-Pakistan APWP (details in text). Swath width = 10°. For legend 1, 2, 4, 5 and 6 refer to Figure 7.1. Hexagonal symbol (3) represents Middle-Triassic pole positions. Linear polar projection.

Table 7.1 Late Palaeozoic to Middle Mesozoic Palaeomagnetic Results from Australia

Rock Unit	Age	South Pole Position Lat.S (°)	Long.E (°)	d_p[1] (°)	d_m[1] (°)	E_{95}[1] (°)	Symbol (Fig.7.2a)	Reference
Main Glacial Stage	L.Carboniferous	53	149	-	-	11	1	Irving (1966)
Rocky Creek Conglomerate	L.Carboniferous	51	138	-	-	17	2	Irving (1966)
Currabubulla Formation	L.Carboniferous	42	135	24	25	-	3	Irving (1966)
Permo-Carboniferous Volcanics	Permo-Carboniferous	44	132	-	-	26	4	McElhinny & Embleton (1974)
Upper Marine Latites	M-L.Permian	46	136	-	-	15	5	Irving & Parry (1963)
Milton Monzonite	L.Permian (240 my)	32	170	-	-	24	6	Robertson (1964)
Patonga Claystone	E.Triassic	30	147	-	-	8	7	Embleton (1980)
Brisbane Tuff	M.Triassic (215-195 my)	57	143	10	11	-	8	Robertson (1963)
Garrawilla Volcanics and Nombi Extrusives	L.Triassic-E.Jurassic (193my, K-Ar)	46	175	-	-	10	9	Schmidt (1976b)
Western Victoria Basalts	E.Jurassic	47	178	11	18	-	10	Schmidt (1976c)
Barenjoey Dyke	Triassic-Tertiary	53	182	-	-	8	11	Robertson (1979)
Minchinbury Intrusives	Triassic-Tertiary	56	179	-	-	14	12	Robertson (1979)
Colleroy Dyke	Triassic-Tertiary	53	180	-	-	9	13	Robertson (1979)
Springfield Basin	L.Triassic	32	170	-	-	24	14	Schmidt et al. (1976)
Hornsby Breccia	Triassic-Tertiary	29	166	-	-	7	15	Embleton (1980)
Erskine Part Igneous Deposit	Triassic-Tertiary	23	151	-	-	9	16	Robertson (1979)
Jurassic Intrusives	Jurassic (170-185 my)	51	186	-	-	11	17	Schmidt (1976b)
Tasmanian Dolerite 1	M.Jurassic (167 my)	51	175	-	-	5	18	Schmidt and McDougall (1977)
Tasmanian Dolerite 2	M.Jurassic (167 my)	48	124	-	-	10	19	Schmidt & McDougall (1977)
Kangaroo Island Basalts	M.Jurassic (170 my)	39	183	-	-	11	20	Schmidt (1976c)
Mt.Dromedary Igneous Complex	Cretaceous (100 my)	56	153	-	-	11	21	Schmidt (1976a)

*1 - for explanation refer to Table 1.1

from the Moroccan region which in parts has been tectonized during the Hercynian and the Alpine orogenies.

a). The APWP for "stable" Africa, shown in Fig. 7.3a, Table 7.2. The PermoCarboniferous trajectory of the APWP for "stable" Africa is based on four pole positions (Fig. 7.3a, Pole Nos. 1-4) which show appreciable polar wandering. The pole positions for younger periods i.e. the Permo-Triassic (Fig. 7.3a, Pole Nos. 5-7), the Late TriassicEarly Jurassic (Fig. 7.3a, Pole Nos. 9-16) and the Middle to Late Jurassic (Fig. 7.3a, Pole Nos. 17 and 18) form a rather loose group with some of the late Triassic pole positions (Pole Nos. 9 and 10) lying further from the main grouping. A very tentative trajectory is drawn in Fig. 7.3a through these pole positions. It shows some similarity with the Indo-Pakistan APWP, although some of the Late Triassic-Early Jurassic pole positions (Fig. 7.3a, Pole Nos. 11 and 13) fall outside the swath.

The "stable" African APWP shows a broad similarity with the Indo-Pakistan APWP in the Permo-Carboniferous loop and possibly also in the Triassic-Jurassic loop.

b). Much palaeomagnetic work has been carried out on rocks from Morocco, NW Africa. An APWP based on the Moroccan data (Table 7.3) is shown in Fig. 7.4a. The Permo -Carboniferous (Fig. 7.4a, Pole Nos. 1-4) to Middle Triassic pole positions (Fig. 7.4a, Pole NOs. 6-11) show an appreciable polar wandering. The Late Triassic part of the Moroccan APWP is not very well defined. The Late Triassic pole position from the Argana red beds (Fig. 7.4a, Pole No. 12) and pole position from the Triassic Teloutet lava which is not very well dated (Fig. 7.4a, Pole No. 5) disagree with the early Mesozoic part of the apparent polar wander path and also with the Early Jurassic (Fig. 7.4a, Pole Nos. 13-16) and Late Jurassic-Early Cretaceous (Fig. 7.4a, Pole No. 17) pole positions.

Figure 7.3 (A) African mainland APWP from L.Carboniferous-E.Permian to Early Cretaceous plotted according to the Smith and Hallam reconstruction. Tentative L.Triassic-M.Jurassic part of trajectory is shown with dotted lines. (B) A comparison of Indo-Pakistan APWP with African mainland APWP from the L.Carboniferous to M.Jurassic. Note the similarity of P-C loop and the tentative Triassic-Jurassic loop of the African mainland with Indo-Pakistan APWP (details in text). Swath width = 10°. For legend, refer to Figure 7.1. Hexagonal symbol (3) represents M-Triassic pole positions. Linear polar Projection.

Table 7.2 Late Palaeozoic to Middle Mesozoic Palaeomagnetic Results from Africa mainland

Rock Unit	Age	South Pole Position Lat.S (°)	Long.E (°)	d_p[1] (°)	d_m[1] (°)	E_{95}[1] (°)	Symbol (Fig.7.3a)	Reference
Dwyka Varves	L.Carboniferous (315-280 my)	26	26	-	-	11	1	McElhinny & Opdyke (1968)
K₃ Beds, Galula Coal Field	L.Carboniferous-E.Permian?	46	40	-	-	8	2	Opdyke (1964a)
K₃ Beds, Galula Coal Field	L.Carboniferous-E.Permian?	40	64	-	-	16	3	Opdyke (1964a)
K₃ Beds, Mchuchuma Coal Field	E.Permian	27	89	-	-	15	4	Opdyke (1964a)
Mazi Ya Chumui Formation	L.Permian-E.Triassic	67	89	-	-	17	5	McElhinny & Brock (1975)
Cassanje Series	L.Permian-E.Triassic	54	77	-	-	7	6	Valencio et al. (1978)
Upper Beaufort Sediments	E.Triassic	67	87	-	-	-	7	Graham (1961)
Shawa Ijolite	M.Triassic (209 m.y.)	64	86	-	-	12	8	Gough & Brock (1964)
Red Sandstone Formation	L.Triassic	68	50	5	6	-	9	Opdyke (1964b)
Freetown Igneous Complex	Triassic (180 my, K-Ar regarded as a min.age)	81	45	-	-	5	10	Briden et al. (1971)
Marangudzi Complex	L.Triassic-E.Jurassic (182-196 my, K-Ar)	64	98	-	-	11	11	Brock (1968)
Karro Lavas	L.Triassic-E.Jurassic	57	84	-	-	8	12	McElhinny et al. (1968)
Ufinza Dykes	L.Triassic-E.Jurassic (190 my, K-Ar)	54	65	12	17	-	13	Piper (1972)
Stormberg Lavas	E.Jurassic	71	89	-	-	15	14	McElhinny et al. (1964)
Diabese Dykes and Sills	E.Jurassic (173-192 my, K-Ar)	68	62	5	3	-	15	Dalrymple et al. (1975)
Dolerite Sills	E.Jurassic (160-180 my, K-Ar)	72	81	18	22	-	16	Bardon et al. (1973) Conrad & Westphal (1975)
Karroo Dolerites	E-M.Jurassic (154-190 my)	66	75	-	-	12	17	McElhinny & Jones (1965)
Hoachanas Lavas	M.Jurassic (161-173 my, K-Ar)	62	72	17	23	-	18	G idskehaug et al.(1975)
Kaoka Lavas	E.Cretaceous (110-128 my, K-Ar)	48	86	3	4	-	19	G idskehaug et al.(1975)
Mlange Massif	E.Cretaceous (116-128 my)	60	82	9	13	-	20	Briden (1967)

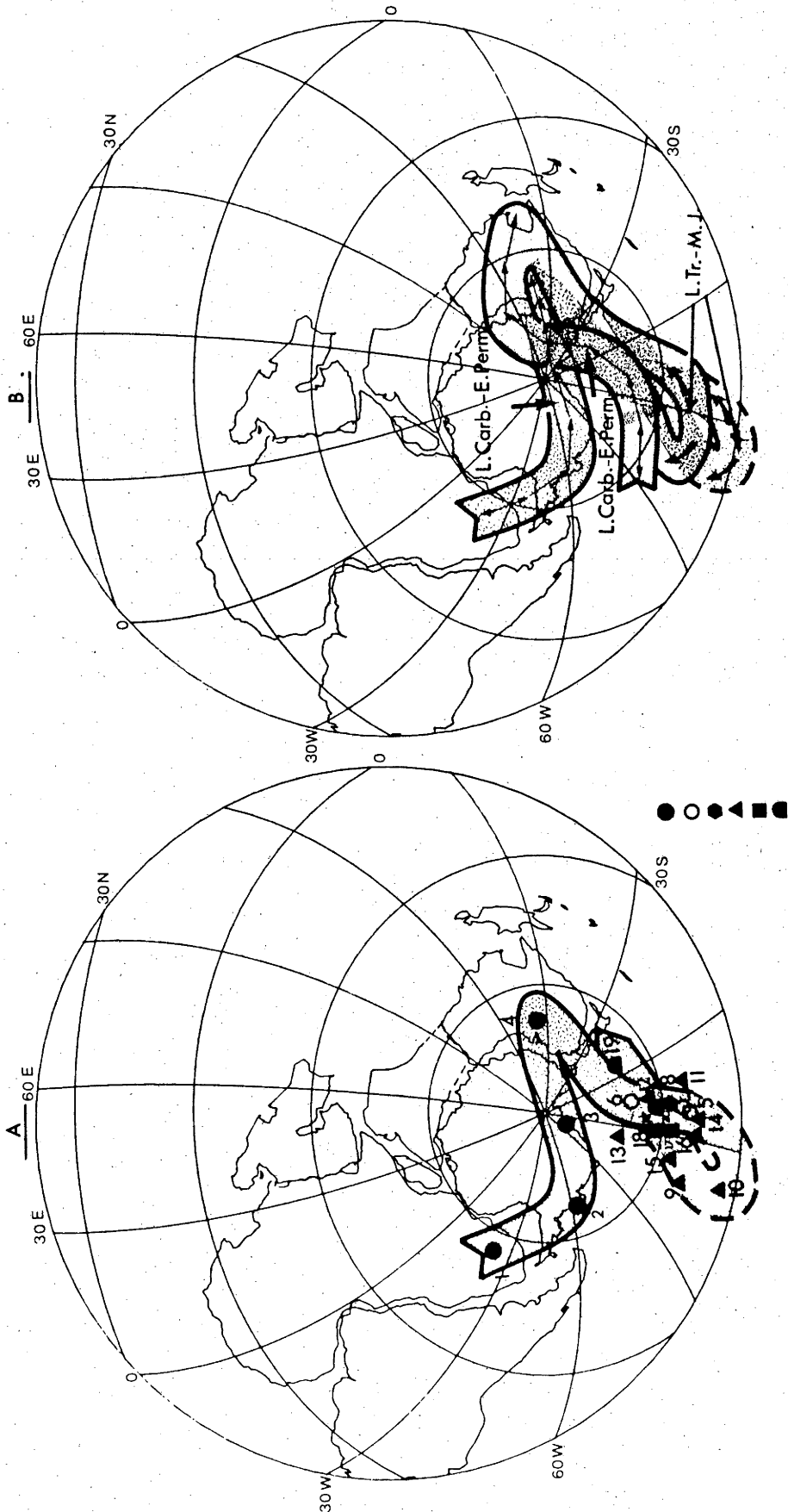*1 - For explanation refer to Table 1.1
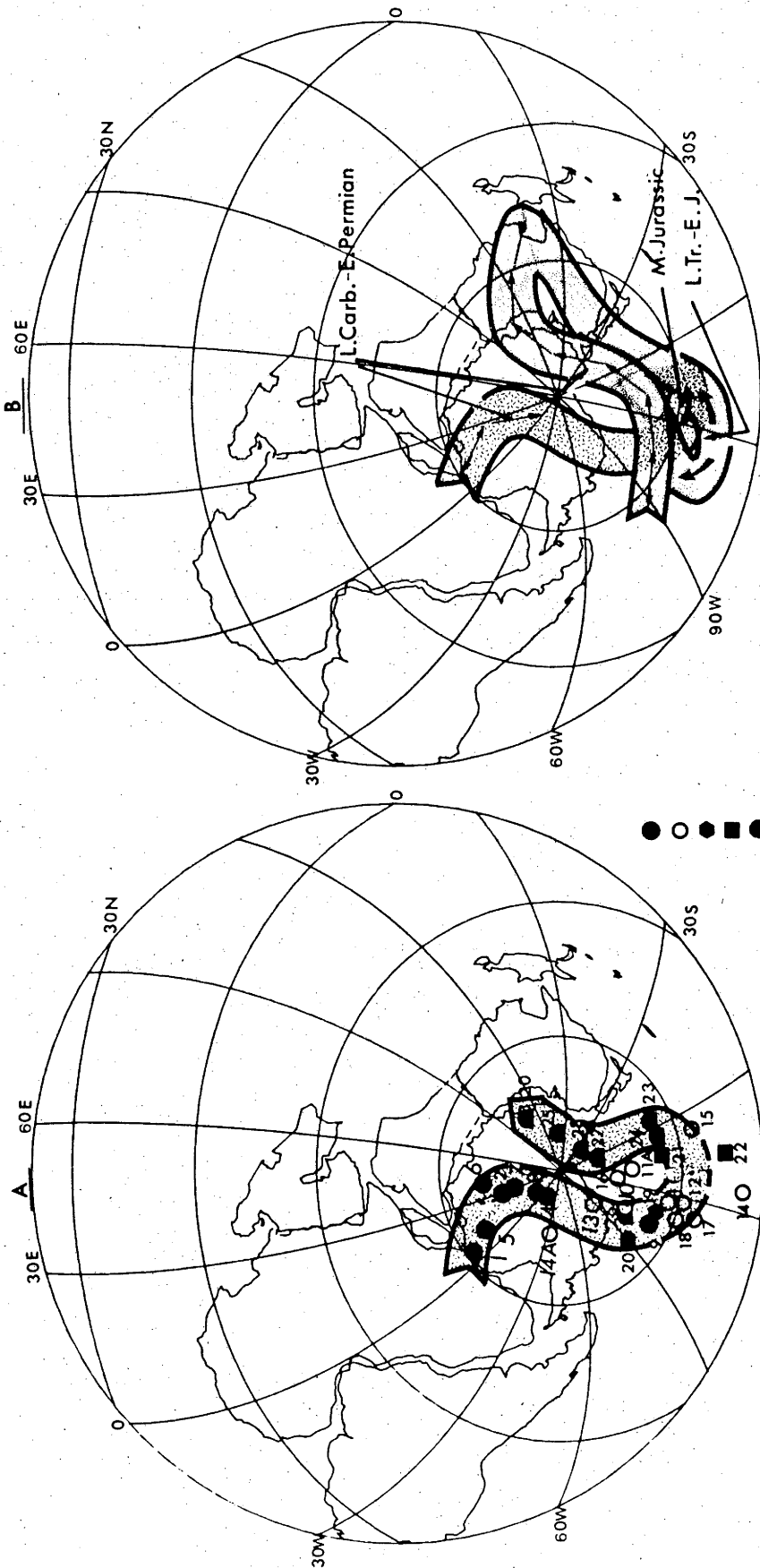
Figure 7.4 (A) NW Africa, Moroccan APWP from late Carboniferous-Early Permian to Early Cretaceous, plotted according to the Smith and Hallam reconstruction, tentative L.Triassic part of the trajectory is shown with dotted lines; (B) A comparison of Indo-Pakistan APWP with NW African APWP show a similarity with the tentative L.Triassic-E.Jurassic loop in NW African APWP whereas extensive P-C loop observed in Indo-Pakistan APWP is not observed in NW African APWP (details in text). Swath widths = 10°. For legend, refer to Figure 7.1, hexagonal symbol (3) represents M.Triassic pole positions. Linear polar projection.

Table 7.3   Late Palaeozoic to Middle Mesozoic Palaeomagnetic Results from NW Africa, Morocco

Rock Unit	Age	South Pole Position Lat.S (°)	Long.E (°)	d_p[*1] (°)	d_m[*1] (°)	D_{95}[*1] (°)	Symbol (Fig.7.4a)	Reference
Basalts, Diorite and Contact	L.Carboniferous (294-297 my, K-Ar)	16	62	-	-	14	1	Martin et al. (1978)
Djebel Tarhat Red Beds	E.Permian	24	64	4	8	-	2	Martin et al. (1978)
Taztot-Trachandesites	E.Permian	38	56	2	4	-	3	Daly and Pozzi (1976)
Chougrane Red Beds	E.Permian	32	64	2	4	-	4	Daly and Pozzi (1976)
Teloutet Lava	Triassic	51	35	12	20	-	5	Martin et al. (1978)
Ait-Aadel Dolerites	M.Triassic	72	74	7	7	-	6	Hailwood (1975)
Titchka Sandstone	M.Triassic	68	87	-	-	22	7	Hailwood (1975)
Sediments, Jerada (combined)	M.Triassic	76	66	3	4	-	8	Daly and Pozzi (1976)
Khenifra Basalts	M.Triassic	58	68	2	3	-	9	Daly and Pozzi (1976)
Beni-Snassen Basalts	M.Triassic	57	72	5	9	-	10	Daly and Pozzi (1976)
Tazzeka Basalts	M.Triassic	78	94	4	6	-	11	Daly and Pozzi (1976)
Argana Red Beds	L.Triassic	50	71	7	14	-	12	Martin et al. (1978)
Middle Atlas Basalts	L.Triassic-E.Jurassic	71	36	-	-	7	13	Michard et al. (1975)
Limestones, Midelt	E.Jurassic	62	30	4	8	-	14	Martin et al. (1978)
Draa Valley Sills	E.Jurassic (180-186 my, K-Ar)	66	50	-	-	4	15	Hailwood & Mitchell (1971)
Foum Zguid Dyke	E.Jurassic (182-187 my, K-Ar)	58	79	-	-	4	16	Hailwood & Mitchell (1971)
Central Atlas	L.Jurassic-E.Cretaceous (119-160 my, K-Ar)	53	82	-	-	24	17	Hailwood & Mitchell (1971)
Infracenomanian Sandstone	E.Cretaceous	75	47	-	-	6	18	Hailwood (1975)
Volcanics, Beni Mellal	E.Cretaceous	44	71	-	-	10	19	Bardon et al. (1973)

*1 - For explanation refer to Table 1.1

Comparison of the Moroccan APWP with the Indo-Pakistan APWP (Fig.
7.4b) shows that the Permo-Carboniferous part of the Moroccan APWP is in
reasonable good agreement with the Indo-Pakistan APWP, but the Moroccan
poles do not show any evidence for a Permo-Carboniferous loop. The
Middle Triassic and Early Jurassic pole positions from Morocco can be
interpreted in terms of an APWP rather similar to that proposed for the
Indo-Pakistan and "stable" Africa.

7.4   Comparison of the Indo-Pakistan APWP with the South American
APWP

An APWP for South America is drawn using the data presented in Table
7.4 (Fig. 7.5a). The Permo-Carboniferous pole positions of South
America are in good agreement, apart from pole position 9, with the
Permo-Carboniferous trajectories of APWP's for the other Gondwanaland
continents. The pole positions for other periods such as the
Permo-Triassic (Fig. 7.5a, Pole Nos. 10-18) and the Middle to Late
Triassic (Fig. 7.5a, Pole Nos. 19 and 20) group reasonably well,
although some Permo-Triassic pole positions (Fig. 7.5a, Pole Nos. 14 and
15) lie further from the main grouping. Two Middle Jurassic pole
positions lie away from the main grouping observed for the Permo
-Triassic pole positions and suggest continuing apparent polar
wandering. This interpretation of the Permo-Carboniferous to Jurassic
part of the South American APWP allows linkage with its Cretaceous
trajectory, which in part may reflect the opening of the South Atlantic
Ocean since the Early Cretaceous (Norton and Sclater, 1979).

A comparison of the South American APWP with the Indo-Pakistan APWP
is shown in Fig. 7.5b. The Permo-Carboniferous pole positions of South
America are in reasonably good agreement with some of the Indo-Pakistan
Permo-Carboniferous pole positions, but do not support the suggested
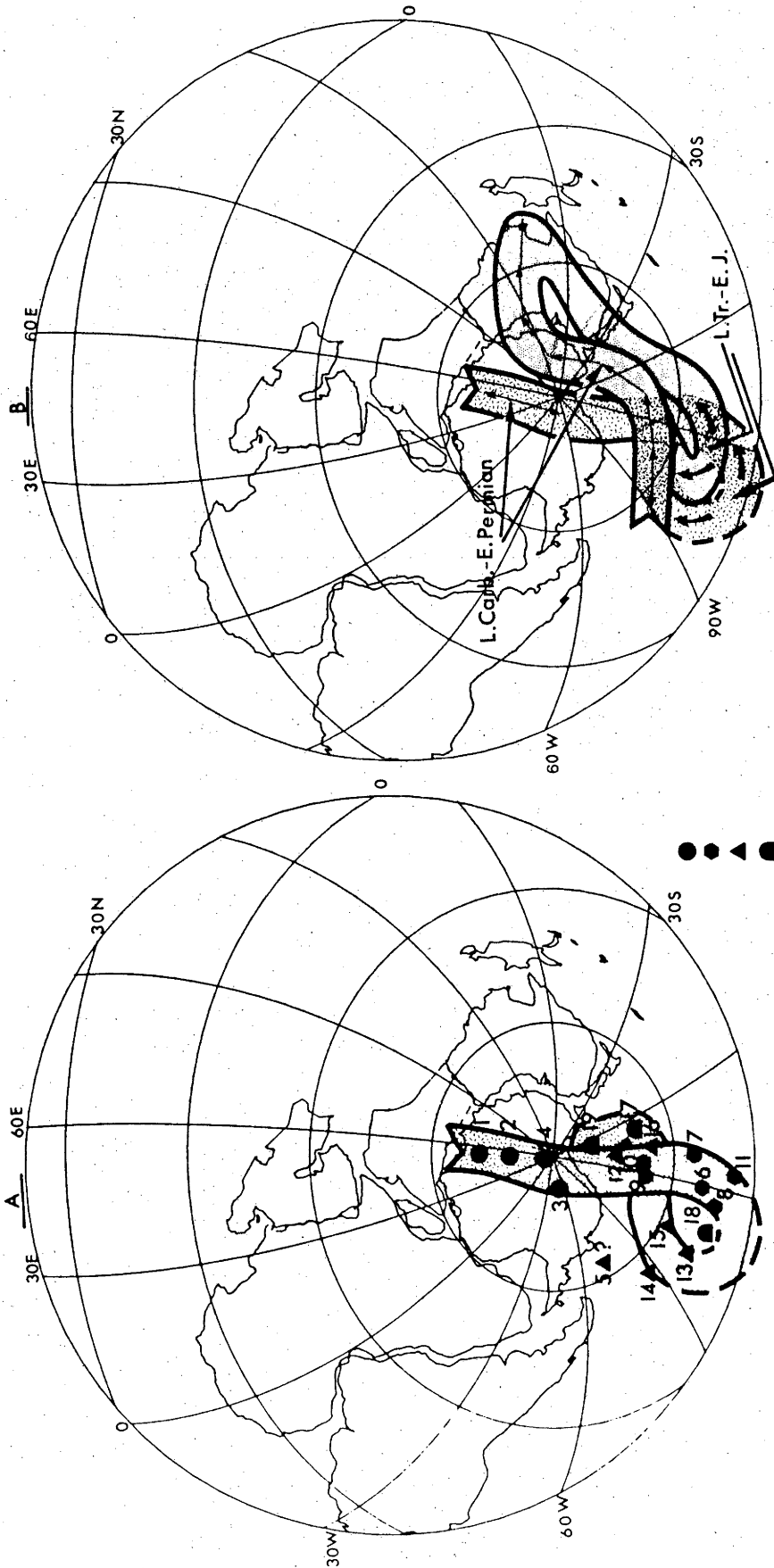
Figure 7.5 (A) South American APWP from the late Carboniferous-Early Permian to Early Cretaceous plotted according to the Smith and Hallam reconstruction. Tentative E.Jurassic part of the trajectory is shown with dotted lines; (B) A comparison of Indo-Pakistan APWP with South American APWP from the L.Carboniferous-M.Jurassic, under Smith and Hallam reconstruction. Note the similarity in L.Triassic-M.Jurassic Indo-Pakistan APWP with tentative E.Jurassic South American APWP but P-C loop interpreted in Indo-Pakistan APWP is not present in South American APWP (details in text). Swath widths = 10°. For legend, refer to Figure 7.1. Linear polar projection.

Table 7.4 Late Palaeozoic to Middle Mesozoic Palaeomagnetic Results from South America

Rock Unit	Age	South Pole Position Lat.S (°)	Long.E (°)	d_p^{*1} (°)	d_m^{*1} (°)	E_{95}^{*1} (°)	Symbol (Fig.7.5a)	Reference
Taiguati	Carboniferous	45	340	-	-	6	1	Creer (1970)
Tubarao	L.Carboniferous	57	357	-	-	15	2	Valencio et al. (1975b)
Lacolina Basalt	L.Carboniferous (295.my, K-Ar)	66	348	-	-	7	4	Thompson (1972)
Piaui Formation	L.Carboniferous	50	345	18	24	-	5	Creer (1970)
Pipiral	Permo-Carboniferous	52	602	-	-	-	6	Creer (1970)
Middle Paganzo II	L.Carboniferous-E.Permian	60	358	-	-	4	7	Embleton (1970)
Red Beds (Paganzo)	Permian	65	347	-	-	6	8	Creer (1965)
La Colina Formation	E.Permian (>266 my, K-Ar)	78	257	3	4	-	9	Valencio et al. (1977)
Cerro Carrizalito	M.Permian (263±5 my)	81	282	-	-	6	10	Creer et al. (1970)
Co.Bola and Colorado	M.Permian	80	228	-	-	10	11	Creer et al. (1970)
Corumbatai Formation	L.Permian	86	294	-	-	14	11a	Valencio et al. (1975b)
Las Tunas and Bonete	L.Permian	78	219	-	-	17	12	Creer et al. (1970)
Middle Paganzo II	L.Permian	74	308	-	-	5	13	Embleton (1970)
Guyana Dykes	L.Permian-E.Triassic	64	209	7	14	-	14	Hargraves (1978)
Anana Formation	L.Permian-E.Triassic	63	329	16	20	-	14a	Valencio et al. (1977)
Paganzo Formation	Permo-Triassic	77	175	-	-	6	15	Creer et al. (1970)
Surinam Dykes	L.Permian-E.Triassic	82	320	10	20	-	16	Veldkamp et al. (1971)
Laqunita Formation (Tuffs)	Triassic	72	233	-	-	-	17	Hargraves (1978)
Igneous Rocks, Puesto - Viezo Formation	E.Triassic (232 my, K-Ar)	76	236	14	18	-	18	Valencio et al. (1975a)
Ischigualasto	M.Triassic (224 my, K-Ar)	79	239	13	15	-	19	Valencio et al. (1975a)
Las Cabras	M.-L.Triassic	74	266	11	18	-	20	Valencio et al. (1969)
Chon Aike Lavas	M.Jurassic (161 my)	85	197	-	-	6	21	Vilas (1974)
Chon Aike Formation	M.Jurassic	69	193	-	-	13	22	Vilas (1974)
Volcanics and Red Beds	E.Cretaceous	84	90	-	-	5	23	Vilas (1976)
Serra Geral Basalts	E.Cretaceous	84	115	-	-	4	24	Pacca and Hiodo (1976)
El Sato-Almafuerte Lavas	E.Cretaceous (119-129my)	72	25	-	-	6	25	Mendia (1978)
Aptrana Formation	E.Cretaceous	80	288	-	-	4	26	Creer (1970)
Sierra de los Condores Group	E.Cretaceous (118.5 my, K-Ar)	81	14	-	-	13	27	Valencio (1972)
Rio de los Molinos Dykes	Cretaceous	78	13	-	1	8	28	Lineares & Valencio (1975)
Sediments and Volcanics	Cretaceous	63	30	-	-	8	29	Creer (1970)

*1 - For explanation refer to Table 1.1.

Permo-Carboniferous loop in the Indo-Pakistan APWP. The other main feature tentatively deduced from the South American APWP is a suggestion of the Triassic-Jurassic loop as observed in the APWP's of most of the other Gondwanaland continents.

7.5   Summary

The Indo-Pakistan APWP suggested here, when compared with the APWP's for other Gondwanaland continents, shows (within the uncertainty limits) a reasonably good agreement for the Permo-Carboniferous to Late Jurassic pole positions. Two main features have been noted in the Indo-Pakistan APWP:

1) The Permo-Carboniferous loop

2) The Triassic-Jurassic loop

1.   The Permo-Carboniferous loop suggested indicates an appreciable polar wandering during Carboniferous and Permian times. A similar loop may exist in data from "stable" Africa but has not been observed in the data from Morroco. The loop can also be seen but not so distinctly in the Australian data. However,It does not appear to be present in the South American data. The reality of the Permo -Carboniferous loop for the APWP of Gondwanaland as a whole must be therefore doubted. More data are needed if the reality of this loop is to be demonstrated.

2). The Triassic-Jurassic loop may reflect the initial break-up of the northern part of Gondwanaland and the formation of the Neotethys during the late Palaeozoic-early Mesozoic. A similar loop has been observed for Australia (Embleton, 1980) and may also exist for Morocco, "stable" Africa and South America. The demonstration of this loop in the data from the latter two fragments of Gondwanaland is rather tentative and awaits further study of Late Triassic and Jurassic rocks. On presently

available data, Triassic-Jurassic loop is suggested for all the Gondwana

continents.

CONCLUSIONS

Thermal and chemical demagnetization results obtained in a palaeomagnetic study of Permo-Carboniferous to possibly Triassic - Jurassic red beds from Gondwana basins in the Koel-Damodar Valley and the Son Valley, N.E. India, have led to the following conclusions.

A). Permo-Carboniferous pole positions from the Talchir Formation (Permo-Carboniferous) and the Barakar Formation (upper Lower Permian) when interpreted as representing a primary magnetization, indicate fast polar wandering during the late Palaeozoic (Fig. 6.1c, Pole Nos. HTB, HTA, TBC, HBA and HBB). The trajectory of the Indo-Pakistan APWP is substantiated by some of the recently obtained pole positions from extrapeninsular Indo-Pakistan, i.e. the Krol Belt (Silurian-Devonian, AT) and the Kashmir Himalaya (Permo-Carboniferous) (Fig. 6.1b, Pole No. 16). But it is more difficult to reconcile this trajectory with earlier established results from peninsular Indo-Pakistan and other results from extrapeninsular Indo-Pakistan, such as from the Krol Belt and the Salt Range. The suggested Permo-Carboniferous trajectory of the Indo-Pakistan APWP is also in agreement with a recently determined, middle Palaeozoic APWP trajectory for SE Australia (Goleby, 1980). (Fig. 6.1c, Pole Nos. BG1, BG2).

An alternative explanation for the Permo-Carboniferous results in terms of a Triassic-Jurassic remagnetization is also suggested because of their similarity with that part of the Indo-Pakistan APWP as proposed by Klootwijk and Bingham (1980) and can be invoked only in case of limited polar wandering. Such an interpretation however, seems less likely because of the predominantly reversed polarities observed whereas a worldwide normal polarity bias is characteristic of the Triassic-Jurassic magnetic interval (McElhinny, 1973, Fig. 6.2).

B) Results from the Late Permian-Early Triassic Panchet Formation agree with previously established results (Fig. 6.1c, Pole No. RPA).

C) Results from the Middle to Late Triassic Tiki Formation and the Parsora Formation are in good agreement with previously established results (Fig. 6.1c, Pole Nos. TPA, JPA, JPB, JPC and JPD). The results support for the broad Triassic-Jurassic loop in the Indo-Pakistan APWP proposed by Klootwijk and Bingham (1980).

D) Comparison of both chemical and thermal demagnetization results in the Tiki Formation and thermal demagnetization results in the Mahadeva Formation indicates a remagnetization processes which are attributed to the Deccan Trap magmatic activity (Fig. 6.1b, Pole Nos. TPA, AMA). Because of the non-blanket character of the overprint, it is argued that hydrothermal activity may have played an important role in their acquisition in addition to regional heating.

E) Chemical demagnetization has been found to be able to separate and remove hard magnetic components, such as those attributed to the Deccan Trap magmatic activity in comparison to thermal demagnetization. For example, the separation of secondary component from the Tiki Formation, TPA (Figs.5.11, 6.1 b,c).

F) Comparison of the suggested Indo-Pakistan APWP with those from the other Gondwanaland continents shows:

(a) A Triassic-Jurassic loop for Indo-Pakistan, Australia and possibly Morocco, "stable" Africa and South America.

(b) Lack of evidence from the other Gondwanaland continents for the primary interpretation suggested for the Permo-Carboniferous results of the Indo-Pakistan, which means no clear support for a Permo-Carboniferous loop.

REFERENCES

Ahmad, F., 1964: The Permian Basin of Peninsular India. 22nd Int.Geol.Colng.New Delhi, 123-138.

Ahmad, F., 1966: Post Gondwana Faulting in Peninsular India and its bearing on the Tectonics of the Subcontinent. Dept.of Geol., AMU, Aligarh, Annals, 2, 1-64.

Ahmad, F. & Ahmad, Z.S., 1977: Tectonic framework of the Gondwana Basins of Peninsular India. In Fourth International Gondwana Symposium, Calcutta, eds. Laskar, B. & Raja Rao, C.S. Hindustan Publishing Corp., Delhi, India, 2, 720-733.

Athavale, R.N., Rao, G.V.S.P. & Rao, M.S., 1979: Palaeomagnetic Results of Two Basic Volcanic Formations from Western Himalaya and a Phanerozoic Polar Wandering Curve for India. In Geophysical Research Bulletin, ed. Kaila, K.L., NGRI, Hyderabad, India, 17, 259-272. Planet.Sci.Lett., 16, 370-378.

Athavale, R.N., Verma, R.K., Bhalla, M.S. & Pullaiah, G., 1970: Drift of the Indian Sub-Continent since Precambrian Times. In Palaeogeophysics, ed., Runcorn, S.K., London Academic Press, 291-305.

Bardon, C., Bossert, A., Hamzeh, R., Rolley, J.P. & Westphal, M., 1973: Etude Palaeomagnetique de Formations Volcaniques du Cretace Inferieur dans I'Atlas de Beni Mellal (Maroc). C.R.Acad.Sci.Paris, 227, 2141-2144.

Bardon, C., Bossert, A., Hamzeh, R. & Westphal, M., 1973: Etude Palaomagnetique de Formations du Trias et du Jurassique de Maroc et du Sahara. C.R.Acad.Sci.Paris, 276, 2356-2360.

Bhalla, M.S. & Verma, R.K., 1969: Palaeomagnetism of Triassic Parsora Sandstones from India. Physics Earth and Planetary Interiors, 2, 138-146.

Bordet, P., 1978: The western Border of the Indian Plate, Implications

for Himalayan Geology. Tectonophysics, 51, T71-T76.

Briden, J.C., 1965: Ancient Secondary Magnetizations in Rocks. Jour.Geophys.Res., 70, 5202-5221.

Briden, J.C., 1967: A New Palaeomagnetic Result from the Lower Cretaceous of East Central Africa. Geophys. J.R.Astr.Soc., 12, 375.

Briden, J.D., Henthorn, D.I. & Rex, D.C., 1971: Palaeomagnetism and Radiometric Evidence for the Age of Freetown Igneous Complex, Sierra Leone, Earth Planet.Sci. Lett., 12, 385.

Brock, A., 1968: Palaeomagnetism of the Nunanetsi Igneous Province and its bearing upon the sequence of Karroo Igneous Activity in Southern Africa. J.Geophys.Res., 73, 1389.

Butler, R.F. & Banerjee, S.K., 1975: Theoretical Single-Domain Grainsize Range in Magnetite and Titanomagnetite. J.Geophys. Res., 80, 4049-4058.

Casshyap, S.M., 1977: Patterns of Sedimentation in Gondwana Basins. In Fourth International Condwana Symposium, Calcutta, eds., Laskar, B. & RajaRao, C.S., Hindustan Publishing Corp., Delhi, 2, 527-551.

Chamalaun, F.H., 1964: Origin of the Secondary Magnetization of Old Red Sandstones of the Anglo-Welsh Cuvette. Jour.Geophys.Res., 6a, 4327-4337.

Chatterji, G.C. & Ghosh, P.K., 1967: Tectonic Framework of the Peninsular Gondwana in India. In Gondwana Stratigraphy, 2, Paris, UNESCO, ed. Amos, A.J., p.924-932.

Chatterjee, S. & Roychowdhury, T., 1974: Triassic Gondwana Vertebrates from India. Ind.Jour.Earth Sci., 1(1), 96-112.

Collinson, D.W., 1965: Origin of Remanent Magnetisation and Initial Susceptibility of Certain Red Sandstones. Geophys. J.Roy.Astron.Soc., 9, 203-217.

Crawford, A.R., 1974: A greater Gondwanaland. Nature, 184, 1179-1181.

Creer, K.M., 1965: A Symposium on Continental Drift, III, Palaeomagnetic data from the Gondwanic Continents. Phil.Trans.Roy.Soc., London, 258, 27-40.

Creer, K.M., 1970: A Palaeomagnetic Survey of South American Rock Formations. Phil.Trans.R.Soc., A267, 457-558.

Creer, K.M., Embleton, B.J.J. & Valencio, D.A., 1970: Triassic and Permo-Triassic Data for S.America. Earth Planet.Sci.Lett., 8, 173-178.

Dalrymple, G.B., Gromme, S.C. & White, R.W., 1975: Potassium-argon Age and Palaeomagnetism of Diabase Dikes in Liberia, Initiation of Central Atlantic Rifting. Geol.Soc.Am.Bull., 86, 399-411.

Daly, L. & Pozzi, J.P., 1976: Resultates Palaeomagnetiques du Permian Inferieur et du Trias Marocain. Comparison aver les donnees Africaines et sud Americaines. Earth. Planet.Sci.Lett., 29, 71-80.

Dunlop, D.J., 1973: Superparamagnetic and Single Domain Threshold Sizes in Magnetite. J.Geophys.Res., 78, 1780-93.

Du Toit, A.L., 1937: Our Wandering Continents. Edinburgh, Oliver and Boyd, 366 p.

Dutt, A.B., 1965: Fenestella sp. from the Talchir of Daltonganj Coal Field. Quart.Jour.Geol.Min.Met.Soc.Ind., 37(3), 133-134.

Dutta, P.K. & Ghosh, S.K., 1972: Triassic Sedimentation in Pali-Tiki Parsora Area, Madhya Pradesh. Proc. 59th Sess.Ind. Sci.Cong.Pt.3, 232-233.

Embleton, B.J.J., 1970: Palaeomagnetic results for the Permian of South America and a Comparison with the African and Australian data. Geophys.J.R.Astr.Soc., 21, 105-118.

Embleton, B.J.J., 1980: Phaerozoic Palaeomagnetism of Australia and Antarctica. Final Report, Study Group 3, of Working Group 10. International Geodynamic Program, M.W. McElhinny and D.A. Valencio

eds., (in press).

Embleton, B.J.J. & Edwards, D.J., 1973: An Instrument for orienting
Rock Samples. Jour.Phys. & Scientific Instruments, 6, 1-13.

Fisher, R.A., 1963: Dispersion on a Sphere. Proc.Roy. Soc.London,
A217, 295-305.

Gansser, A., 1977: The Great Suture between Himalaya and Tibet, A
Preliminary Account. In No 268-Himalaya Sciences de la Terre, Centre
National de la Recherche Scientifique, Paris, 181-191.

Ghosh, S., 1954: Discovery of a New Locality of Marine Gondwana
Formation. Sci.and Cult., 19, 620.

Ghosh, P.K. & Mitra, N.D., 1975: History of Talchir Sedimentation in
Damodar Valley Basins. Mem.Geol.Surv.India., 105, 1-17.

Gidskehaug, A., Creer, K.M. & Mitchell, J.G., 1975: Palaeomagnetism and
K-Ar Ages of the South-West Africa Basalts and their bearing on the
time of Initial Rifting of the South Atlantic Ocean.
Geophys.J.R.Astr. Soc., 42, 1.

Goleby, B.R., 1980: Early Palaeozoic Palaeomagnetism in Southeast
Australia. (Submitted to J.Geomag.Geoelec.) Preprint.

Gough, D.I. & Brock, A., 1964: The Palaeomagnetism of the Shawa
Ijolite. J.Geophys.Res., 698, 2489-2493.

Graham, K.W.T., 1961: Palaeomagnetic Studies on Some South African
Rocks. Ph.D. Thesis, University of Cape Town.

Griffiths, D.H., King, R.F., Rees, A.I., & Wright, A.E. , 1960: The
remanent magnetization of some recent varved sediments. Proc. Roy.
Soc. London, A 256, 359-83.

Griffiths, J.R., 1974: Revised Continental Fit of Australia and
Antarctica. Nature, 249, 336-338.

Hailwood, E.A., 1975: The Palaeomagnetism of Triassic and Cretaceous
Rocks from Morocco. Geophys.J., 41, 219-235.

Hailwood, E.A. & Mitchell, J.C., 1971: Palaeomagnetic and Radiometric Dating Results from Jurassic Intrusions in South Morocco. Geophys.J., 24, 351-364.

Hargraves, R.B., 1978: Problems in Palaeomagnetic synthesis illustrated by results from Permo-Triassic Dolerites in Gyana. Phys.Earth Planet.Int., 16, 277-284.

Hedley, I.G., 1968: Chemical Remanent Magnetization of the FeOOH-Fe O System. Phys.Earth Planet.Interiors, 1, 103-121.

Irving, E. & Major, A., 1964: Post-Depositional detrital remanent magnetization in a synthetic sediment. Sedimentology , 3 , 135-43.

Irving, E., 1964: Palaeomagnetism and its application to Geological Geophysical Problems. Wiley-Interscience, New York, 1-399.

Irving, E., 1966: Palaeomagnetism of Some Carboniferous Rocks from New South Wales and its relation to Geophysical Events. J.Geophys.Res., 71, 6025-51.

Irving, E. & Opdyke, N.D., 1965: The Palaeomagnetism of the Bloomsburg Red Beds and its possible application to the Tectonic History of the Appalachians. Royal Astron.Soc.Geophys.Jour., 9, 153-167.

Irving, E. & Parry, L.G., 1963: The magnetism of some Permian Rocks from New South Wales. Geophys.J., 7, 395-411.

Jaeger, J.C., 1957: The Temperature in the Neighbourhood of a Cooling Intrusive Sheet. Am.Jour.Sci., 255, 306-318.

Jaeger, J.C., 1959: Temperatures Outside a Cooling Intrusive Sheet. Am.Jour.Sci., 257, 44-54.

Jain, A.K., Klootwijk, C.T. & Goswami, K.C., 1979: Late Palaeozoic Diamictites of Garhwal Lesser Himalayas, India. In Prepleistocene Tillites, ed. Harland, W.B., Cambridge University Press, Cambridge, in press.

Kaneoka, I.& Haramura, H., 1973: K/Ar Ages of successive lava Flows from

the Deccan Traps, India. Earth Plan. Sc. Letters , 18 , 229-36.

Kirschvink, J.L., 1979:   The Least-Square Line and Plane and the
  Analysis of Palaeomagnetic Data. Dept.Geol.Geophys. Sci., Princeton
  University, New Jersey, 1-43.

Klootwijk, C.T., 1971: Palaeomagnetism of the Upper GondwanaRajmahal
  Traps, Northern India. Tectonophysics, 12, 449-467.

Klootwijk, C.T., 1973: Palaeomagnetism of Upper Bhander Sandstones from
  Central India and Implications for a Tentative Cambrian Gondwanaland
  Reconstruction. Tectonophysics, 18, 123-145.

Klootwijk, C.T., 1974: Palaeomagnetic Results from some Panchet Clay
  Beds, Karanpura Coal Field, North Eastern India. Tectonophysics, 21,
  79-92.

Klootwijk, C.T., 1975: Palaeomagnetism of Upper Permian Red Beds in the
  Wardha Valley, Central India. Tectonophysics, 25, 115-137.

Klootwijk, C.T., 1976:   The Drift of the Indian Sub-Continent, an
  interpretation of recent palaeomagnetic data.   Geol.Rundsch., 65,
  885-909.

Klootwijk, C.T., 1979a: A Review of Palaeomagnetic Data from the
  Indo-Pakistan Fragment of Gondwanaland, in Geodynamics of Pakistan,
  (eds. De Jong, K.A. & Farah, A.). Geological Survey of Pakistan,
  Quetta, p.41-80.

Klootwijk, C.T., 1979b: A Summary of New Palaeomagnetic Results from
  Extrapeninsular India, Implications for Collision Tectonics.   In
  Structural Geology of the Himalaya, ed. Saklani, P.3., 307-360.

Klootwijk, C.T. & Bingham, D.K., 1980: The Extent of Greater India 3:
  Palaeomagnetic Data from the Tibetan Sedimentary Series, Central Nepal
  Himalaya. Earth Planet.Sci.Lett., (in press).

Klootwijk, C.T. & Peirce, J.W., 1979: India's and Australia's Pole
  Path 3ince Late Mesozoic and the IndiaAsia Collision.   Nature, 282,

605-607.

LeFort, P., 1975: Himalayas, The Collided Range. Present Knowledge of the Continental Arc. Am.Jour.Sci., 275, 1-44.

Lele, K.M., 1964: The Problem of Middle Gondwana in India, 22nd Int.Geol.Cong.Gond., New Delhi, India, 181-202.

Lele, K.M., 1969: Studies in the Indian Middle Gondwana Flora -5, Parsorophyllum Gen.Nov. from the Parsora Beds, South Rewa Gondwana Basin. J.Sen.Mem.Vol., Bot.Soc.Bengal, Calcutta, 313-318.

Linarea, E. & Valencio, D.A., 1975: Palaeomagnetism and K-Ar Ages of the Rio de los Molinos Dikes, Province of Corboda, Argentina. Jour.Geophys.Res., 80, 3315-3321.

Martin, D.L., Nairn, A.E.M., Noltimer, H.C., Petty, M.H., and Schmitt, T.J., 1978: Palaeozoic and Mesozoic Results from Morocco. Tectonophysics, 44, 91-114.

McDougall, I. & McElhinny, M.W., 1970: The Rajmahal Traps of India - K/Ar Ages and Palaeomagnetism. Earth Planet.Sci.Lett., 9, 371-378.

McElhinny, M.W., 1964: Statistical Significance of the Fold Test in Palaeomagnetism. Geophys.J.R.Astr.Soc., 8, 338-340.

McElhinny, M.W., 1968-79: Palaeomagnetic Directions and Pole Positions, Parts VIII-XVI. Geophys.J.R.Astr.Soc., 15, 409-430 (1968a); 116, 207-224 (1968b); 19, 305-327 (1969); 20, 417-429 (1970); 27, 237 (1972a); 30, 281-293 (1972b); 49, 313-356 (1977); 52, 259-276 (1978); List XVI (1979) in press.

McElhinny, M.W., 1973: Palaeomagnetism and Plate Tectonics. Cambridge University Press, Cambridge, 1-358.

McElhinny, M.W. & Brock, A., 1975: A new palaeomagnetic Result from East Africa and Estimates of the Mesozoic Palaeoradius. Earth Planet.Sci.Lett., 27, 321-328.

McElhinny, M.W. & Embleton, B.J.J., 1974: Australian Palaeomagnetism

and the Phanerozoic Plate Tectonics of Eastern Gondwanaland. Tectonophysics, 22, 1-29.

McElhinny, M.W. & Jones, D.L., 1965: Palaeomagnetic measurements on some Karroo Dolerties from Rhodesia. Nature, 206, 921.

McElhinny, M.W. & Opdyke, N.D., 1968: The Palaeomagnetism of some Carboniferous Glacial Varves from Central Africa. J.Geophys.Res., 73, 689-696.

McElhinny, M.W., Cowley, J.A. & Edwards, D.J., 1973: Palaeomagnetism of some Rocks from Peninsular India and Kashmir. Tectonophysics, 50, 41-54.

McElhinny, M.W., Luck, G.R. & Edwards, D.J., 1971: Large Volume Magnetic Field-Free Space for Thermal Demagnetization and other studies in Palaeomagnetism. Pure.Appl.Geophys., 90, 126-130.

McElhinny, M.W., Briden, J.C., Jones, D.L. & Brock, A., 1968: Geological and Geophysical Implications of Palaeomagnetic Results from Africa. Rev.Geophys., 6, 201.

Mendia, J.E., 1978: Palaeomagnetism of Alkaline Lave Flows from El Salto-Almafuerte, Cordoba Province, Argentina. J.Roy.Astro.Soc., 54, 539-546.

Michard, A., Westphal, M., Bossert, A. & Hamzeh, R., 1975: Tectonique de blocs dans le Socle Atlanto-Mesetien du Maroc, une nouvelle interpretation des donnees geologiques et palaeomagnetiques. Earth Planet.Sci.Lett., 24, 363-368.

Mital, G.S., Verma, R.K. & Pullaiah, G., 1970: Palaeomagnetic Study of Satyavedu Sandstones of Cretaceous Age from Andhra Pradesh, India. Pure Appl.Geophys., 81, 177-191.

Morgan, W.J., 1976: Computer Programs for making Maps and Moving Continents. Dept.Geol.Geophys.Sci., Princeton University, New Jersey, 1-225.

Nagata, T., 1961: Rock Magnetism. Maruzen, Tokyo, 2nd Edition, 1-350.

Neel, L., 1955: Some theoretical aspects of rock magnetism. Phil.Mag.Suppl.Adv.Phys., 4, 191-243.

Norton, I. & Molnar, P., 1977: Implications of a revised fit between Australia and Antarctica for the Evolution of the Eastern Indian Ocean. Nature, 267, 338-340.

Norton, I.D. & Sclater, J.G., 1979: A model for the evolution of the Indian Ocean and the Break-Up of Gondwanaland. J.Geophys.Res., 84, 6803-6830.

O'Reilly, W., 1976: Magnetic Minerals in the Crust of the Earth. Rep.Prog.Phys., 39, 857-908.

Opdyke, N.D., 1964a: The Palaeomagnetism of the Permian Red Beds of Southwest Tanganyika, J.Geophys.Res., 69, 2477-2487.

Opdyke, N.D., 1964b: The Palaeomagnetism of some Triassic Red Beds from Northern Rhodesia. J.Geophys.Res., 69, 2495-2497.

Pacca, I.G. & Hiodo, F.M., 1976: Palaeomagnetic Analysis of Mesozoic Serra Geral Basaltic lava flows in Southern Brazil. Symposium on Continental Margins of Atlantic Type, Sao Paulo, Brazil, 1975. An.Acad.Bras.Cienc., 48, 207-214.

Parry, L.G., 1965: Magnetic Properties of Dispersed Magnetite powder. Phil.Mag., 11, 303-312.

Peirce, J.W., 1976: Assessing the Reliability of DSDP palaeolatitudes. Jour.Geophys.Res., 81, 4173-4187.

Peirce, J.W., 1978: The Northward Motion of India Since the Late Cretaceous. Royal Astron.Soc.Geophys.Jour., 52, 277-311.

Piper, J.D.A., 1972: A Palaeomagnetic Study of the Bukoban System, Tanzania. Geophys.J.Roy.Astron.Soc., 28, 111.

Powell, C.McA., 1979: A speculative tectonic history of Pakistan and surroundings, some constrainst from the Indian Ocean. In Geodynamics

of Pakistan, eds. Farah, A., and DeJong, K.A., 5-24.

Powell, C.McA. & Conaghan, P.J., 1973:   Plate   tectonics   and   the
Himalayas.   Earth Planet.Sci.Lett., 20, 1-12.

Powell, C.McA., Johnson, B.D. & Veevers, J.J., 1978:   A Revised Fit of
East and West Gondwanaland.   The Carey Symposium, Hobart,   Feb.   1977,
Tectonophysics (in press).

Pullaiah, G. & Verma, R.K., 1970:   Geomagnetic   Field   Reversal   in
Cretaceous   Tirupati   Sandstone   Formation   from   India.   Earth
Planet.Sci.Lett., 2, 158-162.

Pullaiah, G., Irving, E., Buchan, K.G. & Dunlop, D.J., 1975:
Magnetization Changes caused by Burian and Uplift.   Earth Planet.
Sci.Lett., 28, 133-143.

Rizvi, S.R.A., 1972:   Geology and Sedimentation Trends in Palamau Coal
Fields, Bimar, India.   Mem.Geol.Surv.India, 104, 1-107.

Robertson, W.A., 1963:   Palaeomagnetism of some Mesozoic Intrusives and
Tuffs from Eastern Australia.   J.Geophys.Res., 68, 2299-2312.

Robertson, W.A., 1964:   Palaeomagnetism of the Monzonite   Porphyry   from
Milton, New South Wales.   Pure Appl.Geophys., 59, 93-99.

Robertson, W.A., 1979:   Palaeomagnetic Results from   some   Sydney   Basin
Igneous Rock Deposits.   J.Proc.R.Soc. N.S.W., in press.

Sastry, M.V.A. & Shah, S.C., 1964:   Permian   Marine   Transgression   in
Peninsular   India.   Vol.of   Abst.,   2249,   Int.Geol.Cong.,   Pt.19, New
Delhi, 139-150.

Sastry, M.V.A., Acharya, S.K., Shah, S.C., Satsangi, P.P., Ghosh, S.C.,
Raha, P.K., Singh, G. & Ghosh, R.N., 1977:   Stratigraphic   lexicon   of
Gondwana   Formations of India. Misc.   Pub.No. 36, Geological Survey of
India, 175 p.

Schmidt, P.W., 1976a: The Late Palaeozoic and Mesozoic Palaeomagnetism
of Australia.   Ph.D. Thesis, Australian National University, Canberra,

Australia.

Schmidt, P.W., 1976b: The Non-Uniqueness of the Australian Mesozoic Palaeomagnetic Pole Position. Geophys.J., 47, 285-300.

Schmidt, P.W., 1976c: A New Palaeomagnetic Investigation of Mesozoic Igneous Rocks in Australia. Tectonophysics, 33, 1-13.

Schmidt, P.W. & McDougall, I., 1977: Palaeomagnetic and Potassium-Argon Dating Studies of the Tasmanian Dolerites. J.Geol.Soc.Aust., 25, 321-328.

Schmidt, P.W., Currey, D.T. & Ollier, C.D., 1976: Sub-basaltic Weathering, Dam Sites, Palaeomagnetism and the age of Laterisation. J.Geol.Soc.Aust., 23, 367-370.

Sengor, C.A.M., 1979: Mid-Mesozoic Closure of Permo-Triassic Tethys and Its Implications. Nature, 279, 590-593.

Shah, S.C. & Sastry, M.V.A., 1973: Significance of Early Permian Marina Faunas of Peninsular India. 3rd Int.Symp. on Gond.Strat., I.U.G.S., Canberra, Australia, Abstract, 41 p.

Shah, S.C., Singh, G. & Sastry, M.V.A., 1971: Biostratigraphic classification of Indian Gondwana. Int.Symp.,Strat.Min.Res.Cong. Syst.Annals of Geol. Dept. Aligarh Muslium University,, 5 and 6, 306-326.

Smith, A.G. & Hallam, A., 1970: The Fit of the Southern Continents. nature, 98, 139-144.

Stacey, F.D., 1963: The Physical Theory of Rock Magnetism. Phil.Mag.Supp.Adv.Phys., 12, 46-133.

Stacey, F.D. & Banerjee, S.K., 1974: The Physical Principles of Rock Magnetism. Elsevier, Amsterdam, 1-195.

Stocklin, J., 1977: Structural Correlation of the Alpine Ranges Between Iran and Central Asia. Soc.Geol.France, Mem.H.Ser., 8, 333-353.

Stoneley, R., 1974: On the origin of ophiolite complexes in the

Southern Tethys Region. Tectonophysics, 25, 303-322.

Strangway, D.W., Honea, R.M., McMahon, B.E. & Larson, E.E., 1968: The
Magnetic Properties of Naturally Occurring Goethite.
Geophys.J.Roy.Astron.Soc., 15, 345-359.

Thompson, R., 1972: Palaeomagnetic Results from the Paganzo Basin of
Northwest Argentina. Earth Planet.Sci. Lett., 15, 145-156.

Valencio, D.A., 1969: El palaeomagnetismo de algunas magmatitas del
Triasico superior, Grupo Cacheuta, Provincia de Mendoza, Republica
Argentina.Rev.Asoc. Geol.Argent., 24, 191-198.

Valencio, D.A., 1972: Palaeomagnetism of the lower Cretaceous
Vulcanites Cerro Colorado Formation of the Sierra de los Condores
Group, Province of Corboda, Argentina. Earth
Planet. Sci. Lett.

Valencio, D.A., Mendia, J.G. & Vilas, J.F., 1975a: Palaeomagnetism and
K-Ar Ages of Triassic Igneous Rocks from the Ischiqua-Ischichuca Basin
and Puerto Viezo Formation, Argentina. Earth Planet.Sci.Lett., 26,
319-330.

Valencio, D.A., Rocha Campos, A.C. & Pacca, I.G., 1975b:
Palaeomagnetism of some sedimentary rocks of the late Palaeozoic
Tubarao and Pass Doiss Groups from the Parana Basin, Brazil.
Rev.Bras.Geosci., 53, 186-197.

Valencio, D.A., Rocha-Campos, A.C. & Pacca, I.G., 1978: Palaeomagnetism
of the Cassanje "Series" (Karroo System) Angola.
An.Acad.Brasil.Cienc., 50, 353-364.

Valencio, D.A., Vilas, J.F. & Mendia, J., 1977: Palaeomagnetism of the
Middle and Upper Sections of Paganzo Group (Argentina) and the
Correlation of upper Palaeozoic-lower Mesozoic Rocks. Geophys.J.Roy.
Astr.Soc., 51, 59-74.

Veevers, J.J., Powell, C.McA. & Johnson, B.D., 1975: Greater India's

place in Gondwanaland and in Asia. Earth Planet.Sci. Lett., 27, 383-387.

Veevers, J.J.& Cotterill, D., 1978:

Western margin of Australia: Evolution of a rifted arc system,

Geol. Soc. Amerc. Bull., 89, 337-355.

Verma, R.K. & Bhalla, M.S., 1968: Palaeomagnetism of the Kamthi

Sandstones of Upper Permian Age from Godavary Valley, India.

Jour.Geophys.Res., 73, 703-709.

Vilas, J.F., 1974: Palaeomagnetism of some ingeous rocks of the Middle

Jurassic Chon Aike Formation from Estancia la Reconquista, Province of

Santa Cruz, Argentina. Geophys.J., 39, 511-522.

Vilas, J.F., 1976: Palaeomagnetism of the lower Cretaceous Sierra de

los Condores Group, Province Cordoba, Argentina.

Geophys.J.Roy.Astr.Soc., 46, 295-305.

Walker, T.R., 1976: Diagenetic Origin of Continental Red Beds. In The

Continental Permian in Central, West and South Europe, ed. Falke, H.,

Reidel, Dordrecht, 240-282.

Wegener, A., 1924: The Origin of Continents and Oceans. Dutton & Co.,

New York, 212 p.

Wellman, P. & McElhinny, M.W., 1970: K-Ar Age of the Deccan Traps,

India. Nature, 227, 595-596.

Wensink, H., 1975: The Palaeomagnetism of the Speckled Sandstones of

Early Permian Age from the Salt Range, Pakistan. Tectonophysics, 26,

281-292.

Wensink, H., 1968: Palaeomagnetism of some Gondwana Red Beds from

Central India. Palaeogeogr.Palaeoclimat.Palaeoecol., 5, 323-343.

Wensink, H. & Klootwijk, C.T., 1968: The Palaeomagnetism of the Talchir

Series of the Lower Gondwana System, Central India. Earth

Planet.Sci.Lett., 4, 191-196.

Wensink, H., Belrijk, N.A.I.M., Hebeda, E.H., Priem, H.N.A. ,
   Verdurmen, E.A.I. & Verschure, R.H., 1977: In: Fourth International
   Gondwana Symposium, Calcutta, Vol. 2, 832-49.

Zijderveld, J.D.A., 1967: A.C. Demagnetization of Rocks, Analysis of
   Results. In Collinson et al., (eds.), Methods in Palaeomagnetism,
   Elsevier, Amsterdam, 254-286.